

Verification and Optimization of a Knockdown Factor Formula for Thin- Shell Structures

By

Yuanxi Zhao

Master of Science Project
in Structural Engineering

Committee members
Dr.ir. P.C.J. Hoogenboom (chair)
Ir. A.C.B. Schuurman
Dr.ir. F.P. van der Meer



Preface

First and foremost, I would like to extend my sincerest gratitude to my advisor, Pierre Hoogenboom, for his unwavering tolerance, support, and assistance throughout the course of this thesis. His guidance has been instrumental in shaping the direction of my research and identifying the specific issues that needed to be addressed. Under his mentorship, I have not only gained a deeper understanding of my field of study but also learned how to approach complex problems with a critical mindset. Additionally, I am profoundly thankful to all members of my committee, Frans van der Meer and Marco Schuurman, who meticulously reviewed my work, pinpointed areas that required refinement, and provided invaluable feedback that was crucial in overcoming the challenges encountered during the research process.

Moving forward, I am committed to carrying the lessons learned from this academic journey into my future endeavors. The skills acquired and the knowledge gained through this rigorous process will undoubtedly serve as a solid foundation for whatever path I choose to follow. I hope to continue contributing to the field, applying the principles and methodologies explored in this thesis to real-world scenarios. Moreover, I aspire to foster the same spirit of inquiry and dedication that my mentors have exemplified, thereby helping to expand the boundaries of our collective understanding. My ambition is to remain engaged in research and development, aiming to bridge theory with practice, and contribute positively to society.

I look forward to the opportunities ahead, eager to apply what I've learned and make a meaningful impact in my chosen field.

Yuanxi Zhao
Zhengzhou, China
December 10, 2024

Summary

Shell structures are widely favored due to their ability to bear substantial loads with minimal thickness, aligning with contemporary aesthetic sensibilities. This thesis investigates the buckling behavior of thin-shell structures with the aim to refine a knockdown factor formula. Authored by Yuanxi Zhao under the guidance of Dr.ir. P.C.J. Hoogenboom, Ir. A.C.B. Schuurman, and Dr.ir. F.P. van der Meer, this research addresses the critical issue of load-carrying capacity reduction due to shape imperfections leading to buckling.

A complete range of shell shapes and loading has been studied. The shells buckle in ring mode (1-3, 3-3, 2-1, 2-3), column mode (2-2), mixed column-ring mode (1-1) and in-extensional mode (3-2, 3-1, 1-2) (page 19).

Linear buckling analyses were conducted to explore how parameters such as height, boundary conditions and model size influence the buckling load factor. Geometrical nonlinear analyses were conducted using SCIA Engineer, introducing different imperfection amplitudes to simulate real-world conditions. The knockdown factor was calculated as nonlinear buckling load over linear buckling load. This knockdown factor was compared to a knockdown factor obtained from a formula.

The knockdown factor does not depend on the curvature ratio k_{yy}/k_{xx} or the membrane force ratio n_{xx}/n_{yy} . It only depends on the imperfection amplitude and d/t (page 65) and the slenderness a/t (page 6). The knockdown factor formula produces reasonable values. However, the formula is not accurate (page 62). It is recommended to derive a new knockdown factor formula.

Table of Contents

PREFACE	2
SUMMARY	3
1 INTRODUCTION	6
1.1 RESEARCH OBJECTIVE	6
1.2 RESEARCH PROCEDURE	7
2 EXISTING KNOWLEDGE.....	9
2.1 SHELL STRUCTURES.....	9
2.2 COORDINATE SYSTEMS AND CURVATURES.....	10
2.2.1 <i>Coordinate systems</i>	10
2.2.2 <i>Surface curvature</i>	10
2.2.3 <i>Principal curvature</i>	11
2.2.4 <i>Gaussian curvature</i>	11
2.3 MEMBRANE FORCES, MOMENTS AND SHEAR FORCES	11
2.4 SHELL BUCKLING THEORY	12
2.4.1 <i>Static Instability</i>	12
2.4.2 <i>Bifurcation buckling</i>	13
2.4.3 <i>Imperfection sensitivity</i>	14
2.4.4 <i>Implementation of imperfection</i>	14
2.5 FINITE ELEMENT ANALYSIS	15
2.5.1 <i>Linear buckling analysis</i>	15
2.5.2 <i>Nonlinear finite element analysis</i>	15
3 MODELS AND ANALYSIS METHODS	17
3.1 MODEL GENERATION	17
3.1.1 <i>Shape of Shell Structures</i>	17
3.1.2 <i>Elements</i>	18
3.2 BUCKLING ANALYSIS PROCESS	18
4 LINEAR BUCKLING ANALYSIS	19
5 PARAMETER STUDY OF LINEAR ANALYSIS.....	24
5.1 ELEMENT SIZE STUDY	24
5.1.1 <i>Element size: 0.895 m</i>	24
5.1.2 <i>Element size: 0.671 m</i>	28
5.2 MODEL SCALE STUDY	33
5.2.1 <i>Half-scale model with unchanged load</i>	33
5.2.2 <i>Half-scale model with twice radial load and twice Young's modulus</i>	38

5.3 DEVELOPMENT OF BUCKLING MODES	42
5.4 BUCKLING BEHAVIOR ANALYSIS OF MODEL 2 - 1 WHEN $N_{xx} = 0$	45
5.5 BOUNDARY CONDITIONS STUDY	45
5.6 MODEL HEIGHT STUDY	47
6 GEOMETRICAL NONLINEAR ANALYSIS.....	51
7 PARAMETER STUDY OF THE NONLINEAR ANALYSIS	53
7.1 IMPERFECTION AMPLITUDE STUDY	53
7.1.1 Imperfection amplitude: 100mm (0.5t)	53
7.1.2 Imperfection amplitude: 400mm (2t)	54
7.1.3 Imperfection amplitude: 800mm (4t)	56
7.1.4 Conclusion	58
8 KNOCKDOWN FACTOR CALCULATION	59
8.1 Imperfection amplitude: 200mm (t)	59
8.2 Imperfection amplitude: 100mm (0.5t)	59
8.3 Imperfection amplitude: 400mm (2t)	60
8.4 Imperfection amplitude: 800mm (4t)	60
9 COMPARISON AND DISCUSSION.....	62
10 CURVE FITTED KNOCKDOWN FACTOR FORMULA.....	65
11 CONCLUSIONS AND RECOMMENDATIONS	67
11.1 Linear Analysis Conclusions	67
11.2 Nonlinear Analysis Conclusions	69
11.3 Overall Conclusions and Recommendations.....	69
LITERATURE	70
APPENDIX 1.....	72
APPENDIX 2.....	73
APPENDIX 3.....	79
APPENDIX 4.....	83
APPENDIX 5.....	92
APPENDIX 6.....	93

1 Introduction

1.1 Research objective

Shell structures are very popular in engineering because of their free forms. They have remarkable properties, which is that shells' curvature enables them to carry distributed load as membrane forces. Therefore, they inherently have excellent strength to weight ratio, which makes thinner and more aesthetic designs possible.

Clearly, all possible modes of failure need to be excluded in the design process, such as large deformations, disturbing vibrations (serviceability load combinations) yielding, crushing, fatigue and buckling (ultimate limit state load combinations). In thin shell structures, the buckling failure mode often governs the design[1]. The most serious flaw in applying shell structures is that shell buckling is a sudden event and it does not occur gradually, which means that shells often do not show enough deformation as a warning before collapsing. Therefore, it's necessary to study the buckling condition and behavior of thin-shell structures.

Experimental buckling results show a wide scatter and the obtained ultimate loads are much smaller than the critical loads of the established linear buckling theory (See Figure 1.1.1). Previous research shows that this is caused by initial geometric imperfections[2].

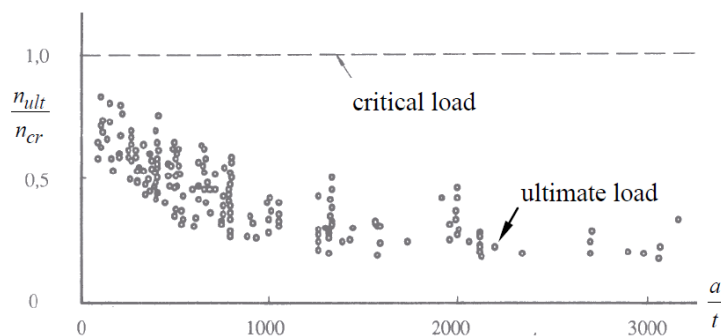


Figure 1.1.1 Experimental ultimate loads of 172 axially loaded aluminum cylinders [3]

In designing shell structures, finite element analyses are made to check shell designs. There are two ways to predict the buckling load, 1) linear buckling analysis corrected by a knockdown factor, or 2) geometrical nonlinear analysis including shape imperfections[4]. The first method is quick but not accurate. The second method is accurate but time consuming.

The knockdown factor can vary between 1/10 and 1. Often, 1/6 is used, which is based on the lower bound of many aluminum cylinder experiments performed after 1930. This kind of lower bound limit is conservative but not accurate, which restricts the development of thin shell structures.

A possibly better estimate of the knockdown factor is provided by a formula that was

derived in 2019[4].

$$C = \frac{\left(\frac{k_{xx}}{k_{yy}} - 1 - 2\eta \frac{d}{t}\right)^2}{4 \left(\frac{k_{xx}}{k_{yy}} - \frac{n_{yy}}{n_{xx}} - 3\eta \frac{d}{t}\right) \left(\frac{k_{xx}}{k_{yy}} - 2\eta \frac{d}{t}\right)} \quad \eta = \frac{\sqrt{3(1-\nu^2)}}{1-C} \quad (1.1)$$

where

- C knockdown factor
- n_{xx}, n_{yy} membrane forces ($n_{xy} = 0$)
- k_{xx}, k_{yy} curvatures ($k_{xy} = 0$)
- d amplitude of the shape imperfection
- t shell thickness
- ν Poisson's ratio

The formula shows that the knockdown factor depends on the amplitude d of the imperfection. The formula applies to local buckling, therefore, it does not apply to global buckling (in-extensional deformation), for which the knockdown factor is just 1. The objective of this research is to verify the knockdown factor formula (1.1) by geometrical nonlinear analysis considering initial shape imperfections. Physical nonlinearities are not considered in this research.

1.2 Research procedure

Nine thin shell structures of various shapes and sizes have been designed and modelled. The specific parameters of these models can be found in subsection 3.1. The software SCIA Engineer was used. Supports were designed such that global buckling (in-extensional deformation) and edge buckling were prevented as much as possible. The local buckling loads were predicted by 1) linear elastic analyses with the formula knockdown factor and 2) geometrically nonlinear analysis including shape imperfections. The two predictions were compared for the nine designs to verify the results of the knockdown factor formula.

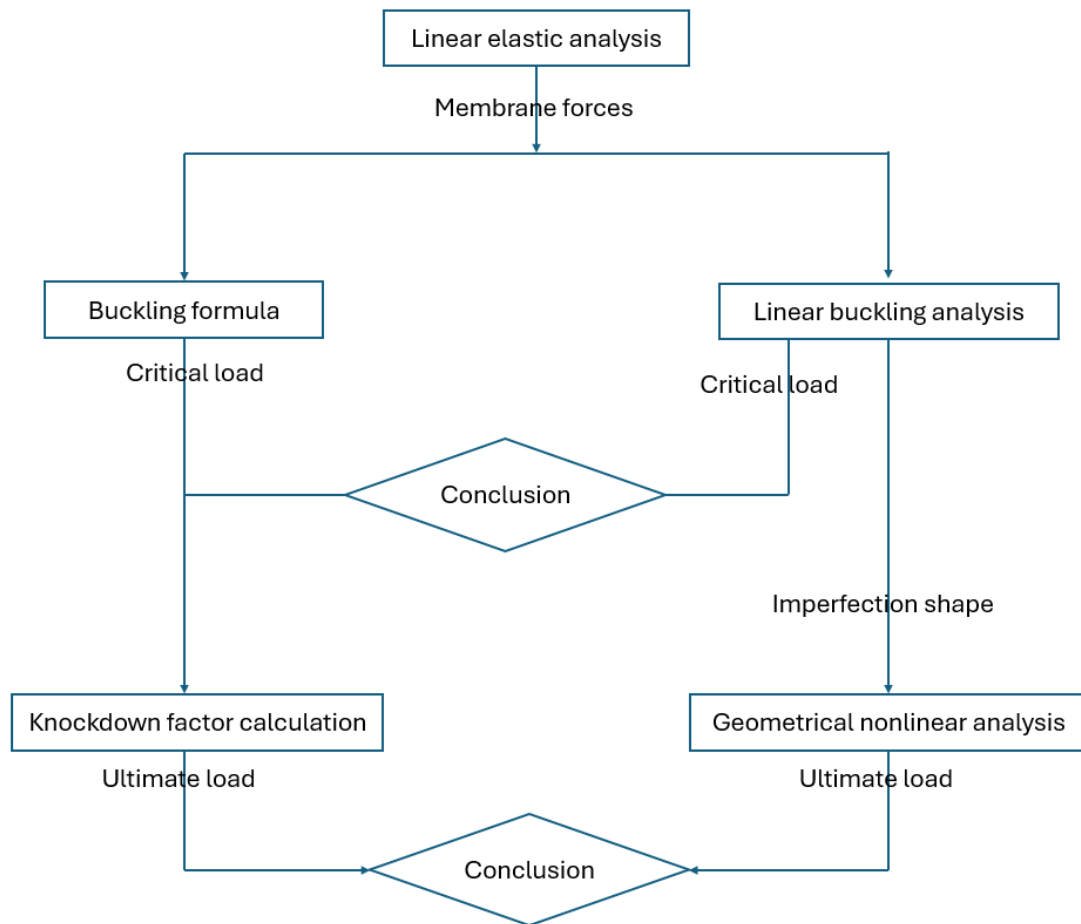


Figure 1.3.1 Research process

2 Existing Knowledge

2.1 Shell structures

The term "shell" refers to structures that have strength and stiffness owing to their thin, natural, and curved form, such as an egg shell, a nut, a human skull, and a tortoise shell. The related parameters of a shell, the radius a , the span l and the sagitta s , are defined as the figure below.

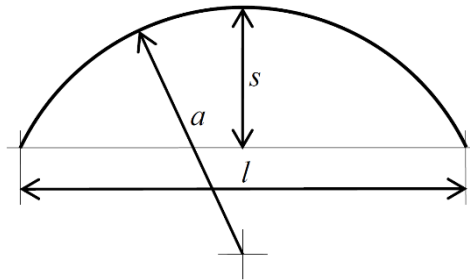


Figure 2.1.1 Geometry of a shell [4]

Generally, shells can be classified based on their radius-to-thickness ratio[4]:

- Very thick shell ($a/t < 5$) : needs to be modelled three-dimensionally; structurally it is not a shell
- Thick shell ($5 < a/t < 30$) : membrane forces, out of plane moments and out of plane shear forces occur; all associated deformations need to be included in modelling its structural behavior
- Thin shell ($30 < a/t < 4000$): membrane forces and out of plane bending moments occur; out of plane shear forces occur, however, shear deformation is negligible; bending stresses vary linearly over the shell thickness
- Membrane ($4000 < a/t$): membrane forces carry all loading; out of plane bending moments and compressive forces are negligible; for example a tent

Shells can carry the distributed surface load by their membrane forces instead of bending moments, allowing for much thinner designs compared with plate structures [5][6][7]. Thin-shell structures are lightweight shell-based structures. These curving components are put together to form huge constructions. Aircraft fuselages, boat hulls, and the roofs of large building are all examples of typical uses.

Thin-shell structures are preferred by architects and structural designers due to their good appearance and excellent strength to weight ratio, especially for large span structures. An example of thin-shell structures, the Sydney Opera House (Australia), is shown below.



Figure 2.1.2 Sydney Opera House (Australia)

2.2 Coordinate systems and curvatures

2.2.1 Coordinate systems

In shell analysis three coordinate systems are used (Figure 2.2.1); 1) a global coordinate system to describe the shape of the shell, 2) a local coordinate system to define curvature, displacements, membrane forces, moments and loading, 3) a curvilinear coordinate system to derive and solve the shell equations[4].

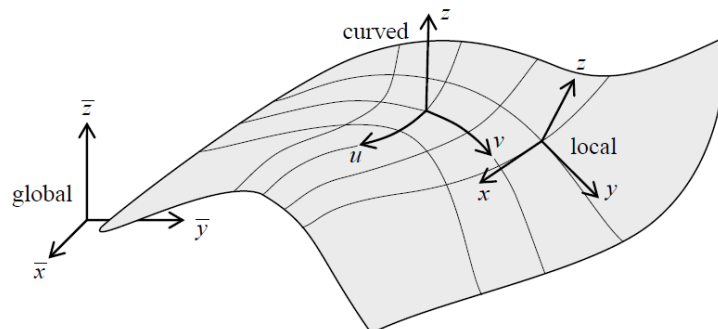


Figure 2.2.1.1 Global, local and curvilinear coordinate systems [1]

2.2.2 Surface curvature

The curvatures for surfaces can be defined. Draw a plane through a normal vector z of a surface, and this normal plane will intersect the surface in a curved line. The curvature of this line is referred to as normal section curvature k . If the circle lies at the positive side of the z axis the normal section curvature is positive. If the circle lies at the negative side of the z axis the normal section curvature is negative. The direction of the z axis can be chosen freely (pointing inward or outward)[4].

The z axis is part of a local coordinate system. When the normal plane includes the x direction vector the curvature is k_{xx} . When the plane includes the y direction vector the curvature is k_{yy} . These curvatures can be calculated by

$$k_{xx} = \frac{\partial^2 z}{\partial x^2}, \quad k_{yy} = \frac{\partial^2 z}{\partial y^2} \quad (2.1)$$

The twist of the surface k_{xy} is defined as

$$k_{xy} = \frac{\partial^2 z}{\partial x \partial y} \quad (2.2)$$

2.2.3 Principal curvature

In a point of a surface many normal planes are possible. If we consider all of them and compute the normal section curvatures then there will be a minimum value k_2 and a maximum value k_1 . These minimum and maximum values are the principal curvatures at this point[4].

$$k_1 = \frac{1}{2}(k_{xx} + k_{yy}) + \sqrt{\frac{1}{4}(k_{xx} - k_{yy})^2 + k_{xy}^2} \quad (2.3)$$

$$k_2 = \frac{1}{2}(k_{xx} + k_{yy}) - \sqrt{\frac{1}{4}(k_{xx} - k_{yy})^2 + k_{xy}^2} \quad (2.4)$$

The directions in the tangent plane in which the minimum and maximum occur are perpendicular.

$$\alpha = \frac{1}{2} \arctan \frac{2k_{xy}}{k_{xx} - k_{yy}}, \quad \frac{1}{2} \pi + \frac{1}{2} \arctan \frac{2k_{xy}}{k_{xx} - k_{yy}} \quad (2.5)$$

2.2.4 Gaussian curvature

The Gaussian curvature of a surface in a point is the product of the principal curvatures in this point $k_G = k_1 k_2$. It can be shown that also $k_G = k_{xx} k_{yy} - k_{xy}^2$. The Gaussian curvature is independent of how we choose the directions of the local coordinate system. A positive value means the surface is bowl-like. A negative value means the surface is saddle-like. A zero value means the surface is flat in at least one direction (plates, cylinders, and cones have zero Gaussian curvature)[4].

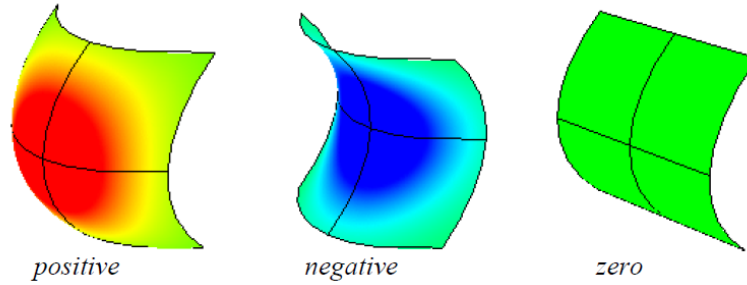


Figure 2.2.4.1 Gaussian curvature (contour plot)

2.3 Membrane forces, moments and shear forces

In thin shells the membrane forces, the moments and the shear forces are defined in the same way as in plates.

$$n_{xx} = \int_{-\frac{1}{2}t}^{\frac{1}{2}t} \sigma_{xx} dz \quad (2.6)$$

$$n_{yy} = \int_{-\frac{1}{2}t}^{\frac{1}{2}t} \sigma_{yy} dz \quad (2.7)$$

$$\frac{1}{2}(n_{xy} + n_{yx}) = \int_{-\frac{1}{2}t}^{\frac{1}{2}t} \sigma_{xy} dz \quad (2.8)$$

$$m_{xx} = \int_{-\frac{1}{2}t}^{\frac{1}{2}t} \sigma_{xx} z dz \quad (2.9)$$

$$m_{yy} = \int_{-\frac{1}{2}t}^{\frac{1}{2}t} \sigma_{yy} z dz \quad (2.10)$$

$$m_{xy} = \int_{-\frac{1}{2}t}^{\frac{1}{2}t} \sigma_{xy} z dz \quad (2.11)$$

$$v_x = \int_{-\frac{1}{2}t}^{\frac{1}{2}t} \sigma_{xz} dz \quad (2.12)$$

$$v_y = \int_{-\frac{1}{2}t}^{\frac{1}{2}t} \sigma_{yz} dz \quad (2.13)$$

The positive directions of these internal forces are defined as follows.

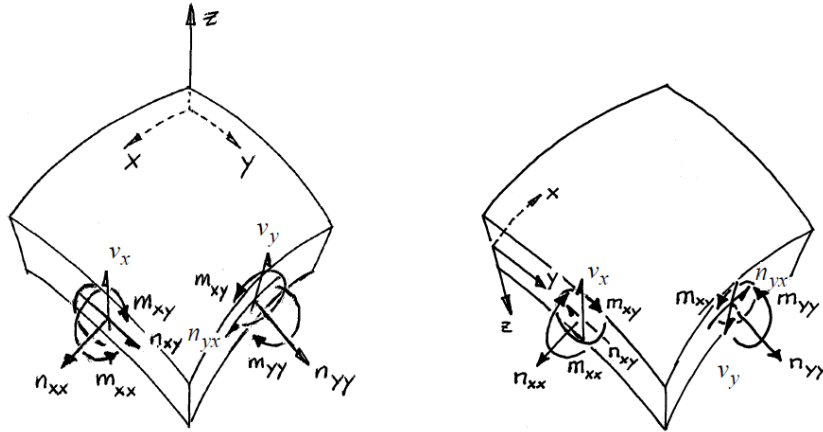


Figure 2.3.1 Positive internal forces of shell parts [4]

2.4 Shell buckling theory

Because of their curvature, shells are thin and may carry distributed surface loads as membrane forces. The ability of shells to retain membrane strain energy without significant deformation gives them their thinness. Shells may become statically unstable and fail severely if this energy is transferred into bending energy[8].

2.4.1 Static Instability

Static instability, often known as buckling, occurs when a structural member or system loses its load-carrying capability[7]. Buckling may be classified into two types: 1) equilibrium bifurcation (Figure 2.4.1.1, point B) and 2) collapse at the limit load without prior bifurcation (point A). A rapid transition in the load-carrying route, such as from axial (or membrane) forces to bending moments, and accompanying

deformations, is an example of bifurcation. This form of instability may be seen in columns, plates, and cylindrical shells. Shallow arches and spherical caps experience the second kind of instability, commonly known as nonlinear buckling or "snap-through" [1][7]. Nevertheless, even arches and spherical caps, given initial geometric imperfections, are prone to fail in an asymmetric mode owing to bifurcation prior to their limit load, i.e. curve 0-B-D in Fig. 2.4.1.1 [1][7][9].

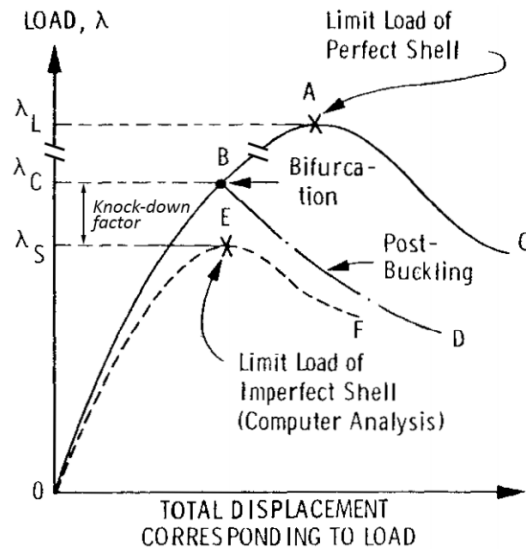


Figure 2.4.1.1 Load-deflection curves showing limit and bifurcation points: path 0AC presents axisymmetric deformation, 0BD non axisymmetric deformation, 0EF for a real structure (or GNLA with imperfection). Snap through occurs at point E. [1]

The loads of Figure 2.4.1.1 can be obtained by multiplying the load factors λ with a reference load. λ_C is the critical buckling load factor at the bifurcation point. λ_L , the limit load factor, is related to the maximum load that can be achieved without prior bifurcation. λ_S is related to the maximum load that can be achieved by a structure with initial geometric imperfections before static instability is reached [9]. λ_S is calculated by a geometrically nonlinear analysis (GNA). However, obtaining λ_S need detailed finite element analysis including initial geometric imperfections. An analysis that includes such imperfections is referred to as a geometrically nonlinear analysis with initial geometric imperfections (GNIA).

2.4.2 Bifurcation buckling

The theoretical buckling membrane force of an axially loaded thin-shell cylinder can be obtained by the formula below[4].

$$n_{cr} = \frac{-1}{\sqrt{3(1-\nu^2)}} \frac{Et^2}{a} \approx -0.6 \frac{Et^2}{a} \quad (2.14)$$

Equation (2.14) is also valid for axially loaded hyperboloids and for externally

pressurized closed cylinders, spherical shells, domes, and hyperbolic paraboloids[4]. The fact that Eq. (2.14) makes no reference to the number of waves found in the buckling pattern helps to explain its broad applicability [1].

2.4.3 Imperfection sensitivity

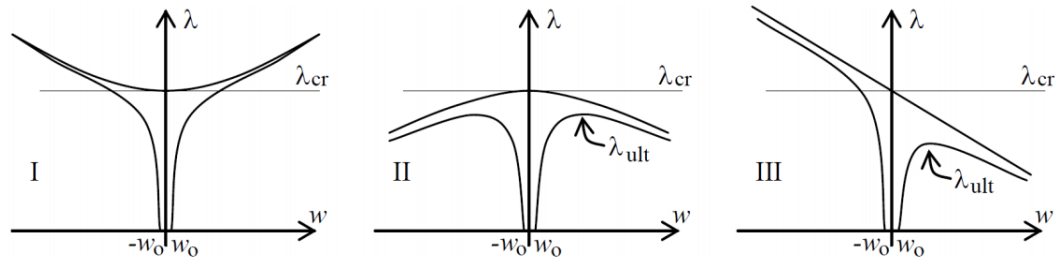


Figure 2.4.3.1 Buckling behavior, left: stable, unstable, asymmetric [4]

Koiter [10] identified three post-buckling behaviors: stable, unstable and asymmetric. He also noticed that for structures with unstable post-buckling behavior, small initial geometric imperfections may have a significant influence, causing the ultimate loads smaller than the critical loads. This kind of structures can be considered as imperfection-sensitive.

2.4.4 Implementation of imperfection

Shell structures are subjected to loose quality control and large construction tolerances due to their size and manufacturing scale (often unique). Because it is difficult to entirely remove all imperfections, different approaches for accounting for the influence of imperfections in finite element calculations of shell load capacity have been developed.

For shell structures with constant curvature, it's possible to develop an analytical solution. However, for complex shell structures, finite element analysis is usually the most realistic method. To apply some imperfection on the model, that imperfection must be identified. With unknown imperfection, the worst situation should be considered (i.e. the 'worst' imperfection should be applied).

Several methods of applying imperfection have been used in previous researches. Koiter imposes imperfection only in the shape of buckling modes in his initial theory. The argument was that any imperfection shape may be decomposed into a series of periodic pattern with Fourier series. He then extended his approach to a more localized, but still periodic, imperfection and found the same sort of imperfection-sensitivity.

Cederbaum and Arbocz constructed a reliability design theory by taking a probabilistic approach to Koiter's theory by varying two critical parameters, initial imperfection amplitude and the allowable load [11].

Tian Chen[12] used 4 different methods to apply imperfections, one single modal shape

with variations, combination of multiple modal shapes, Gaussian random imperfection shape and periodic buckling wave imperfection. He found that for a moderately sensitive structure such as the hyperbolic cooling tower, all the above imperfection shapes are similarly applied. However, after many attempts, the first mode still governs the buckling behavior of the structure. And for a structure with closely spaced eigenvalues, imperfection sensitivity is severe in general. For such a structure, imperfection in the shape of the first mode may not govern the capacity. Cylinder is an extreme example of such a structure, where imperfection in the shape of higher modes, combinations of mode, or sinusoidal waves may govern. Besides geometrical imperfections, he has also applied boundary layer imperfection and stress/strain/displacement imperfection, but it's shown that geometrical imperfection has a far larger impact on the buckling capacity of a thin-shell than other types of imperfections.

2.5 Finite element analysis

2.5.1 Linear buckling analysis

Finite element programs can compute critical load factors and the associated normal modes. This is called a linear buckling analysis. A finite element model has as many critical load factors as the number of degrees of freedom. We can specify how many of the smallest critical load factors the software will compute. If the second smallest buckling load is very close (say within 2%) to the smallest buckling load we can expect the structure to be highly sensitive to imperfections.

The critical load factors need to be multiplied by the knockdown factor. The results need to be larger than 1. Consequently, if all critical load factors are larger than 6, the structure is safe for buckling.

Linear buckling analyses are performed on shell models without imperfections. We could add shape imperfections, however, this would not solve anything. The shape imperfections grow slowly during loading and this is not included in a linear buckling analyses. For imperfections to grow we need to perform a nonlinear finite element analysis[13].

2.5.2 Nonlinear finite element analysis

When a shell design is ready it is sensible to check its performance by nonlinear finite element analyses. In these analyses the loading is applied in small increments for which the displacements are computed. Figure 2.5.2.1 shows the results of different finite element analyses of a simply supported shallow dome[14].

The ultimate load is mainly affected by shape imperfections, support stiffness imperfections and inelastic effects. When these are measured and included in the finite element model then the predicted ultimate load has a deviation less than 10% of the

experimental ultimate load[15].

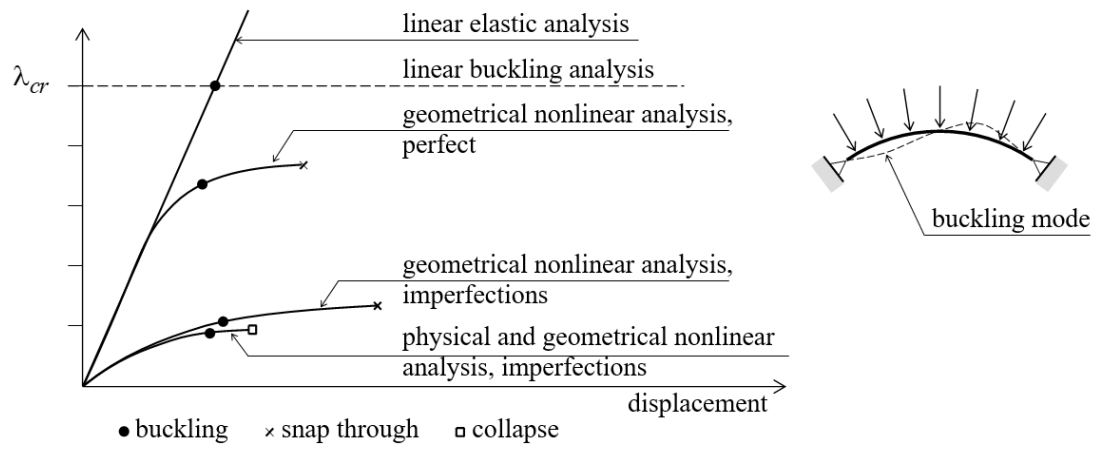


Figure 2.5.2.1 Shell finite element analyses of a steel spherical dome [14]

3 Models and analysis methods

3.1 Model Generation

Nine typical shell models are generated for the verification of the knockdown factor formula.

Model 1-1: perfect cylinder under axial compression

Model 1-2: perfect cylinder under axial compression and radial compression

Model 1-3: perfect cylinder under axial compression and radial tension

Model 2-1: nearly cylinder with positive Gaussian curvature under axial compression

Model 2-2: nearly cylinder with positive Gaussian curvature under axial compression and radial compression

Model 2-3: nearly cylinder with positive Gaussian curvature under axial compression and radial tension

Model 3-1: nearly cylinder with negative Gaussian curvature under axial compression

Model 3-2: nearly cylinder with negative Gaussian curvature under axial compression and radial compression

Model 3-3: nearly cylinder with negative Gaussian curvature under axial compression and radial tension

3.1.1 Shape of Shell Structures

This research focus on thin-shell structures, so the radius-to-thickness ratio of the shell structures is set at 500. The dimensions of the models are as follows.

Table 3.1.1 Dimensions of the models

	Models	Thickness t [mm]	Radius a [m]	Height [m]
Perfect cylinder	1-1; 1-2; 1-3	200	100	100
Nearly cylinder with positive Gaussian curvature	2-1; 2-2; 2-3	200	100 (top and bottom) 105 (middle) 252.5 m (vertical)	100
Nearly cylinder with negative Gaussian curvature	3-1; 3-2; 3-3	200	100 (top and bottom) 95 (middle) 252.5 m (vertical)	100

S235 steel is used for these shells. Young's modulus is 210 000 MPa and Poisson's ratio is 0.3. To focus on the buckling in the middle of the shell, the bottom support is completely fixed, and the translations in x and y directions and the rotations of all three directions of the top support are fixed. The top support is free in the z direction only.

The axial compression is applied as a vertical line load (2000 kN/m) on the top edge of the shell. The radial loads are applied as uniform out-of-plane pressure on the shell surface and their values are determined to make the membrane forces in axial and circumferential directions to be similar. The radial load values are shown in table 3.1.2 below. The determination of these radial load values involves calculations conducted using Maple (Appendix 1), followed by validation through linear elastic analysis in SCIA Engineer. Should the calculated values not meet the aforementioned condition of similarity in membrane forces, minor adjustments are made iteratively until the required condition is fulfilled.

Table 3.1.2 Radial Loads

Model	1-1	1-2	1-3	2-1	2-2	2-3	3-1	3-2	3-3
Radial Load [kN/m ²]	0	-20	20	0	-27	10	0	-12	32.5

3.1.2 Elements

The standard shell element in SCIA Engineer is used. The influence length of a cylinder shell is $2.4\sqrt{at}$, where a is the radius and t is the thickness[4]. The element size is set as 1/6 of the influence length. Using this formula, the element size should be 1.79 m for our model dimension.

3.2 Buckling analysis process

Firstly, a linear elastic analysis is performed to obtain the membrane force of the model. Then we need to do the linear buckling analysis to observe the buckling modes of the structure and obtain the buckling load factor. The critical membrane force can thus be calculated by the membrane force obtained above multiplied with the buckling load factor. Finally we can estimate the ultimate load by multiplying the critical buckling load with the knockdown factor.

This estimation of the ultimate load can be verified by the geometrical nonlinear analysis of the structure, during which the initial imperfection is set as the first buckling mode and the amplitude is chosen as the thickness of shell.

Comparing the results of these two method, we can verify the knockdown factor formula.

4 Linear buckling analysis

In this chapter, the radial loads of the models (model 1-2, 1-3, 2-2, 2-3, 3-2 and 3-3) are set to make the membrane forces of the axial and circumferential directions similar in the area where buckling occurs. Linear buckling analyses of the 9 shell models are performed and the first buckling mode is shown in Figure 4.1.1. The membrane forces in the table occur near the middle height of the shells, where the points buckles most.

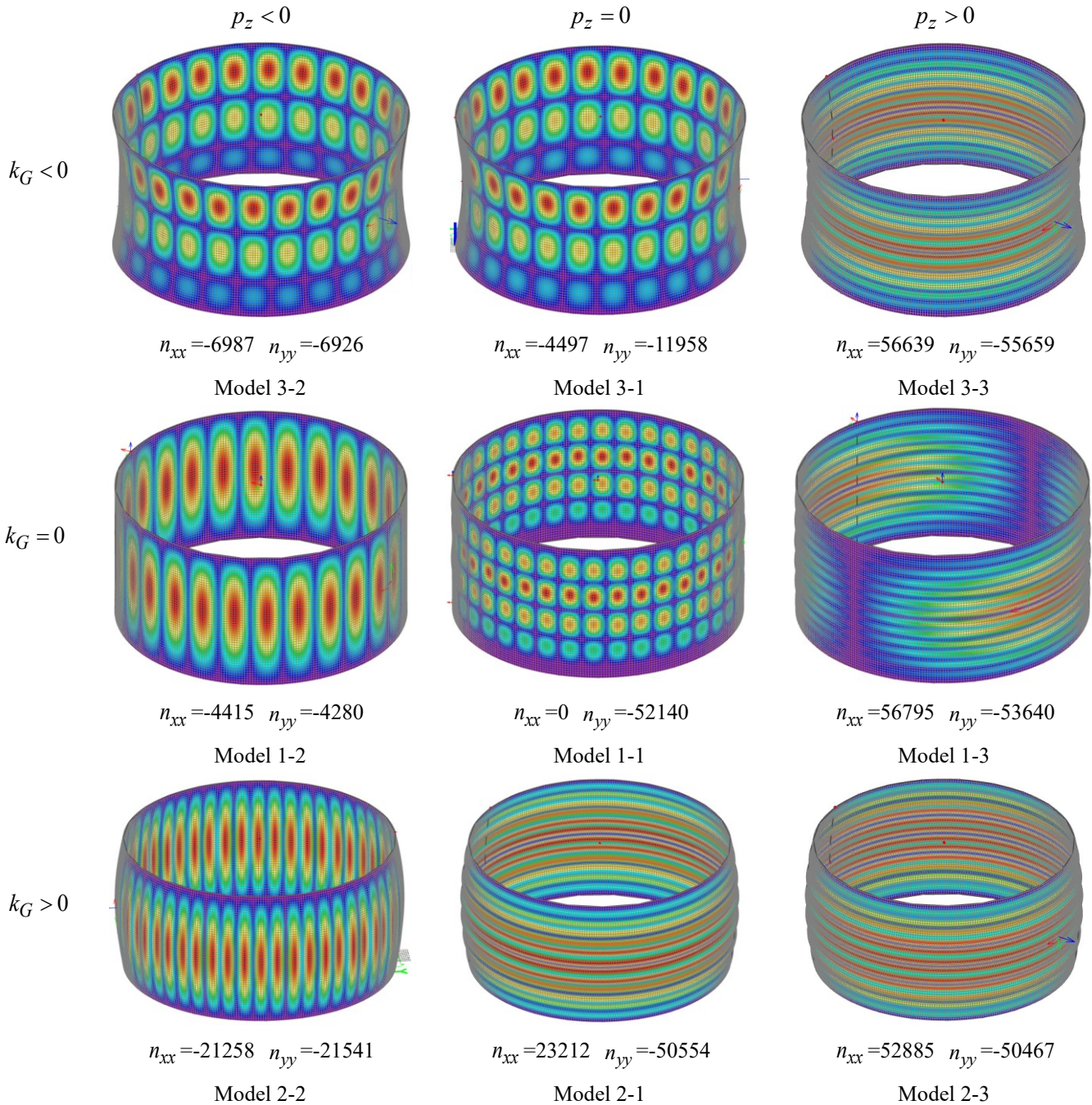


Figure 4.1.1 The 1st buckling mode of the 9 shell structures (element size 1.79 m)

From the figures above we can notice that the ring and column pattern occurs in model 1-1, model 3-1 and model 3-2. The column buckling mode develops in models 1-2 and 2-2. A special half ring buckling mode occur in model 1-3, which will be analyzed in detail in Chapter 5. In the other models, the ring buckling pattern develops.

In Figure 4.1.1, the membrane forces labeled under the buckling mode images refer to the critical membrane forces. They are calculated by multiplying the membrane forces obtained from the linear elastic analyses with the buckling load factors acquired from the linear buckling analyses. Taking the calculation of the critical membrane force in the axial direction, n_{yy} , for model 1-1 as an example, the membrane force in the axial direction obtained from the linear elastic analysis for model 1-1 is -2000 kN/m. The buckling load factor derived from the linear buckling analysis is 26.07. Therefore, the critical membrane force, n_{cry} , in the axial direction for model 1-1 is $-2000 \times 26.07 = -52140$ kN/m. The distributions of membrane forces in the axial and circumferential directions for the 9 models, obtained from the linear elastic analysis, are shown below.

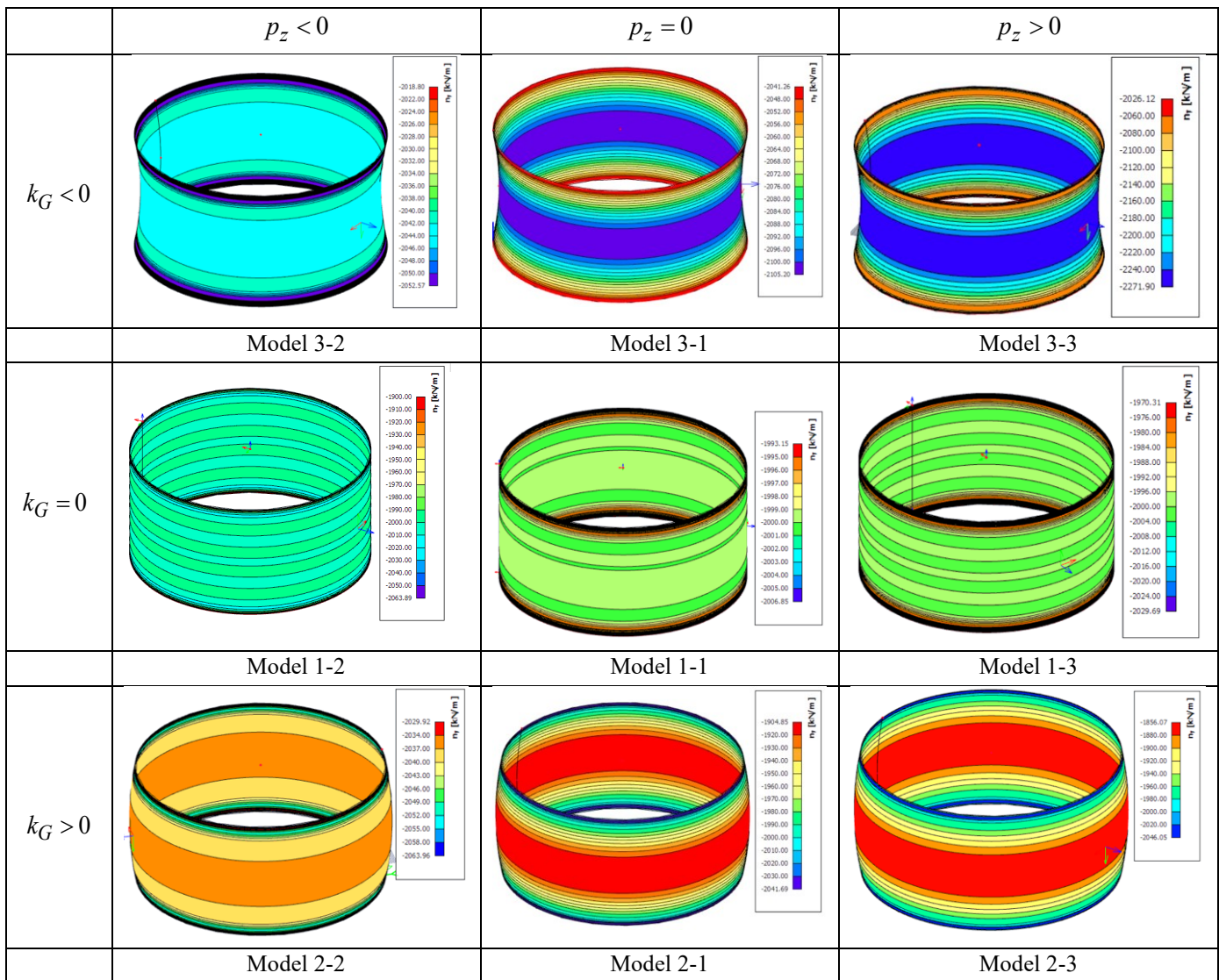


Figure 4.1.2 Membrane force distribution in the axial direction obtained from linear elastic analysis

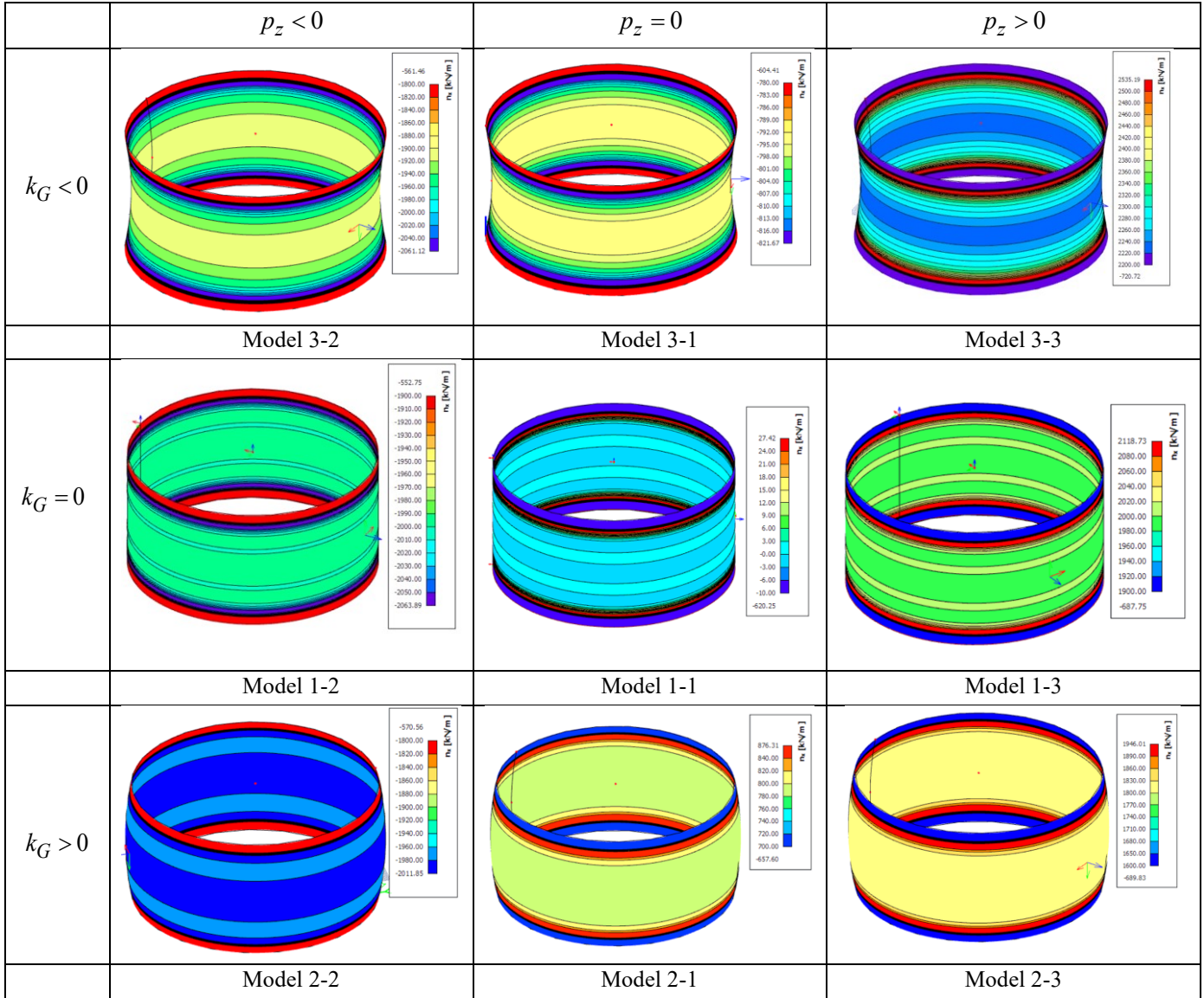


Figure 4.1.3 Membrane force distribution in the circumferential direction obtained from linear elastic analysis

With the membrane forces that we obtain from linear elastic analysis and the buckling load factor from the linear buckling analysis, we can get the critical membrane force. With the shell buckling formula (4.1) [1], we can also get the critical membrane force, with which we can better understand the buckling phenomenon of the 9 shell structures and we can verify the critical membrane force we obtain above.

$$n_{cr} \approx -0.6 \frac{Et^2}{a} \quad (4.1)$$

Table 4.1.1 Critical membrane force in the axial direction from buckling formula and FEM analysis. This analysis is valid for models 1-1, 1-3, 2-1, 2-3 and 3-3 only. (element size 1.79m)

	radius a_x [m]	n_{cry} [kN/m] (Buckling formula)	n_y (FEM)	λ_{cr} (FEM)	n_{cry} [kN/m] (FEM)
model 1-1	100.00	-50400.00	-2000.00	26.07	-52140.00
model 1-2	100.00	-50400.00	-2000.00	2.14	-4280.00
model 1-3	100.00	-50400.00	-2000.00	26.82	-53640.00
model 2-1	105.00	-48000.00	-1904.84	26.54	-50554.45
model 2-2	105.00	-48000.00	-2036.00	10.58	-21540.88
model 2-3	105.00	-48000.00	-1856.07	27.19	-50466.54
model 3-1	95.00	-53052.63	-2105.20	5.68	-11957.54
model 3-2	95.00	-53052.63	-2043.00	3.39	-6925.77
model 3-3	95.00	-53052.63	-2271.91	24.93	-56638.72

Table 4.1.2 Critical membrane force in the circumferential direction from buckling formula and FEM analysis. This analysis is valid for models 1-1 and 2-2 only. (element size 1.79m)

	radius a_y [m]	n_{crx} [kN/m] (Buckling formula)	n_x (FEM)	λ_{cr} (FEM)	n_{crx} [kN/m] (FEM)
model 1-1	∞	0.00	0.00	26.07	0.00
model 1-2	∞	0.00	-2063.00	2.14	-4414.82
model 1-3	∞	0.00	2117.65	26.82	56795.37
model 2-1	252.50	-19960.40	874.60	26.54	23211.88
model 2-2	252.50	-19960.40	-2009.29	10.58	-21258.29
model 2-3	252.50	-19960.40	1945.01	27.19	52884.82
model 3-1	252.50	-19960.40	-791.85	5.68	-4497.71
model 3-2	252.50	-19960.40	-2061.19	3.39	-6987.43
model 3-3	252.50	-19960.40	2232.60	24.93	55658.72

From Table 4.1.1, it is clear that for models 1-1 (ring and column buckling pattern), 1-3 (ring buckling pattern), 2-1 (ring buckling pattern), 2-3 (ring buckling pattern) and 3-3 (ring buckling pattern), the critical membrane forces in the axial direction that we obtain from linear buckling analysis and linear elastic analysis are similar to those we obtain from the buckling formula. From Table 4.1.2, it can be noticed that for models 1-1 (ring and column buckling pattern), 2-2 (column buckling pattern), the critical membrane forces in the circumferential direction that we obtain from linear buckling analysis and linear elastic analysis are similar to those we obtain from the buckling formula.

For models 1-2 (perfect cylinder: axial and radial compression), 2-2 (positive Gaussian curvature cylinder: axial and radial compression), 3-1 (negative Gaussian curvature cylinder: axial compression) and 3-2 (negative Gaussian curvature cylinder: axial and radial compression), it's obvious that the buckling load factor is much lower than others. The buckling behavior of shell structures is complex and influenced by multiple factors such as geometry, boundary conditions, and material properties. In the given models,

different characteristics lead to variations in the buckling load factor.

For model 2-2, the low buckling load factor is due to the occurrence of the column buckling pattern. In a cylinder with positive Gaussian curvature (model 2-2) under axial and radial compression, the column buckling pattern can dominate. This is because the geometry and loading conditions may be such that the structure behaves more like a column in terms of buckling. Column buckling typically has a lower critical load compared to shell buckling in some cases. When the structure buckles in a column-like manner, the load-carrying capacity is reduced, resulting in a lower buckling load factor. For models 1-2, 3-1 and 3-2, the low buckling load factor means that the third mode for in-extensional buckling is occurring [1]. In a perfect cylinder (model 1-2 under axial and radial compression) or negative Gaussian curvature cylinders (model 3-1 under axial compression and model 3-2 under axial and radial compression), in-extensional buckling can occur. In this type of buckling, the loads are carried mostly by bending instead of membrane forces. Since membrane forces usually contribute significantly to the load-carrying capacity of shells, when the load is carried mainly by bending, the overall load-carrying capacity is reduced, leading to a lower buckling load factor. Also, the critical membrane forces obtained from linear buckling analysis and linear elastic analysis being smaller than those from the buckling formula further supports the occurrence of in-extensional buckling and its impact on reducing the load-carrying capacity.

We can conclude that:

- 1) When ring buckling pattern occurs (models 1-3, 2-1, 2-3 and 3-3), the critical membrane forces in the axial direction that we obtain from the linear elastic analysis and the linear buckling analysis are similar to those we obtain from the buckling formula.
- 2) When the column buckling pattern occurs (2-2), the critical membrane forces in the circumferential direction that we obtain from linear buckling analysis and linear elastic analysis are similar to those we obtain from the buckling formula.
- 3) When the ring and column buckling pattern is observed (model 1-1), the critical membrane forces in both the axial and circumferential directions that we obtain from the FEM analysis will be similar to those we obtain from the buckling formula.
- 4) When the in-extensional buckling pattern occurs (models 1-2, 3-1 and 3-2), the critical membrane forces in both the axial and circumferential directions that we obtain from the FEM analysis is much smaller than those we obtain from the buckling formula.

And the similarity between the FEM results and the results obtained from the buckling formula further proves that the FEM models are reliable.

5 Parameter study of linear analysis

5.1 Element size study

The influence length (the distance from one point of zero deflection to the next point of zero deflection) can be used to choose a finite element mesh. The influence length of a cylinder shell is $2.4\sqrt{a t}$, where a is the radius and t is the thickness. We need at least 6 elements in the influence length in order to do the analysis with some accuracy. According to Table 3.1.1, the radius of our initial model is 100 m and the thickness is 0.2 m. Then the elements size should be 1.79 m.

However, when the element size $0.4\sqrt{a t} = 1.79$ m is used, for some models (1-3, 2-1, 2-3, 3-3) there are less than 6 elements in the buckling length, which might lead to an inaccurate result. So the parameter study of element size is carried out and models with an element size of $0.2\sqrt{a t} = 0.895$ m and $0.15\sqrt{a t} = 0.671$ m are analyzed.

5.1.1 Element size: 0.895 m

The first buckling modes of the 9 models with the element size of 0.895 m are shown in Figure 5.1.1.1. As before, the membrane forces shown in the figure are near the middle height of the shells, where the shells buckle most.

Comparing Figure 5.1.1.1 with Figure 4.1.1, it can be noticed that for most models, the 1st buckling mode shapes just have some slight changes with a smaller element size. The only one that has a remarkable change is model 1-3, which has a so-called half ring buckling pattern in the previous analysis with an element size of 1.790 m. However, when the element size is 0.895 m, its buckling pattern will become a complete ring buckling pattern. As mentioned before, the model 1-3 has less than 6 elements in the buckling length with an element size of 1.79 m, thus we can conclude that a smaller element size can indeed improve the accuracy of model 1-3 and the requirement of at least 6 elements in the buckling length is necessary.

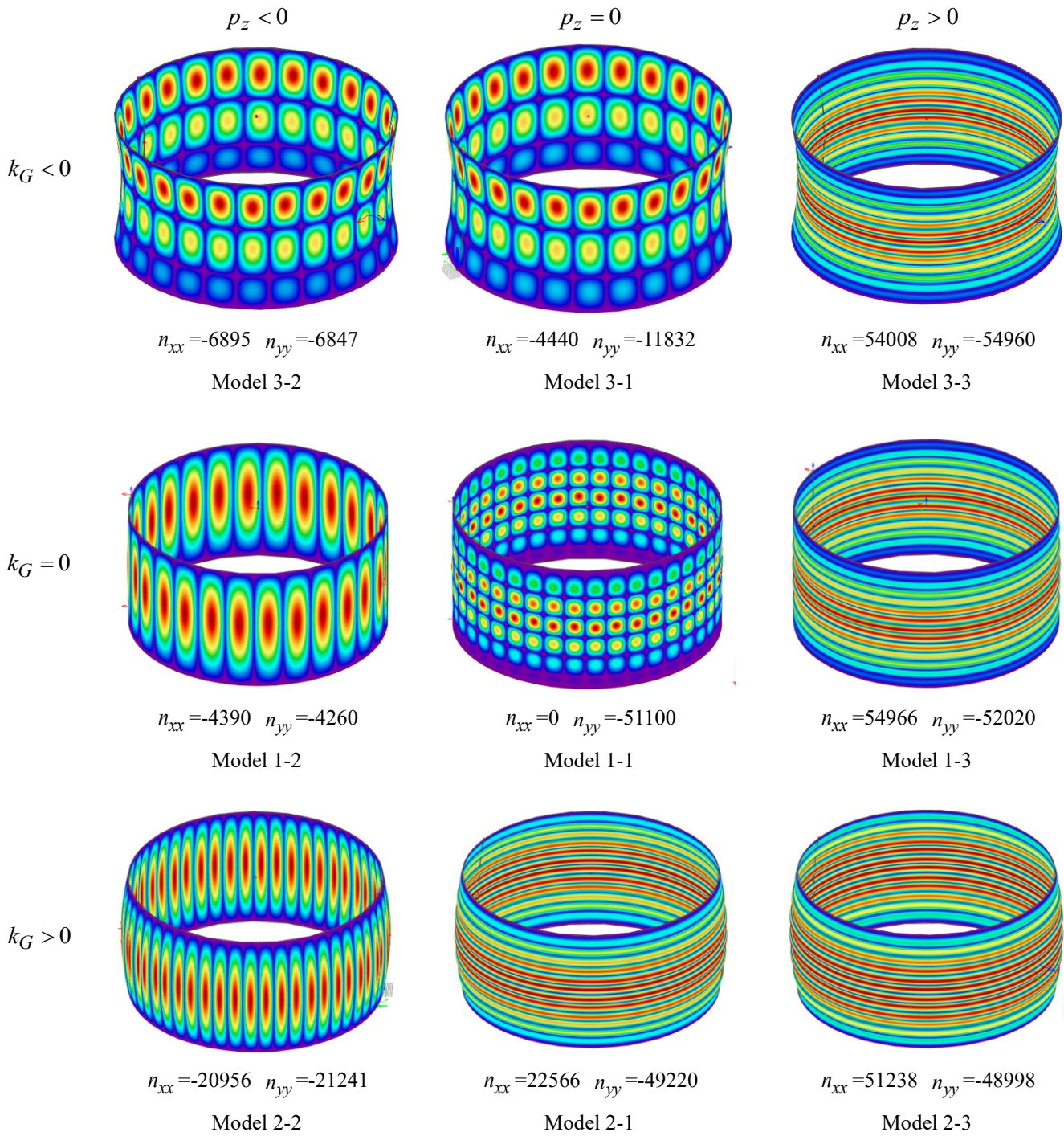


Figure 5.1.1.1 The 1st buckling mode of the 9 shell structures (element size 0.895m)

The distributions of membrane forces in the axial and circumferential directions for the 9 models, obtained from the linear elastic analysis, are shown below.

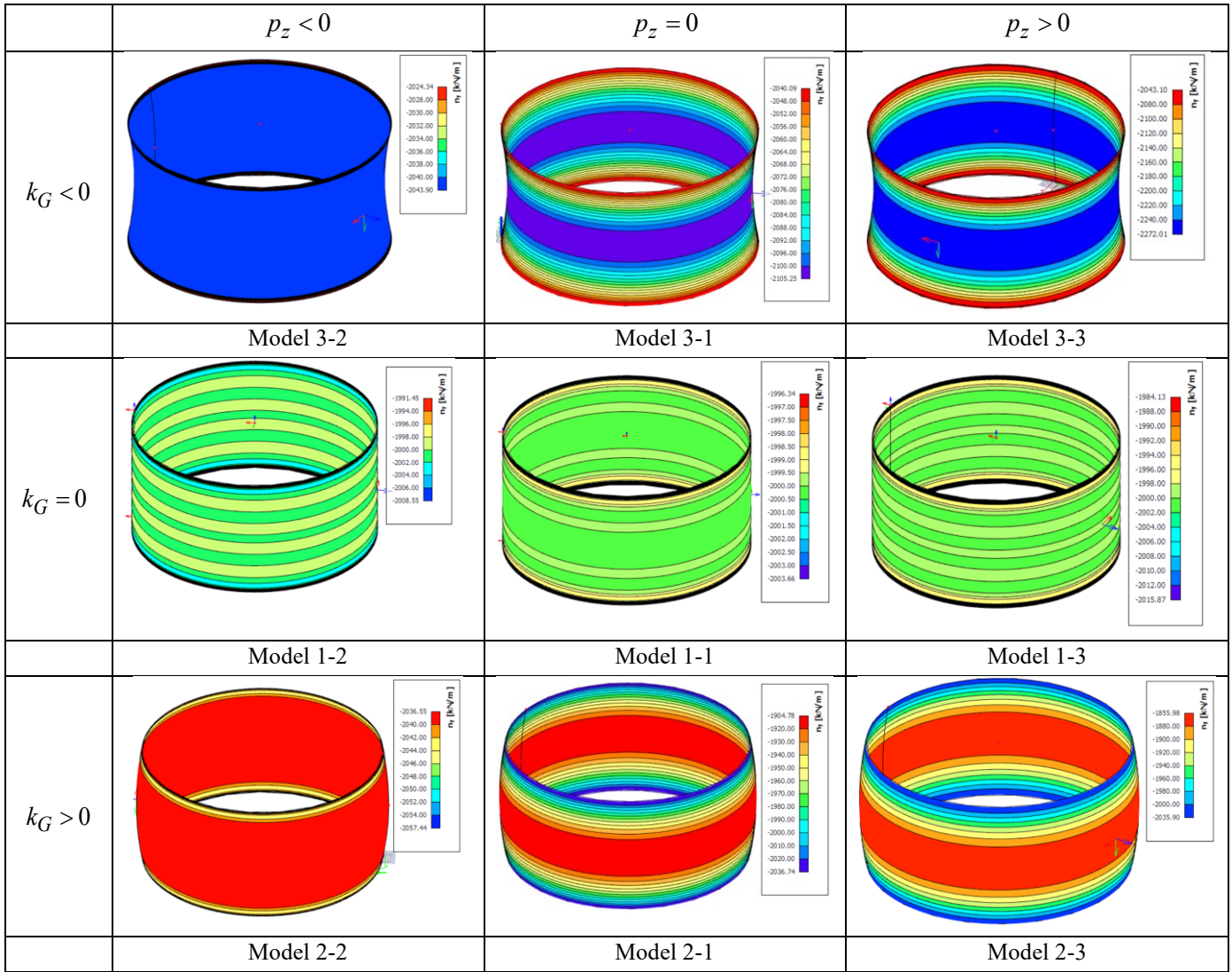


Figure 5.1.1.2 Membrane force distribution in the axial direction obtained from linear elastic analysis

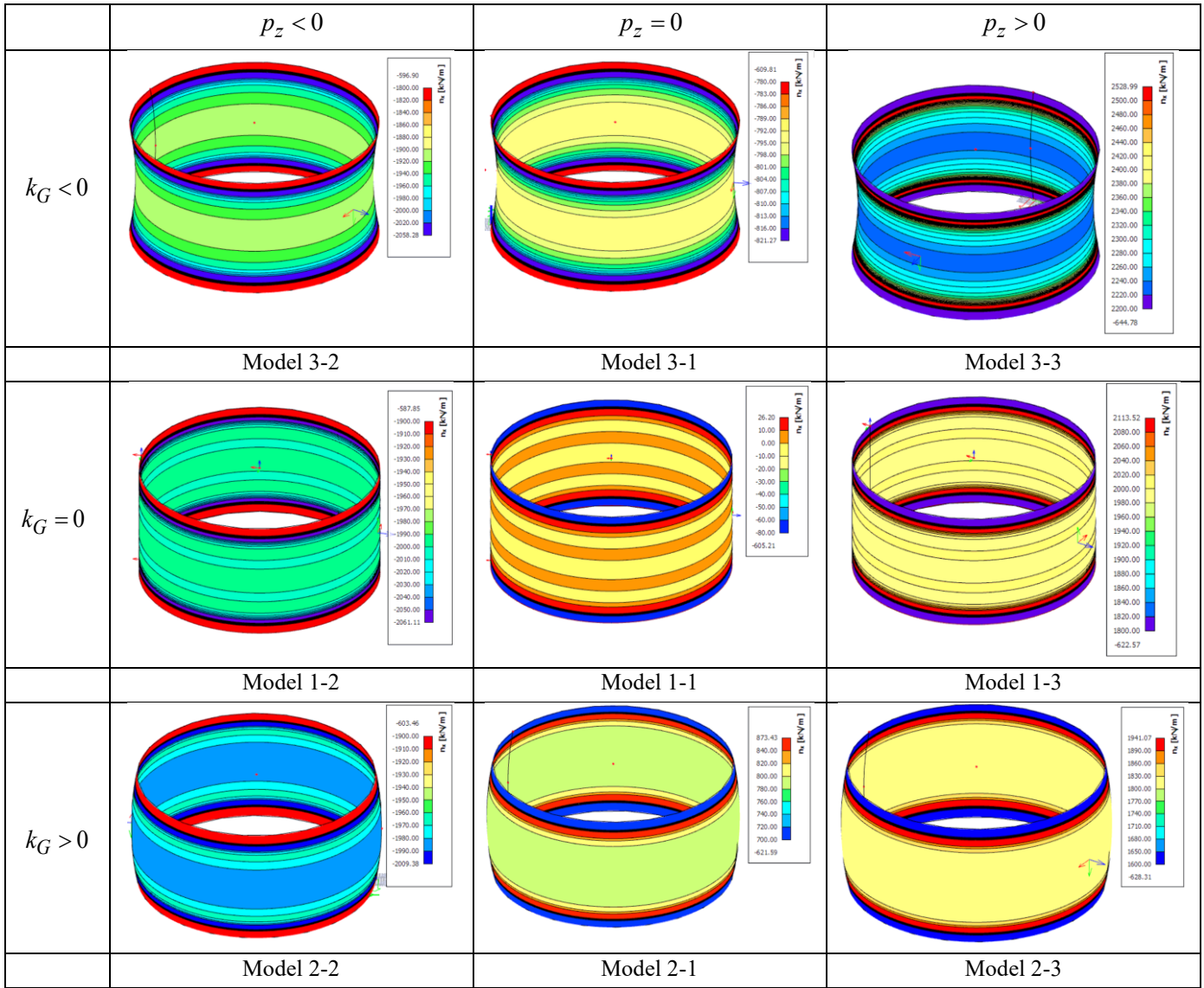


Figure 5.1.1.3 Membrane force distribution in the circumferential direction obtained from linear elastic analysis

The critical membrane forces of the axial directions and the circumferential directions from the buckling formula and the FEM analysis with the element size of 0.895 m are as follows.

Table 5.1.1.1 Critical membrane force in the axial direction from buckling formula and FEM analysis
(element size 0.895m)

	radius a_x [m]	n_{cry} [kN/m] (Buckling formula)	n_y (FEM)	λ_{cr} (FEM)	n_{cry} [kN/m] (FEM)	% Difference from Chapter 4
model 1-1	100.00	-50400.00	-2000.00	25.55	-51100.00	-1.99%
model 1-2	100.00	-50400.00	-2000.00	2.13	-4260.00	-0.47%
model 1-3	100.00	-50400.00	-2000.00	26.01	-52020.00	-3.02%
model 2-1	105.00	-48000.00	-1904.78	25.84	-49219.52	-2.64%
model 2-2	105.00	-48000.00	-2036.55	10.43	-21241.22	-1.39%
model 2-3	105.00	-48000.00	-1855.98	26.40	-48997.87	-2.91%
model 3-1	95.00	-53052.63	-2105.25	5.62	-11831.51	-1.05%
model 3-2	95.00	-53052.63	-2043.90	3.35	-6847.07	-1.14%
model 3-3	95.00	-53052.63	-2272.01	24.19	-54959.92	-2.96%

Table 5.1.1.2 Critical membrane force in the circumferential direction from buckling formula and FEM
analysis (element size 0.895m)

	radius a_y [m]	n_{crx} [kN/m] (Buckling formula)	n_x (FEM)	λ_{cr} (FEM)	n_{crx} [kN/m] (FEM)	% Difference from Chapter 4
model 1-1	∞	0.00	0.00	25.55	0.00	0.00%
model 1-2	∞	0.00	-2060.97	2.13	-4389.87	-0.57%
model 1-3	∞	0.00	2113.25	26.01	54965.63	-3.22%
model 2-1	252.50	-19960.40	873.28	25.84	22565.56	-2.78%
model 2-2	252.50	-19960.40	-2009.24	10.43	-20956.37	-1.42%
model 2-3	252.50	-19960.40	1940.83	26.40	51237.91	-3.11%
model 3-1	252.50	-19960.40	-790.00	5.62	-4439.80	-1.29%
model 3-2	252.50	-19960.40	-2058.13	3.35	-6894.74	-1.33%
model 3-3	252.50	-19960.40	2232.65	24.19	54007.80	-2.97%

Compared Table 5.1.1.1 and 5.1.1.2 with Table 4.1.1 and 4.1.2, it can be noticed that critical membrane forces and the buckling load factors that we obtained from the models of a element size of 0.895 m are similar to those we obtained from the models of a element size of 1.79 m, with a difference of less than 5%.

Therefore, we can conclude that the formula $2.4\sqrt{a t}$ for the influence length is useful for most cases, although an extra check is needed to ensure there are at least 6 elements in an influence length, and a smaller element size may be required when there are less than 6 elements in the influence length.

5.1.2 Element size: 0.671 m

There are slight differences between the buckling modes with an element size of $0.4\sqrt{a t}$ and those with an element size of $0.2\sqrt{a t}$. For example, according to Figure 4.1.1, the model 1-1 has 4 rows of ‘chess’ when the element size is $0.4\sqrt{a t}$, but it has 5 rows of ‘chess’ with an element size of $0.2\sqrt{a t}$ in Figure 5.1.1.1. Another example is the model 2-2, the buckles of which in Figure 5.1.1.1 are mostly identical, while in Figure

4.1.1, it can be noticed that some buckles of model 2-2 are deep and others are light. Based on these differences, the analysis with an even smaller element size, $0.15\sqrt{(a t)} = 0.671$ m is carried out to check whether the results from the element size of $0.2\sqrt{(a t)}$ are accurate or not.

The first buckling modes of the 9 models with the element size of 0.671 m are as follows. The membrane forces below are near the middle height of the shells, where the points buckles most.

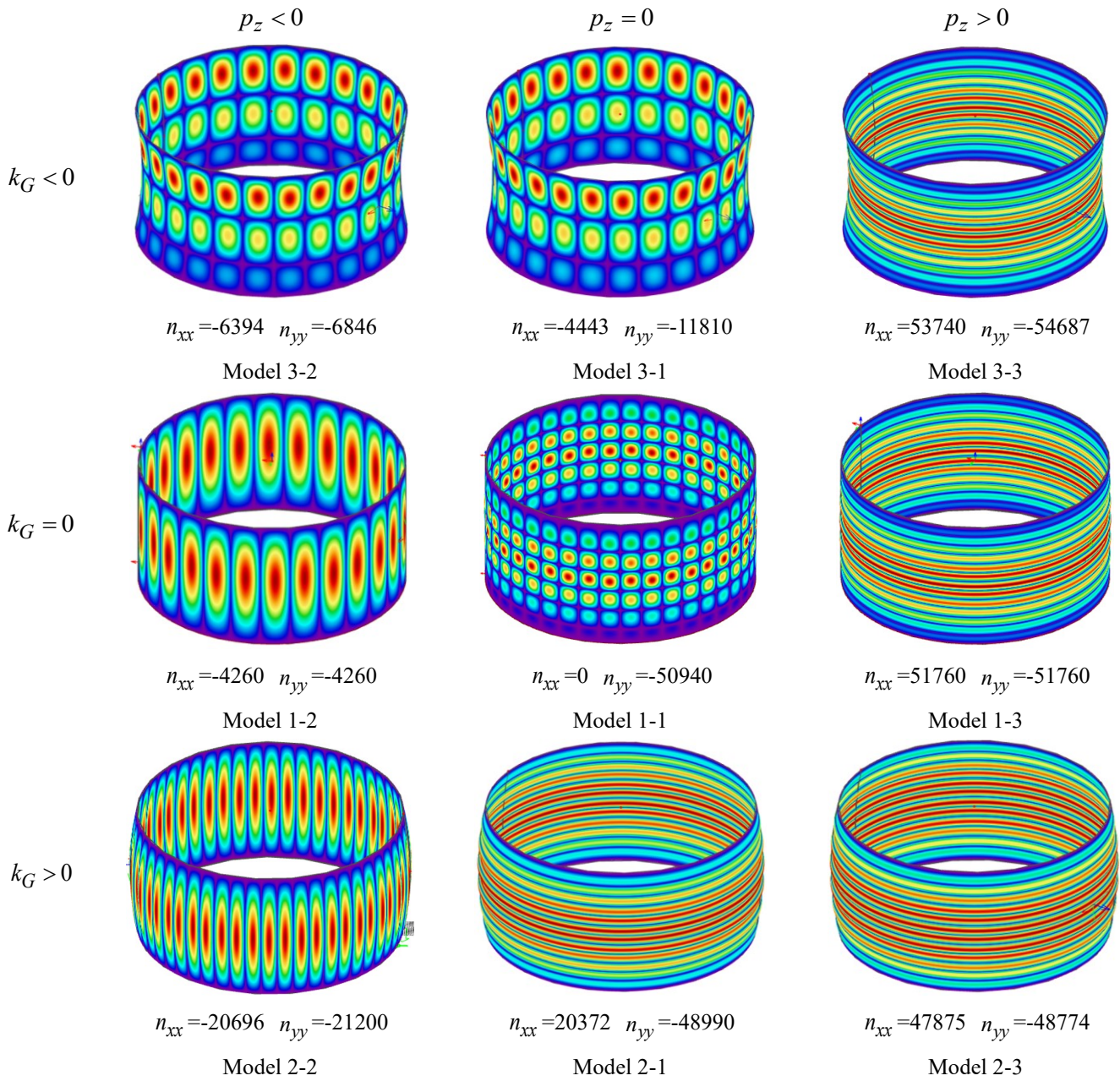


Figure 5.1.2.1 The 1st buckling mode of the 9 shell structures (element size 0.671m)

It is obvious that the buckling modes in Figure 5.1.2.1 are very similar to those in Figure 5.1.1.1.

The distributions of membrane forces in the axial and circumferential directions for the 9 models, obtained from the linear elastic analysis, are shown below.

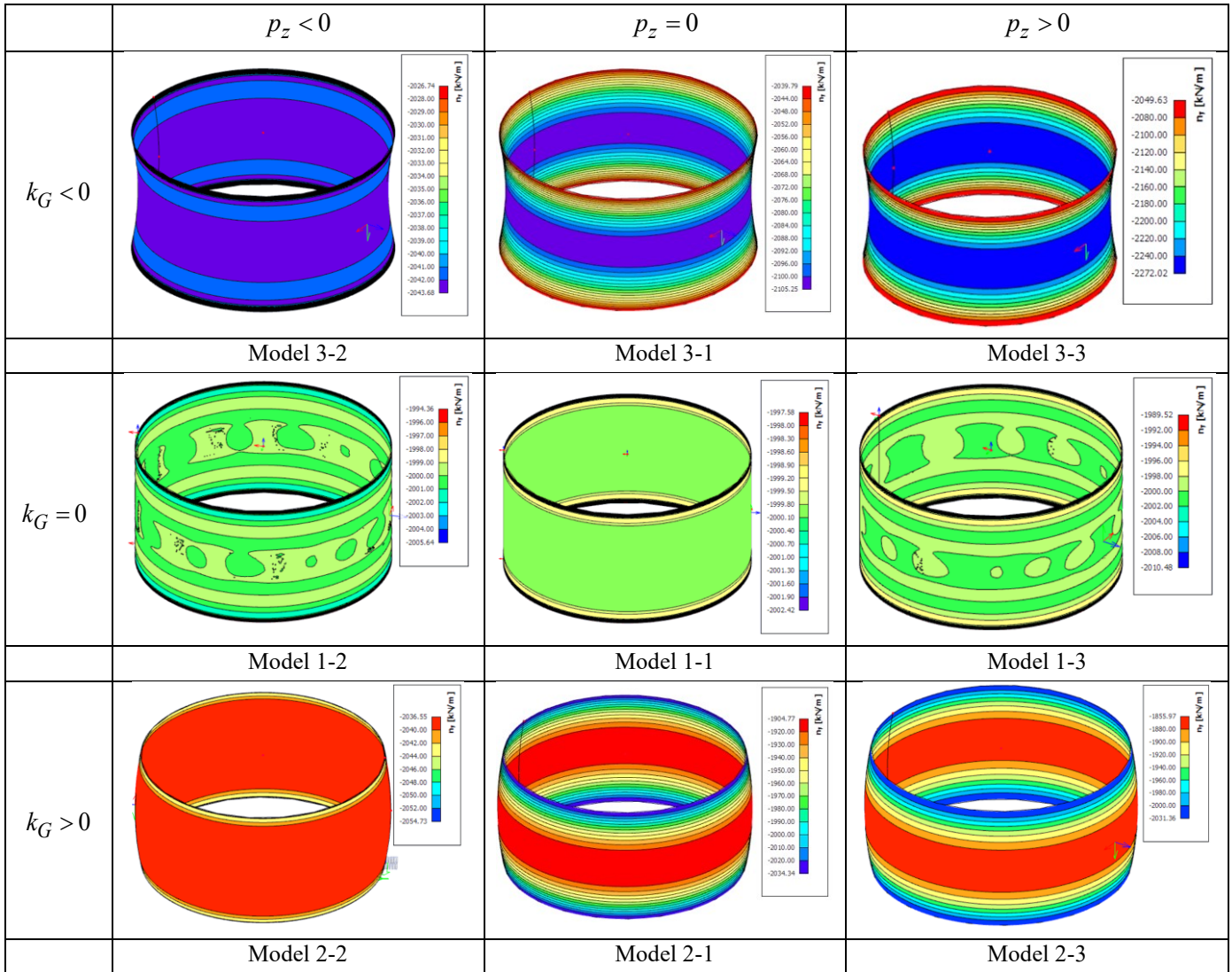


Figure 5.1.2.2 Membrane force distribution in the axial direction obtained from linear elastic analysis

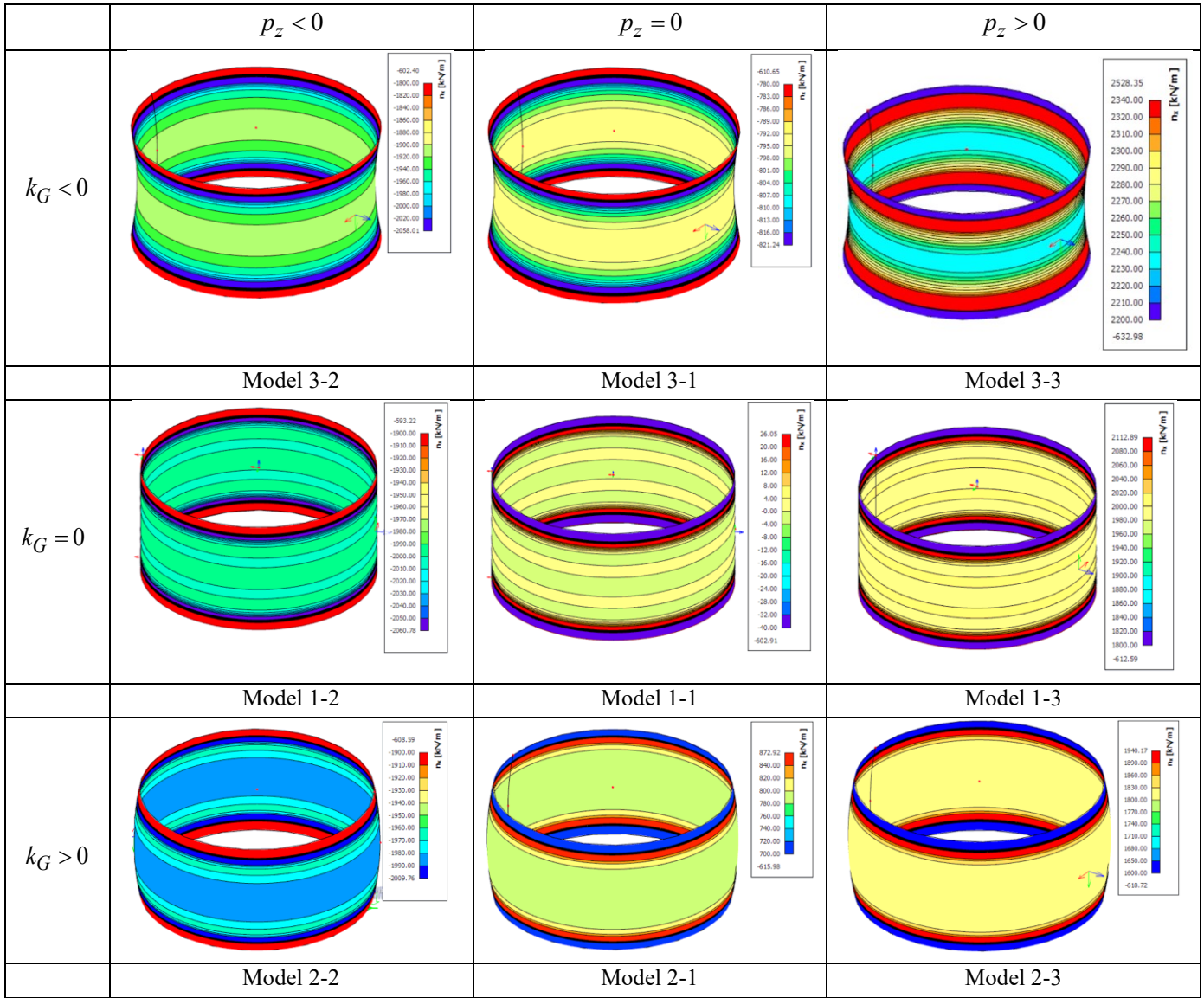


Figure 5.1.2.3 Membrane force distribution in the circumferential direction obtained from linear elastic analysis

The critical membrane forces of the axial directions and the circumferential directions from the buckling formula and the FEM analysis with the element size of 0.671 m are as follows.

Table 5.1.2.1 Critical membrane force in the axial direction from buckling formula and FEM analysis
(element size 0.671m)

	radius a_x [m]	n_{cry} [kN/m] (Buckling formula)	n_y (FEM)	λ_{cr} (FEM)	n_{cry} [kN/m] (FEM)	% Difference from subsection 5.1.1
model 1-1	100.00	-50400.00	-2000.00	25.47	-50940.00	-0.31%
model 1-2	100.00	-50400.00	-2000.00	2.13	-4260.00	0.00%
model 1-3	100.00	-50400.00	-2000.00	25.88	-51760.00	-0.50%
model 2-1	105.00	-48000.00	-1904.77	25.72	-48990.68	-0.46%
model 2-2	105.00	-48000.00	-2036.55	10.41	-21200.49	-0.19%
model 2-3	105.00	-48000.00	-1855.97	26.28	-48774.89	-0.46%
model 3-1	95.00	-53052.63	-2105.26	5.61	-11810.51	-0.18%
model 3-2	95.00	-53052.63	-2043.68	3.35	-6846.33	-0.01%
model 3-3	95.00	-53052.63	-2272.02	24.07	-54687.52	-0.50%

Table 5.1.2.2 Critical membrane force in the circumferential direction from buckling formula and FEM
analysis (element size 0.671m)

	radius a_y [m]	n_{crx} [kN/m] (Buckling formula)	n_x (FEM)	λ_{cr} (FEM)	n_{crx} [kN/m] (FEM)	% Difference from subsection 5.1.1
model 1-1	∞	0.00	0.00	25.47	0.00	0.00%
model 1-2	∞	0.00	-2000.00	2.13	-4260.00	-2.96%
model 1-3	∞	0.00	2000.00	25.88	51760.00	-5.83%
model 2-1	252.50	-19960.40	792.07	25.72	20372.04	-9.72%
model 2-2	252.50	-19960.40	-1988.11	10.41	-20696.23	-1.24%
model 2-3	252.50	-19960.40	1821.76	26.28	47875.85	-6.56%
model 3-1	252.50	-19960.40	-792.07	5.61	-4443.51	0.08%
model 3-2	252.50	-19960.40	-1908.89	3.35	-6394.78	-7.25%
model 3-3	252.50	-19960.40	2232.66	24.07	53740.13	-0.50%

Compared Table 5.1.2.1 and 5.1.2.2 with Table 5.1.1.1 and 5.1.1.2, it can be noticed that the membrane forces obtained from the FEM analyses with an element size of 0.671m are similar to those with an element size of 0.895m. Based on the fact that the buckling patterns and the critical membrane forces are extremely similar to those in subsection 5.1.1, we can conclude that an element size of $0.2\sqrt{(a t)}$ is accurate for our analysis and there is no need to use smaller elements.

5.2 Model scale study

5.2.1 Half-scale model with unchanged load

Our initial model has a radius of 100 m and a thickness of 0.2 m. The element size, $0.4\sqrt{(a t)}$, is only related to the radius and thickness of the model. If the radius-to-thickness ratio is not changed, it was expected that scaling the model dimensions will not affect the result of our investigation. To demonstrate this, 9 models with the

following dimension were analyzed.

Table 5.2.1.1 Dimensions of the models

	Models	Thickness t [mm]	Radius a [m]	Height [m]
Perfect cylinder	1-1; 1-2; 1-3	100	50	50
nearly cylinder with positive Gaussian curvature	2-1; 2-2; 2-3	100	50 (top and bottom) 52.5 (middle)	50
nearly cylinder with negative Gaussian curvature	3-1; 3-2; 3-3	100	50 (top and bottom) 47.5 (middle)	50

The element size for this model is still $0.4\sqrt{at}$, which is 0.895 m. The radial and axial loads are the same as the loads in Chapter 4. The first buckling modes of the 9 models with the element size of 0.895 m are shown in figure 5.2.1.1. The membrane forces shown in the figure are near the middle height of the shells, where the points buckles most.

Comparing Figure 5.2.1.1 with Figure 4.1.1, the buckling patterns have changed in Figure 5.2.1.1. This is due to the fact that the scaling of the dimension makes the membrane forces of the axial and circumferential directions not similar anymore.

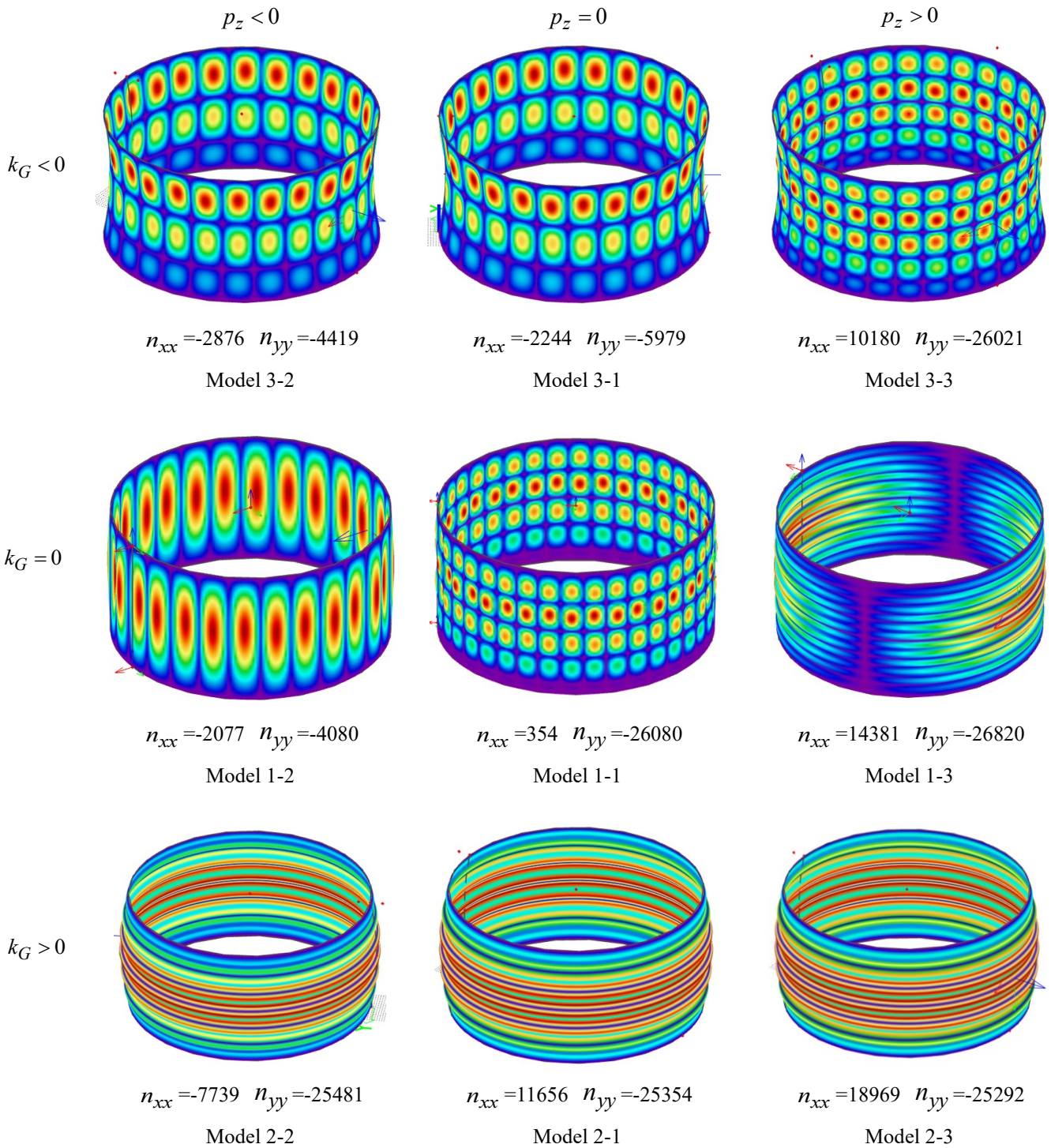


Figure 5.2.1.1 The 1st buckling mode of the 9 shell structures

The distributions of membrane forces in the axial and circumferential directions for the 9 models, obtained from the linear elastic analysis, are shown below.

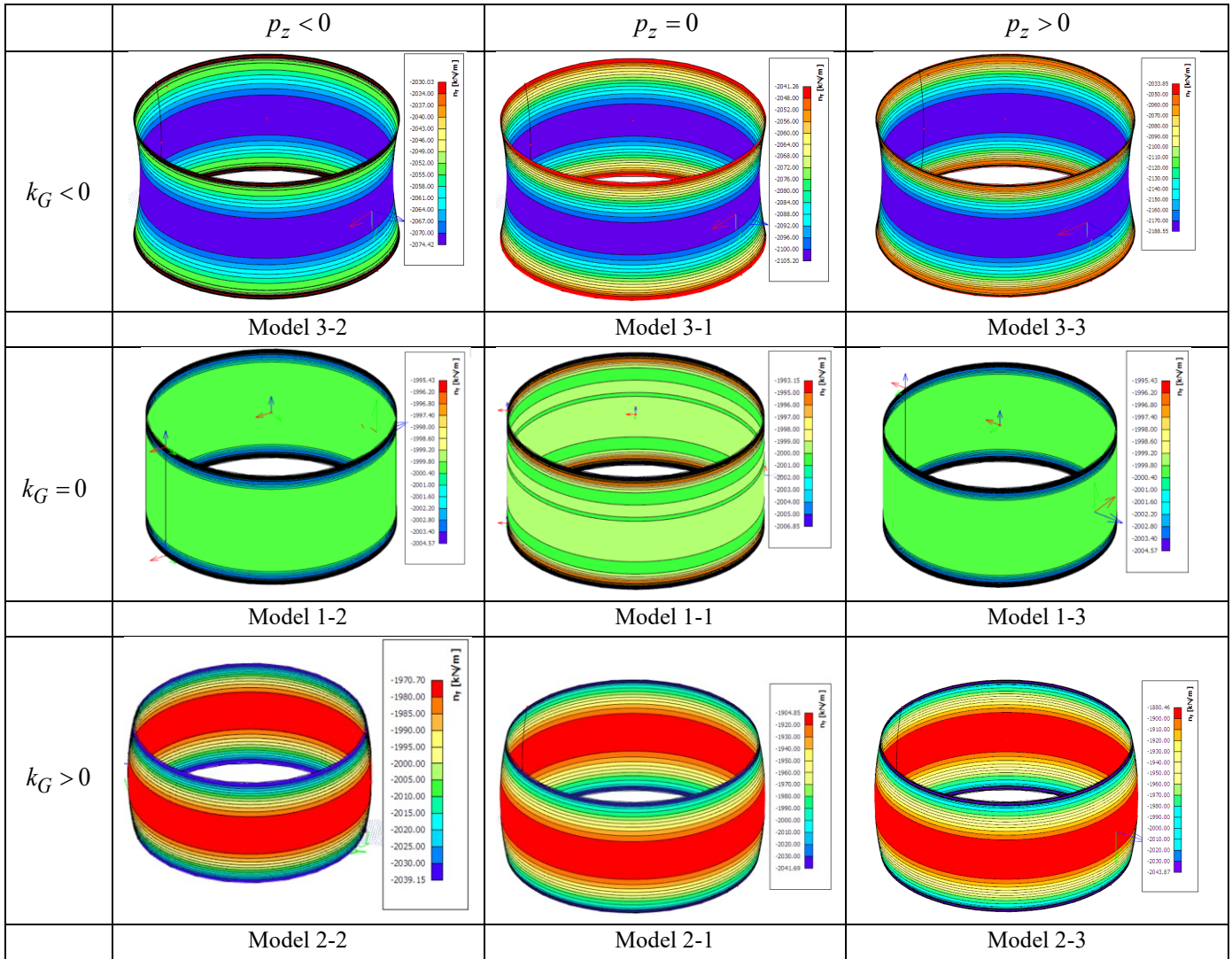


Figure 5.2.1.2 Membrane force distribution in the axial direction obtained from linear elastic analysis

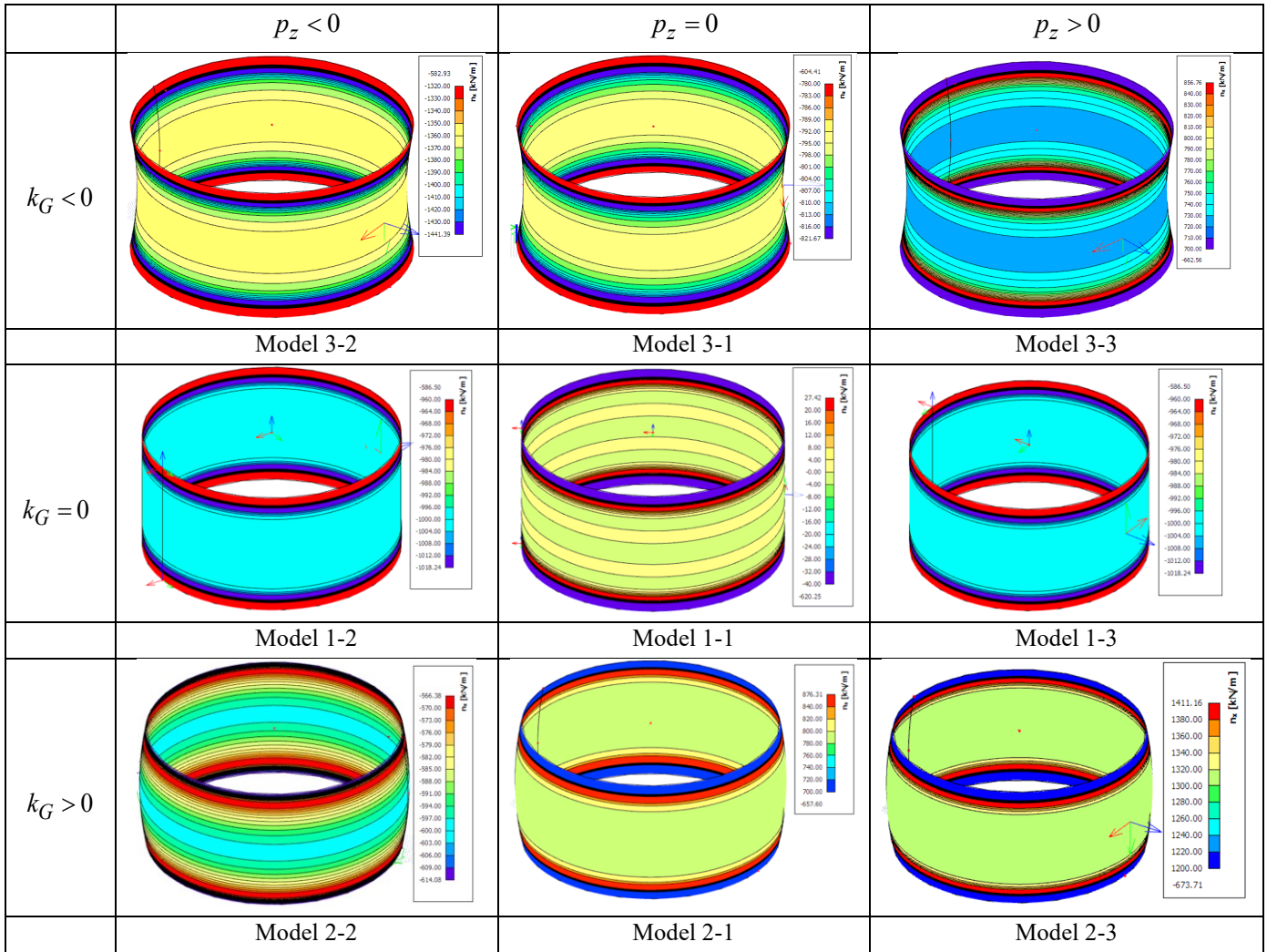


Figure 5.2.1.3 Membrane force distribution in the circumferential direction obtained from linear elastic analysis

The critical membrane forces of the axial directions and the circumferential directions from the buckling formula and the FEM analysis are as follows

Table 5.2.1.2 Critical membrane force in the axial direction from buckling formula and FEM analysis

	radius a_x [m]	n_{cry} [kN/m] (Buckling formula)	n_y (FEM)	λ_{cr} (FEM)	n_{cry} [kN/m] (FEM)	% Difference from Chapter 4
model 1-1	50.00	-25200.00	-2000.00	13.04	-26080.00	-49.98%
model 1-2	50.00	-25200.00	-2000.00	2.04	-4080.00	-4.67%
model 1-3	50.00	-25200.00	-2000.00	13.41	-26820.00	-50.00%
model 2-1	52.50	-24000.00	-1904.85	13.31	-25353.55	-49.85%
model 2-2	52.50	-24000.00	-1970.70	12.93	-25481.15	18.29%
model 2-3	52.50	-24000.00	-1880.46	13.45	-25292.19	-49.88%
model 3-1	47.50	-26526.32	-2105.20	2.84	-5978.77	-50.00%
model 3-2	47.50	-26526.32	-2074.42	2.13	-4418.51	-36.20%
model 3-3	47.50	-26526.32	-2188.55	11.89	-26021.86	-54.06%

Table 5.2.1.3 Critical membrane force in the circumferential direction from buckling formula and FEM analysis

	radius a_y [m]	n_{crx} [kN/m] (Buckling formula)	n_x (FEM)	λ_{cr} (FEM)	n_{crx} [kN/m] (FEM)	% Difference from Chapter 4
model 1-1	∞	0.00	0.00	13.04	0.00	0.00%
model 1-2	∞	0.00	-1018.07	2.04	-2076.86	-52.96%
model 1-3	∞	0.00	1072.40	13.41	14380.88	-74.68%
model 2-1	126.25	-9980.20	875.73	13.31	11655.97	-49.78%
model 2-2	126.25	-9980.20	-598.50	12.93	-7738.61	-63.60%
model 2-3	126.25	-9980.20	1410.37	13.45	18969.48	-64.13%
model 3-1	126.25	-9980.20	-790.00	2.84	-2243.60	-50.12%
model 3-2	126.25	-9980.20	-1350.00	2.13	-2875.50	-58.85%
model 3-3	126.25	-9980.20	856.16	11.89	10179.74	-81.71%

It can be noticed that most buckling load factors of Table 5.2.1.2 and 5.2.1.3 are about half of those of Table 4.1.1 and 4.1.2, which is logical based on the formula (4.1) since both the radius and the thickness have become half of the ones before.

5.2.2 Half-scale model with twice radial load and twice Young's modulus

In subsection 5.2.1, the buckling modes in Figure 5.2.1.1 are different with those in Figure 4.1.1, which is caused by the fact that the scaling of the dimension makes the membrane forces of the axial and circumferential directions not similar any more. Thus in this subsection the radial load is doubled to make the ratio of the axial and circumferential membrane forces to be the same as that in chapter 4.

The buckling load factors of Table 5.2.1.2 and Table 5.2.1.3 are about half of those of Table 4.1.1 and 4.1.2. This is logical since in formula (4.1) both the radius and the thickness are half of before. To obtain the same critical membrane force, the Young's modulus is also doubled in this subsection.

The dimension in this subsection is the same as that in subsection 5.2.1 and half of that in chapter 4. The axial load in this subsection is the same as that in subsection 5.2.1 and chapter 4. The element size is $0.4\sqrt{at}$, which is 0.895m. The first buckling modes of the 9 models with the element size of 0.895m are as follows. Again, the membrane forces below are near the middle height of the shells, where the points buckles most.

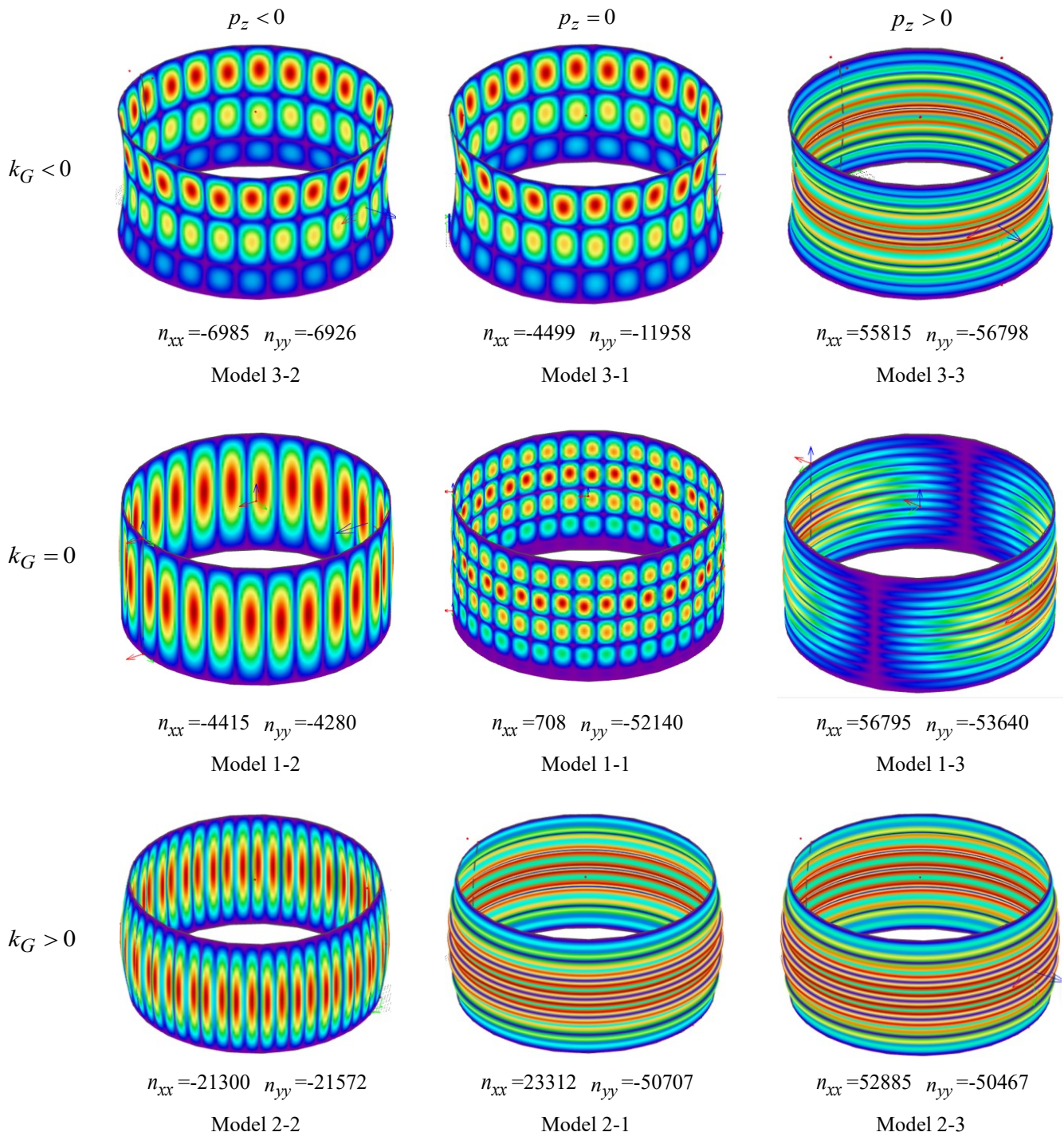


Figure 5.2.2.1 The 1st buckling mode of the 9 shell structures

Compared with Figure 4.1.1, the buckling patterns almost have not changed at all. Thus it can be concluded that the scale of the dimension will not affect the buckling patterns.

The distributions of membrane forces in the axial and circumferential directions for the 9 models, obtained from the linear elastic analysis, are shown below.

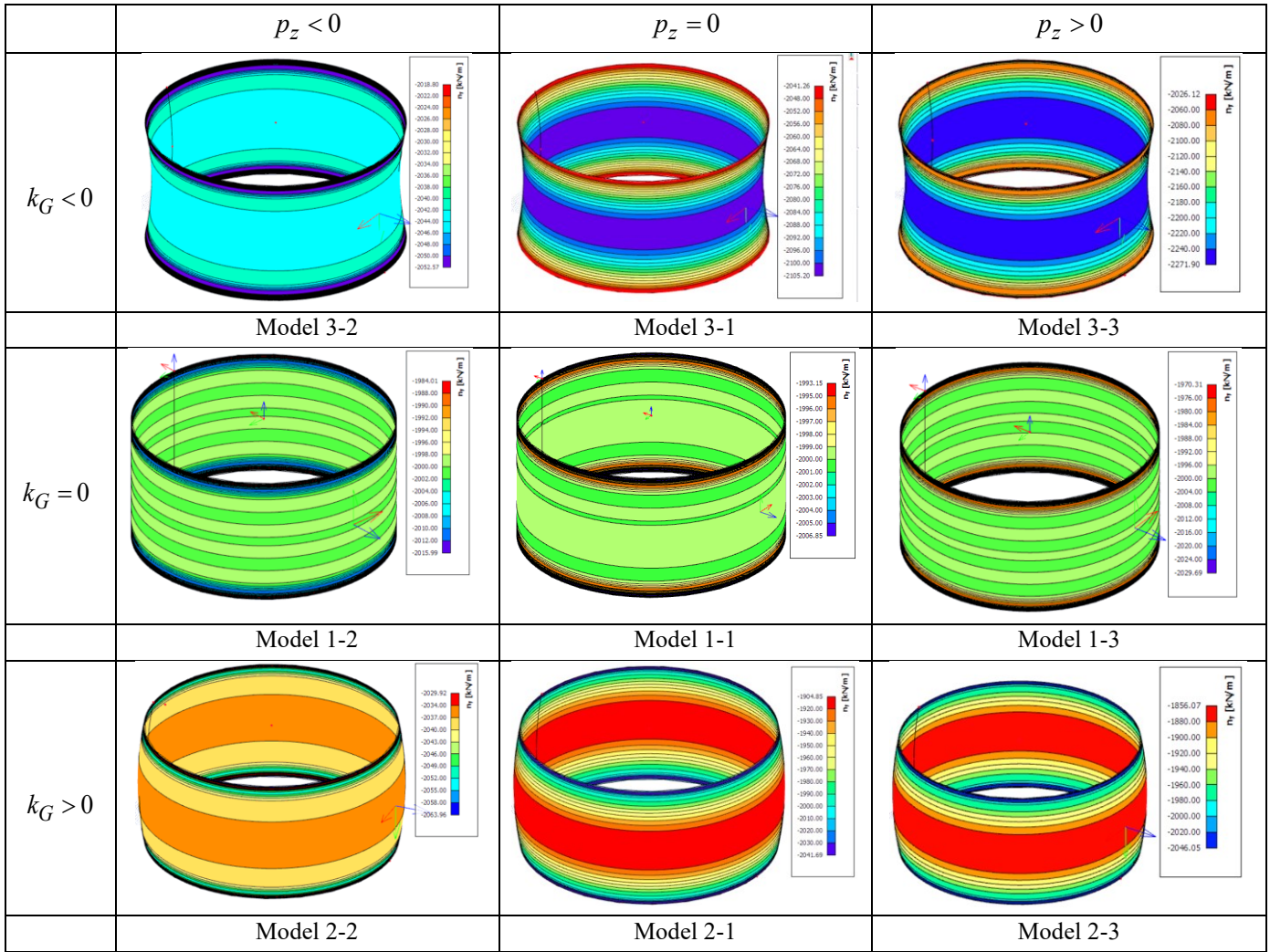


Figure 5.2.2.2 Membrane force distribution in the axial direction obtained from linear elastic analysis

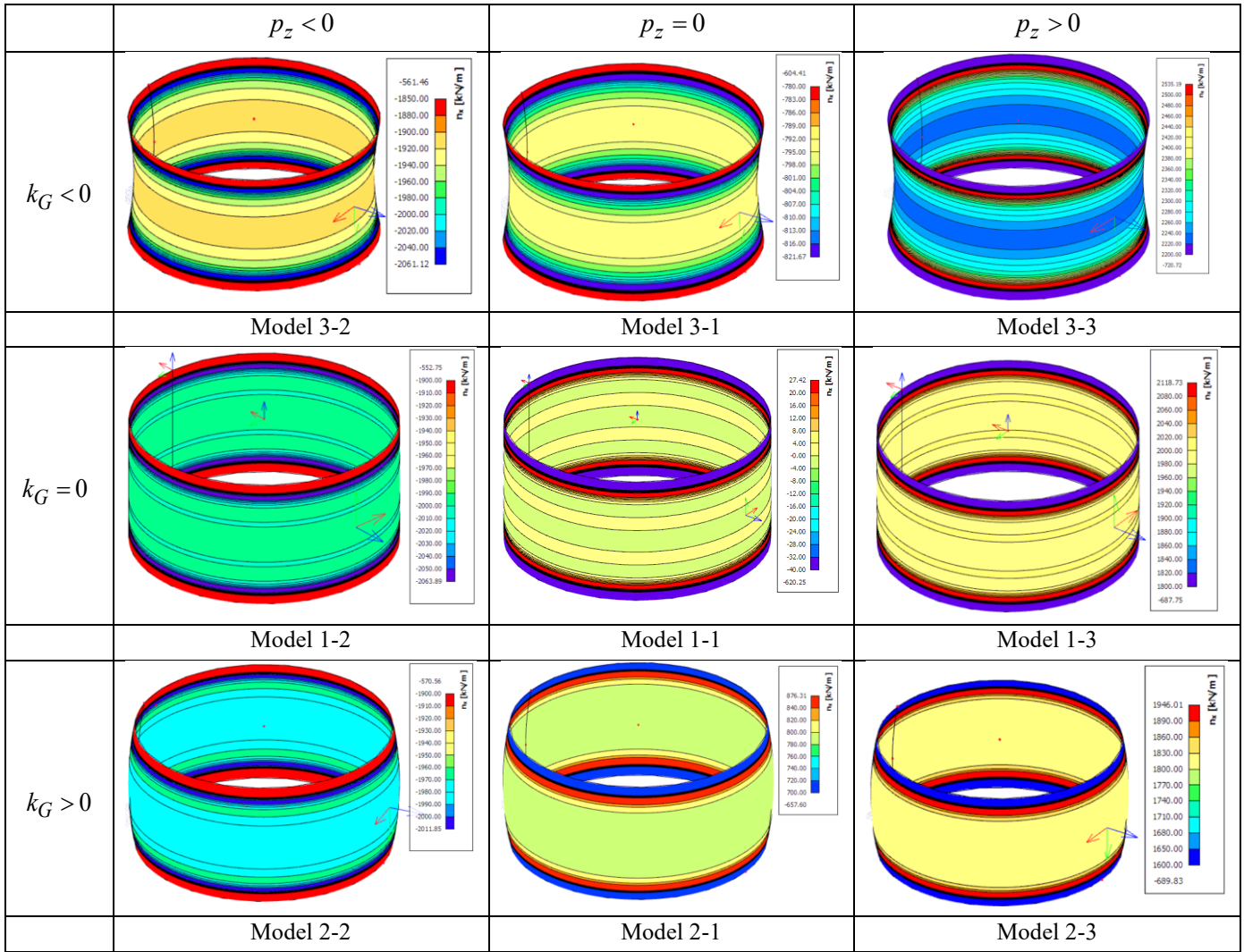


Figure 5.2.2.3 Membrane force distribution in the circumferential direction obtained from linear elastic analysis

The critical membrane forces of the axial directions and the circumferential directions from the buckling formula and the FEM analysis are as follows

Table 5.2.2.1 Critical membrane force in the axial direction from buckling formula and FEM analysis

	radius a_x [m]	n_{cry} [kN/m] (Buckling formula)	n_y (FEM)	λ_{cr} (FEM)	n_{cry} [kN/m] (FEM)	% Difference from Chapter 4
model 1-1	50.00	-50400.00	-2000.00	26.07	-52140.00	0.00%
model 1-2	50.00	-50400.00	-2000.00	2.14	-4280.00	0.00%
model 1-3	50.00	-50400.00	-2000.00	26.82	-53640.00	0.00%
model 2-1	52.50	-48000.00	-1904.85	26.62	-50707.11	0.00%
model 2-2	52.50	-48000.00	-2037.00	10.59	-21571.83	0.00%
model 2-3	52.50	-48000.00	-1856.07	27.19	-50466.54	0.00%
model 3-1	47.50	-53052.63	-2105.20	5.68	-11957.54	0.00%
model 3-2	47.50	-53052.63	-2043.00	3.39	-6925.77	0.00%
model 3-3	47.50	-53052.63	-2271.90	25.00	-56797.50	0.00%

Table 5.2.2.2 Critical membrane force in the circumferential direction from buckling formula and FEM analysis

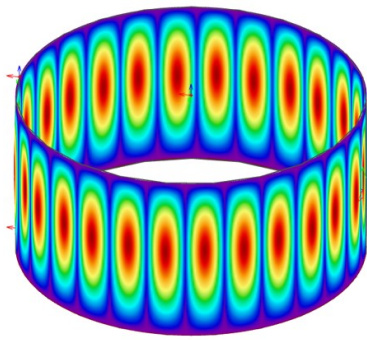
	radius a_y [m]	n_{crx} [kN/m] (Buckling formula)	n_x (FEM)	λ_{cr} (FEM)	n_{crx} [kN/m] (FEM)	% Difference from Chapter 4
model 1-1	∞	0.00	0.00	26.07	0.00	0.00%
model 1-2	∞	0.00	-2063.30	2.14	-4415.46	0.00%
model 1-3	∞	0.00	2117.63	26.82	56794.84	0.00%
model 2-1	126.25	-19960.40	875.73	26.62	23311.93	0.00%
model 2-2	126.25	-19960.40	-2011.32	10.59	-21299.88	0.00%
model 2-3	126.25	-19960.40	1945.01	27.19	52884.82	0.00%
model 3-1	126.25	-19960.40	-792.02	5.68	-4498.67	0.00%
model 3-2	126.25	-19960.40	-2060.52	3.39	-6985.16	0.00%
model 3-3	126.25	-19960.40	2232.60	25.00	55815.00	0.00%

The values in Table 5.2.2.1 and 5.2.2.2 are very close to those in Table 4.1.1 and 4.1.2. Thus it can be concluded that the scale of the dimension will not affect the critical membrane forces of the 9 models.

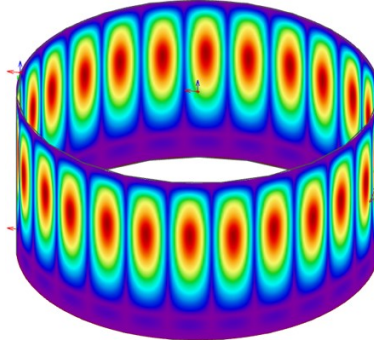
The analysis above points to the conclusion that the scale of dimension will not affect the result of our investigation.

5.3 Development of buckling modes

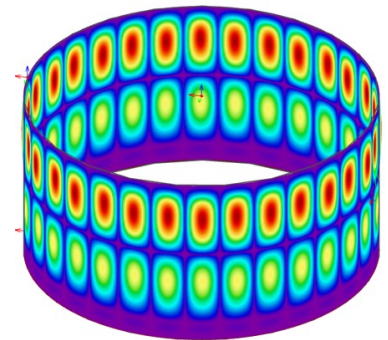
From Table 4.1.1, it can be noticed that a half ring buckling pattern occurs for model 1-3 (perfect cylinder under axial compression and radial tension). In fact, this half ring buckling pattern could be regarded as a transition state between the ring and column buckling pattern and ring buckling pattern. To find out how the buckling pattern develops, a cylinder under axial compression (2000 kN/m) and different radial loads (from compression to tension) is analyzed. The element size is 0.895m. The first buckling modes of this cylinder under different loads are as follows.



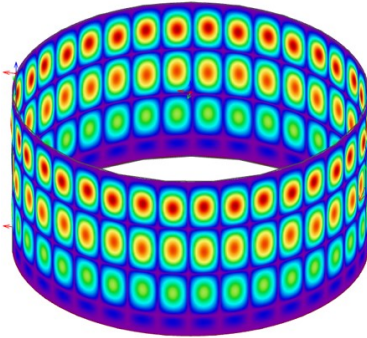
Radial compression: 20 kN/m²
Buckling load factor: 2.13



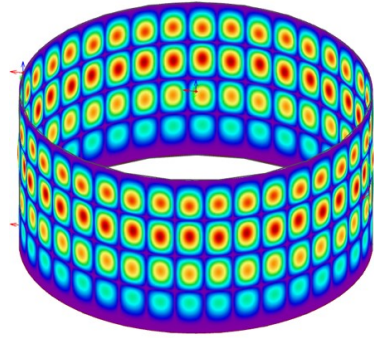
Radial compression: 0.5 kN/m²
Buckling load factor: 23.82



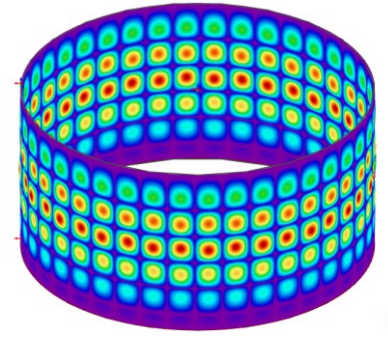
Radial compression: 0.45 kN/m²
Buckling load factor: 24.10



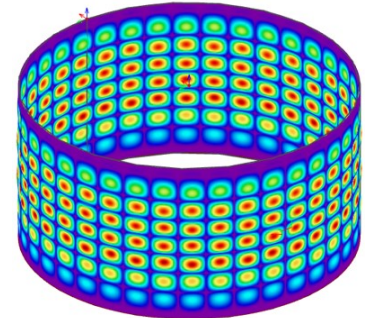
Radial compression: 0.23 kN/m²
Buckling load factor: 25.09



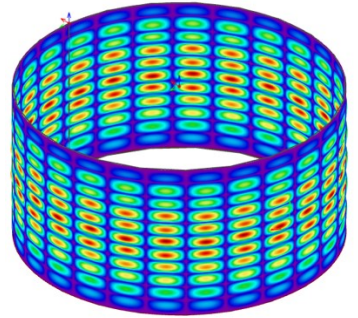
Radial compression: 0.15 kN/m²
Buckling load factor: 25.29



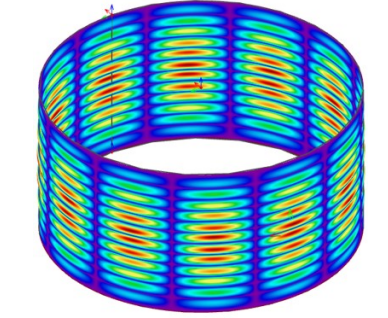
Radial load: 0 kN/m²
Buckling load factor: 25.55



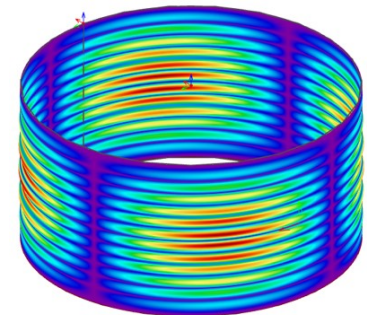
Radial tension: 0.3 kN/m²
Buckling load factor: 25.89



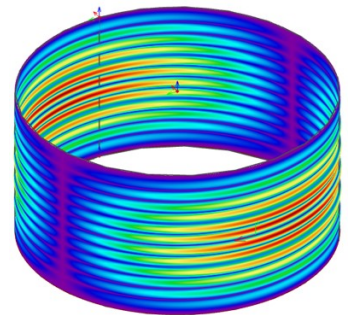
Radial tension: 0.5 kN/m²
Buckling load factor: 25.98



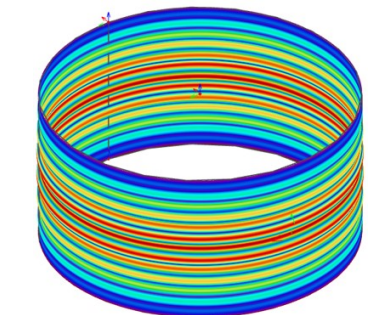
Radial tension: 0.75 kN/m²
Buckling load factor: 26.00



Radial tension: 1.0 kN/m²
Buckling load factor: 26.00



Radial tension: 1.5 kN/m²
Buckling load factor: 26.00



Radial tension: 15 kN/m²
Buckling load factor: 26.01

Figure 5.3.1 Buckling modes of a cylinder shell under an axial compression of 2000 kN/m and various radial loads

In Figure 5.3.1, it can be noticed that when the radial load is 0 and the cylinder shell is under pure compression, the ring and column buckling pattern occurs, which means buckling is occurring in both axial and circumferential directions.

With the increase of the radial compression, the buckling in the axial direction becomes less and less and finally there is just buckling in the circumferential direction, which called the column buckling pattern.

When the radial tension is applied to the cylinder shell, there will be more buckling in the axial direction and less buckling in the circumferential direction. In the end, with the increase of the radial tension, the buckling in the circumferential direction disappears and the ring buckling pattern occurs.

Below is a figure showing the buckling load factor as a function of the radial tension.

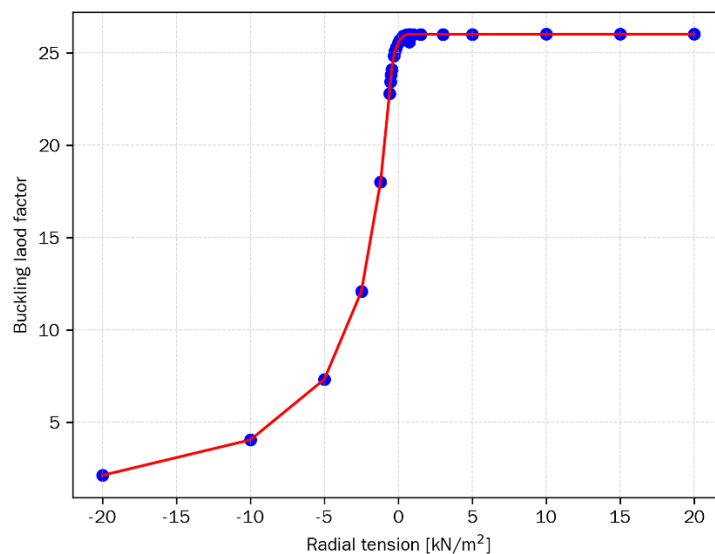


Figure 5.3.2 Line graph of the buckling load factor as a function of the radial tension

From Figure 5.3.2, it can be observed that when the radial tension is less than 0 kN/m² (i.e., in the compression range), the buckling load factor decreases rapidly with the increase of the radial compression magnitude. For example, as the radial compression increases from 0.5 kN/m² to 20 kN/m², the buckling load factor drops from 23.82 to 2.13. This shows that radial compression has a significant negative impact on the buckling load factor of the cylinder shell, greatly reducing its ability to resist buckling.

When the radial tension is greater than 0 kN/m², the buckling load factor initially increases rapidly. As the radial tension increases from 0 kN/m² to around 1 kN/m², the buckling load factor rises from 25.55 to approximately 26.00. However, as the radial tension continues to increase further (beyond 1 kN/m²), the growth rate of the buckling load factor slows down and gradually approaches a relatively stable value around 26. This indicates that while radial tension can enhance the buckling load factor, the strengthening effect becomes less pronounced as the radial tension reaches a certain

level.

Overall, the buckling load factor is highly sensitive to the change of radial load, especially in the compression range where the negative impact is substantial, and in the tension range, it shows a trend of first increasing rapidly and then approaching a stable value.

5.4 Buckling Behavior Analysis of Model 2 - 1 when $n_{xx} = 0$

In this subsection, we explore the buckling behavior of Model 2 - 1 under a special loading condition. While keeping other conditions unchanged, a radial compressive load of -7.68 kN/m^2 is added to Model 2 - 1. This particular load is applied to result in the circumferential membrane force (n_{xx}) in the middle of the positively curved shell being zero. The membrane force distributions in the axial and circumferential directions, obtained from the linear elastic analysis, are as follows. Additionally, the buckling mode and the associated buckling load factor, obtained from the linear buckling analysis, are presented below.

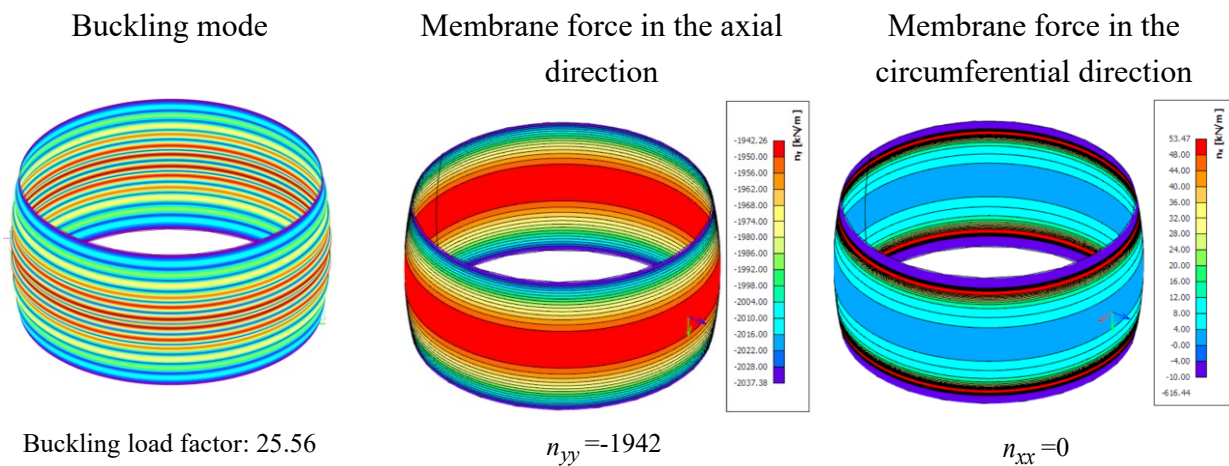


Figure 5.4.1 Membrane force distributions, buckling mode and buckling load factor of positively curved shell when $n_{xx} = 0$

The buckling pattern observed is a ring buckling pattern. We may now conclude that the curvature in the y -direction is not important up to $n_{xx} = 0$. The hoop force n_{xx} does not change the buckling mode or buckling load factor. This also confirms the shell buckling Formula (4.1).

5.5 Boundary conditions study

In the precious research, the bottom support is completely fixed. The top support is restricted in the x and y directions and is prevented from rotating, allowing movement only in the z direction. In this subsection, how the shells behave with hinged supports will be researched. The bottom of the shell will be supported by a hinge, while the top

support is designed to restrict the movement in x and y directions and be free to translate in the z direction and rotate in all three directions. The first buckling modes of the 9 models with hinged supports are as follows.

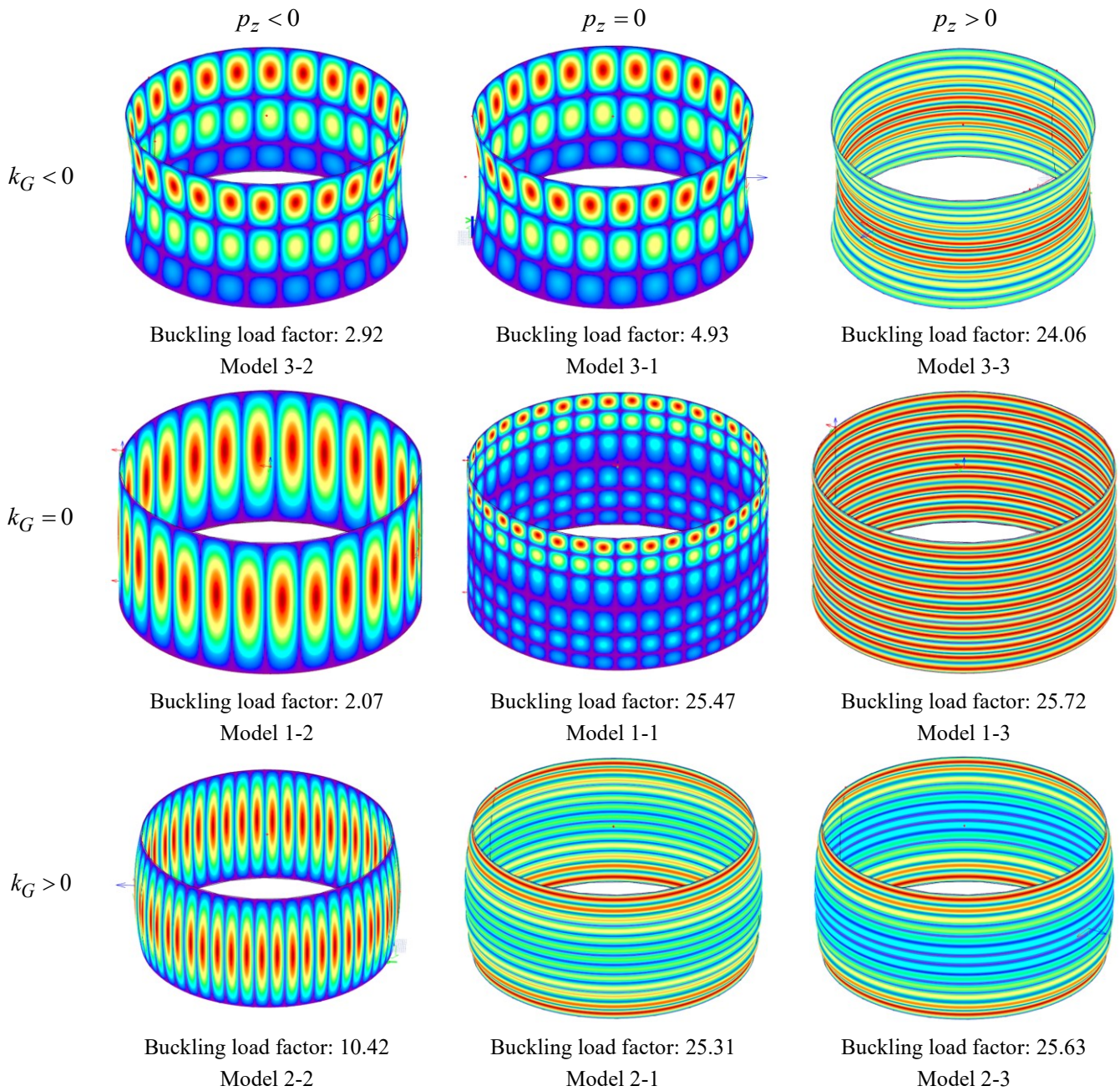


Figure 5.4.1 The 1st buckling mode of the 9 shell structures (hinged support)

It's obvious that the buckling patterns of the shells with hinged supports are similar to those with fixed supports in subsection 5.1.1, except in the regions near the support edges. Shells with hinged supports undergo more intense buckling in the vicinity of the supports, which is attributable to the fact that hinged supports do not restrict rotations, thereby contributing to the buckling phenomenon. Another point to note is that the buckling load factors obtained from the analysis using hinged supports are nearly

identical to those with fixed supports, although the buckling load factors for shells with hinged supports are marginally lower than those for shells with fixed supports.

In summary, the support conditions have a limited impact on the shell's buckling patterns and buckling load factors. The difference is that shells with hinged supports are more likely to buckle near the support areas compared to those with fixed supports, and they tend to have slightly lower buckling load factors.

5.6 Model height study

In this subsection, the impact of model height on the buckling behavior of shell structures is investigated. Three representative models of three different buckling patterns, model 1-1 (exhibiting the ring and column buckling pattern), model 1-2 (displaying the column buckling pattern), and model 1-3 (showing the ring buckling pattern), are selected for analysis. The heights of these models are varied as 50m, 75m, 100m, 125m, and 150m. The buckling modes and buckling load factors obtained from the linear buckling analyses are as follows.

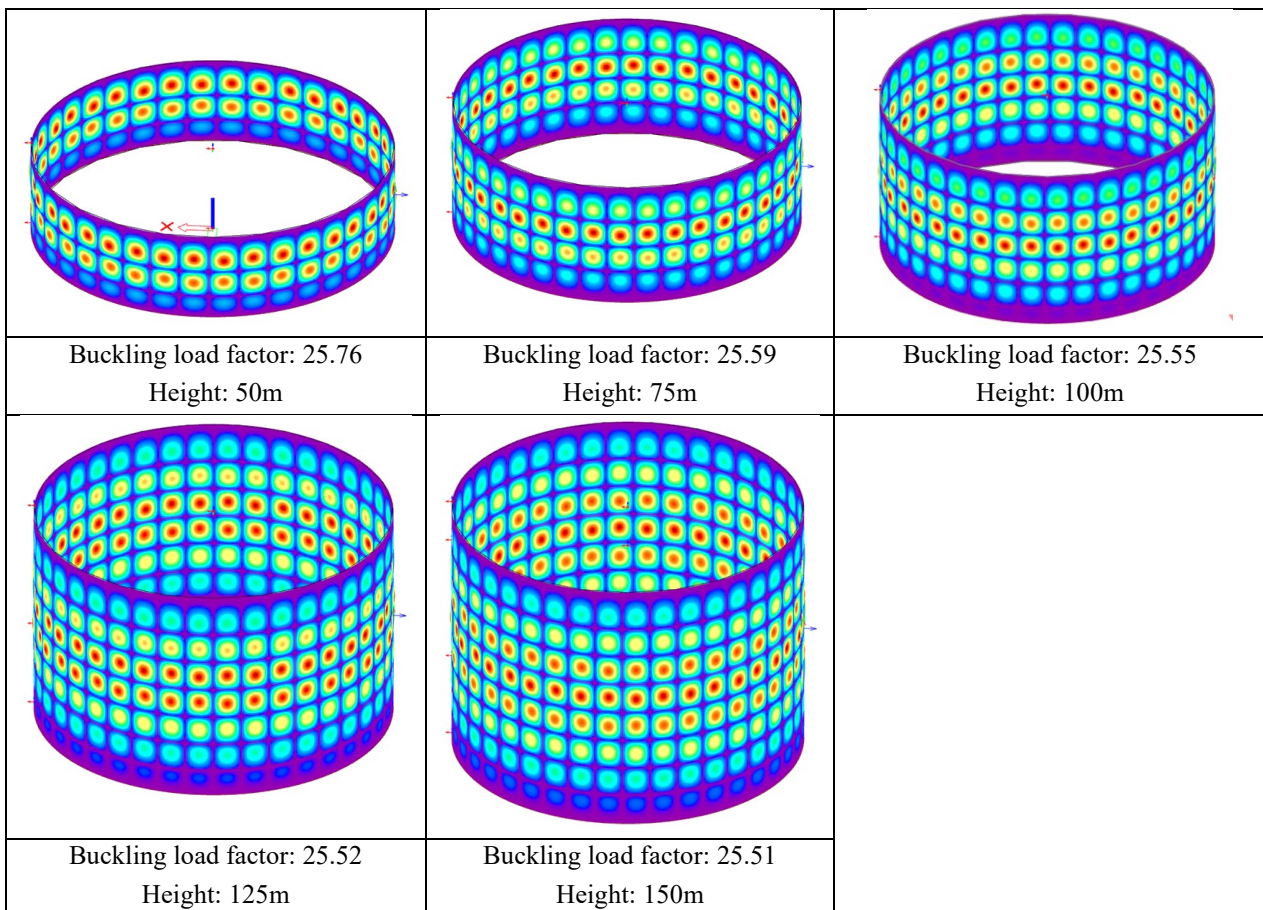


Figure 5.5.1 The 1st buckling modes of model 1-1 with different model heights

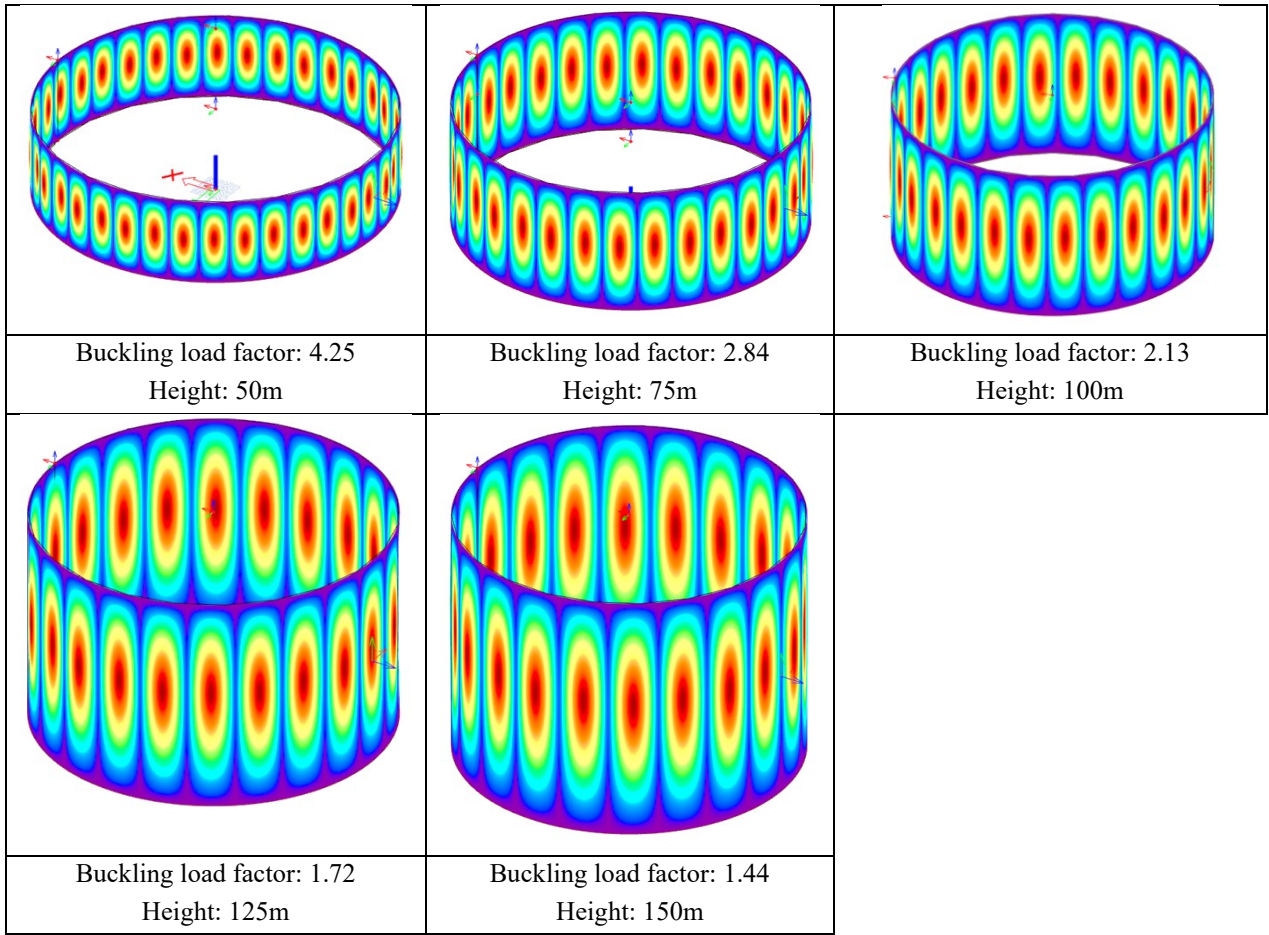


Figure 5.5.2 The 1st buckling modes of model 1-2 with different model heights

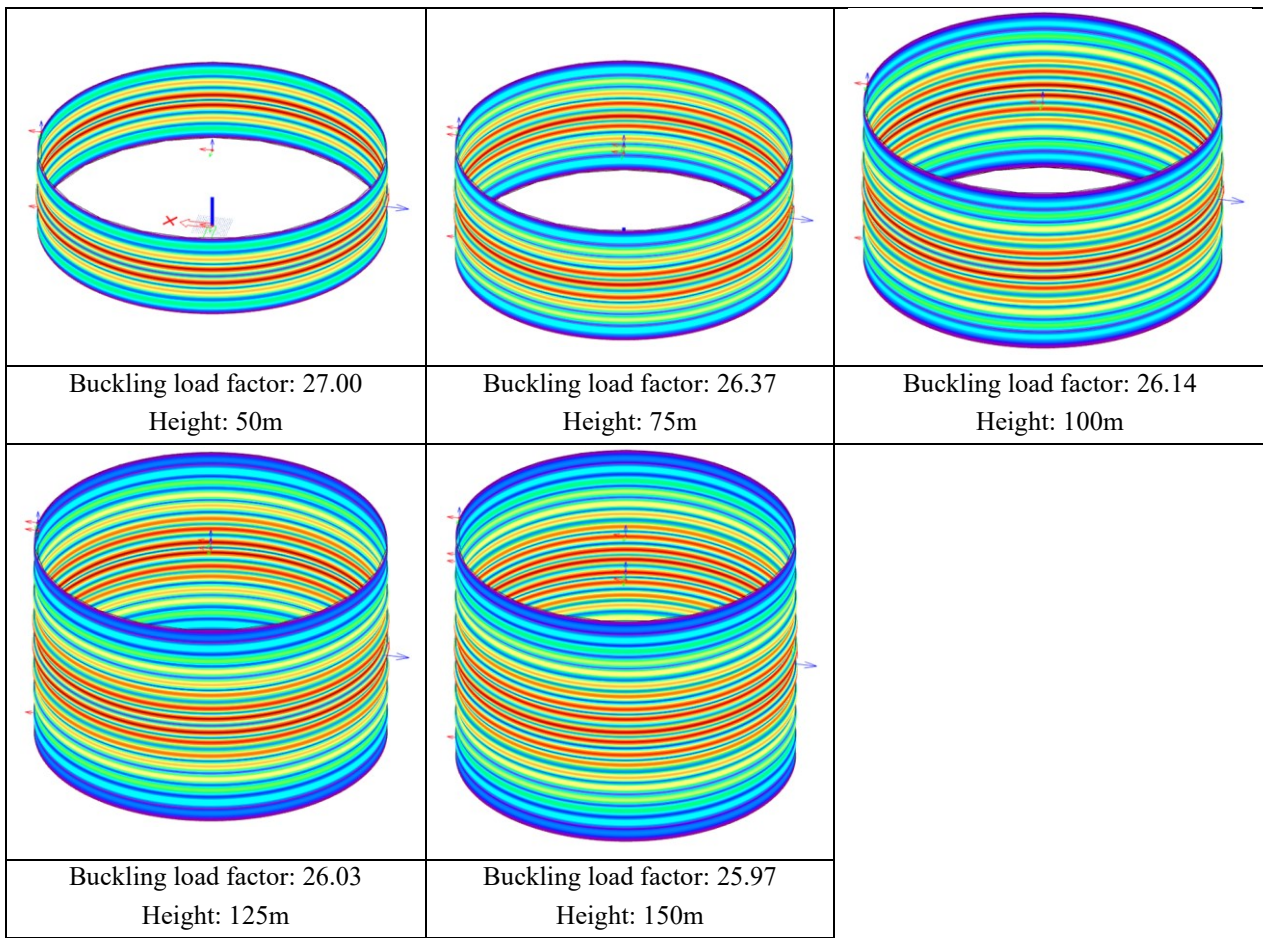


Figure 5.5.3 The 1st buckling modes of model 1-3 with different model heights

For model 1-1 with the ring and column buckling pattern, as the height increases from 50m to 150m, the buckling load factor only shows a slight decrease from 25.76 to 25.51. The change in the buckling load factor is relatively small, with a decrease of approximately $(25.76 - 25.51) / 25.76 \times 100\% \approx 0.97\%$. The buckling mode remains relatively consistent, maintaining the characteristic of the ring and column pattern throughout the height variations, although the number of "rows" in the ring and column pattern seems to increase with height. This indicates that the height has a limited impact on the overall buckling behavior and load-carrying capacity of this type of model. Theoretically, in the ring and column buckling pattern, the load is distributed relatively evenly in both the axial and circumferential directions. The increase in height does not significantly alter the stress distribution and the interaction between different parts of the shell, resulting in only a minor change in the buckling load factor.

Model 1-2, which has the column buckling pattern, experiences a more significant change in the buckling load factor. It decreases from 4.25 at a height of 50m to 1.44 at 150m. The decrease percentage is $(4.25 - 1.44) / 4.25 \times 100\% \approx 66.12\%$, which is a relatively large change. Theoretically, as the height increases, the slenderness ratio of the columns in the axial direction effectively increases. According to the Euler buckling

theory, the critical buckling load is inversely proportional to the square of the slenderness ratio. Therefore, the buckling load factor decreases significantly with the increase in height. Regarding the column buckles, it is observed that as the overall height of the model increases, the height of each individual column buckle becomes relatively less prominent or shorter compared to the overall height increase. This might be because the increased height allows for more distribution of the buckling behavior, resulting in relatively shorter column buckles. At a height of 50m, a certain number of columns are present, and as the height increases to 150m, the number of visually distinguishable columns is approximately half of that at 50m. This change in the number of columns is a direct visual observation and may have implications for the structural behavior and load-carrying capacity of the model.

In the case of model 1-3 with the ring buckling pattern, the buckling load factor decreases gradually from 27.00 at 50m to 25.97 at 150m. The decrease is about $(27.00 - 25.97) / 27.00 \times 100\% \approx 3.81\%$. The number of ring buckles appears to increase with the increase in height. Theoretically, in the ring buckling pattern, the axial deformation is the dominant factor that drives the formation of the ring pattern. Axial compression causes the shell to buckle in the axial direction, which in turn leads to circumferential deformation and the appearance of the ring buckling pattern. This type of buckling involves a circumferential wave pattern around the shell, making it a more global deformation mode that is primarily influenced by the overall axial behavior and geometry of the shell, rather than local variations. The increase in height may affect the distribution of axial stress and the interaction between different axial segments of the shell, resulting in a relatively small decrease in the buckling load factor. However, compared to the column buckling pattern, where individual columns or segments are more susceptible to changes in height due to increased slenderness, the impact of height on the ring buckling pattern is relatively small. This is because ring buckling is a more global deformation mode, dependent on the entire shell's response, rather than localized instabilities.

In general, The buckling load factor decreases with the increase of the model height. The height of the shell structure has different degrees of influence on the buckling behavior and load-carrying capacity of the shell structure depending on the buckling pattern. For the ring and column buckling pattern, the influence is relatively small; for the column buckling pattern, the influence is significant; and for the ring buckling pattern, the influence is moderate. When designing shell structures, the height factor needs to be considered comprehensively according to the specific buckling characteristics to ensure the structural safety and stability.

6 Geometrical nonlinear analysis

In this chapter, geometrical nonlinear analyses are conducted. The first buckling modes obtained from the linear stability analyses are chosen as the initial geometrical imperfections with imperfection amplitudes of ± 200 mm (shell thickness). These two imperfection amplitudes correspond to two distinct nonlinear combinations, labeled as NC1 (200mm) and NC2 (-200mm), respectively. The element size is $0.2\sqrt{a t}$, which is 0.895 m. The Newton-Raphson method is used. The initial load factor in the nonlinear combination is set as 50. The load is applied in 80 steps. The ultimate load is defined as the product of the applied load and $50 (n - 0.5)/80$, where n is the load step at which divergence of the iterations occurs. And $50 (n - 0.5)/80$ is the buckling load factor for the geometrical nonlinear analysis. The nonlinear buckling patterns of the 9 models obtained from geometrical nonlinear analyses with imperfection amplitudes of 200 mm (NC1) are shown in Figure 6.1.

In Figure 6.1, the membrane forces labeled under the buckling patterns are calculated using the Sanders-Koiter equations[4], and the calculation details are shown in Appendix 2.

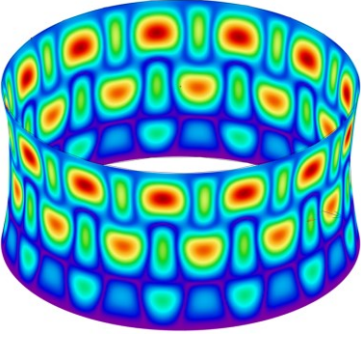
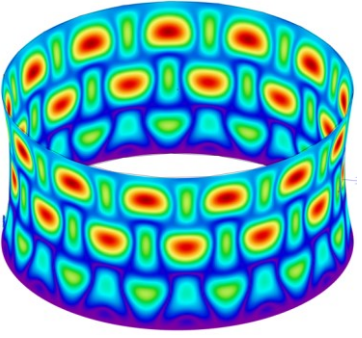
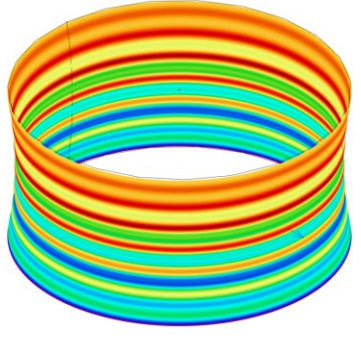
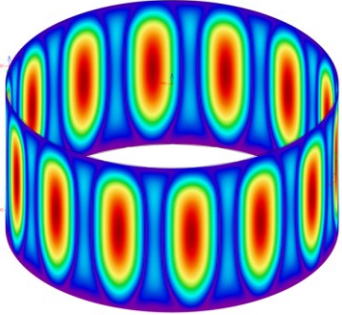
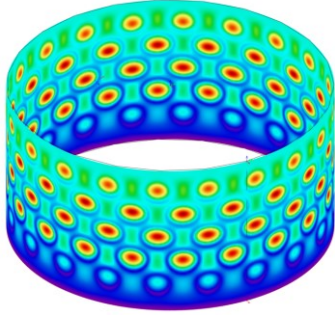
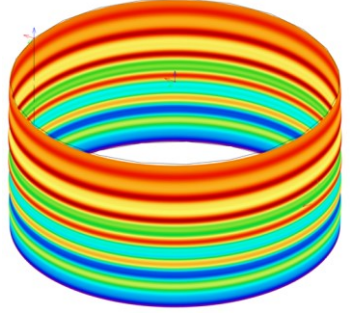
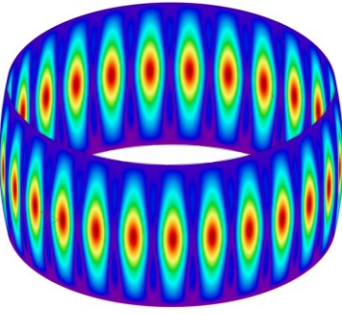
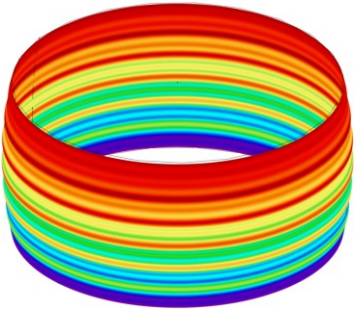
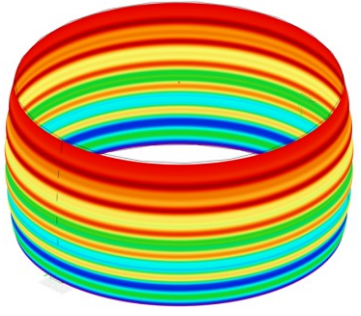
	$p_z < 0$	$p_z = 0$	$p_z > 0$
$k_G < 0$			
	Model 3-2 $n_{xx} = -7844$ $n_{yy} = -8547$ Buckling load factor: 4.06	Model 3-1 $n_{xx} = -5196$ $n_{yy} = -13811$ Buckling load factor: 6.56	Model 3-3 $n_{xx} = 15057$ $n_{yy} = -13811$ Buckling load factor: 6.56
$k_G = 0$			
	Model 1-2 $n_{xx} = -5620$ $n_{yy} = -5620$ Buckling load factor: 2.81	Model 1-1 $n_{xx} = 0$ $n_{yy} = -21880$ Buckling load factor: 10.94	Model 1-3 $n_{xx} = 14380$ $n_{yy} = -14380$ Buckling load factor: 7.19
$k_G > 0$			
	Model 2-2 $n_{xx} = -5740$ $n_{yy} = -5352$ Buckling load factor: 2.81	Model 2-1 $n_{xx} = 5196$ $n_{yy} = -12495$ Buckling load factor: 6.56	Model 2-3 $n_{xx} = 13245$ $n_{yy} = -13695$ Buckling load factor: 7.19

Figure 6.1 The buckling patterns of the 9 shell structures (NC1), membrane forces and nonlinear buckling load factors included

The buckling patterns of NC2 (imperfection amplitude : -200 mm) are identical to those of NC1 (imperfection amplitude : 200 mm), with the exception of being rotated by a certain angle, and thus they are not included here. The specific images can be referred to in Appendix 3. Additionally, NC2 and NC1 share the same buckling load factor.

7 Parameter study of the nonlinear analysis

7.1 Imperfection amplitude study

In Chapter 6, the imperfection amplitudes used for the geometrical nonlinear analyses are 200mm (NC1) and -200mm (NC2), the absolute values of which are equal to the shell thickness t . In this section, different imperfection amplitudes are applied.

7.1.1 Imperfection amplitude: 100mm (0.5t)

In this subsection, the first buckling modes obtained from the linear stability analyses are still chosen as the initial geometrical imperfections with the imperfection amplitudes of ± 100 mm (half of the shell thickness). These amplitudes correspond to two separate nonlinear analyses, identified as NC1 (with +100 mm) and NC2 (with -100 mm). The element size remains at $0.895t$ ($0.2\sqrt{a t}$). The Newton-Raphson method is used. The nonlinear buckling patterns of the 9 models obtained from geometrical nonlinear analyses with imperfection amplitudes of 100 mm (NC1) are as follows and the buckling patterns of NC2 can be referred to in Appendix 3.

In Figure 7.1.1.1, the membrane forces labeled under the buckling patterns are calculated using the Sanders-Koiter equations[4], and the calculation details are shown in Appendix 2.

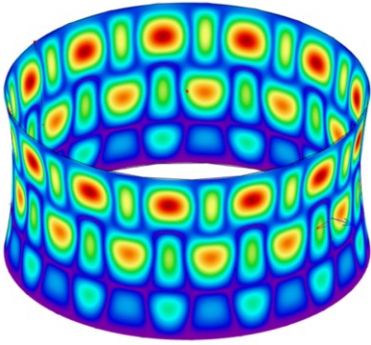
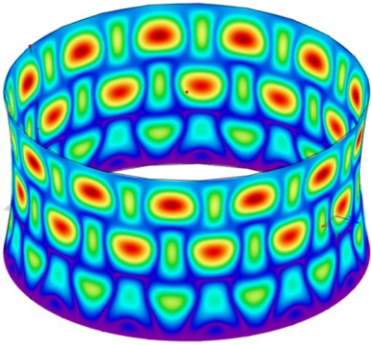
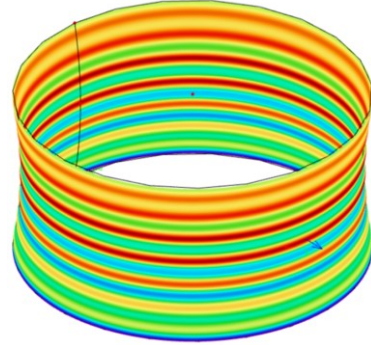
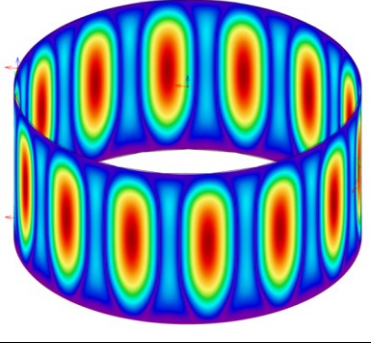
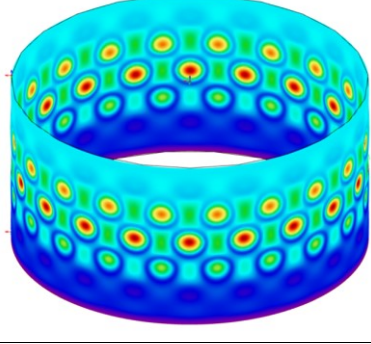
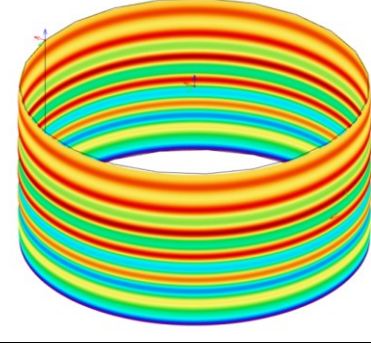
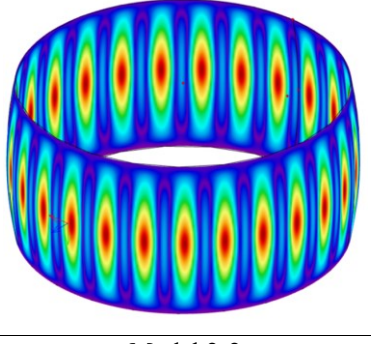
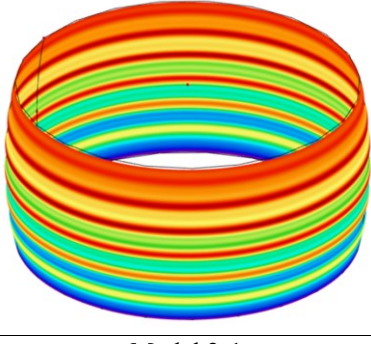
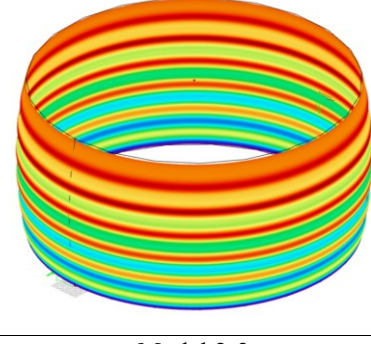
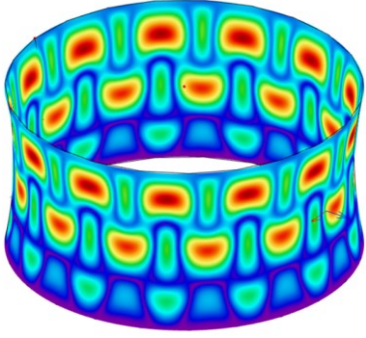
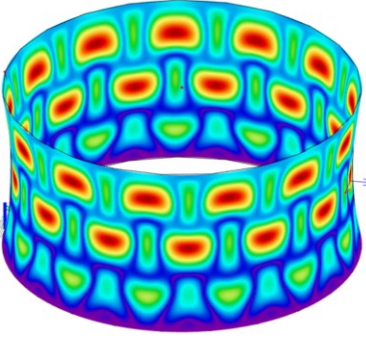
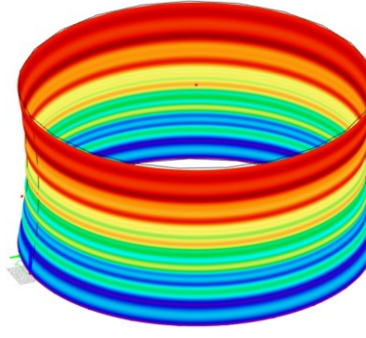
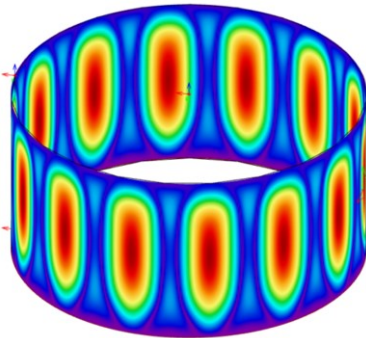
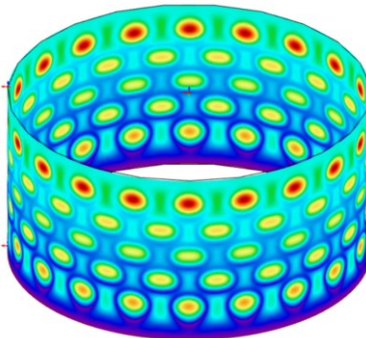
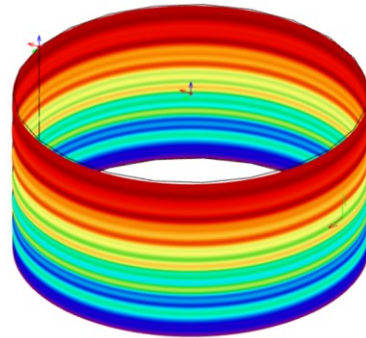
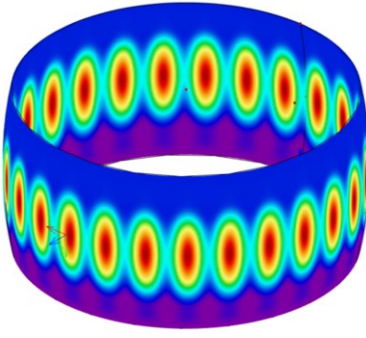
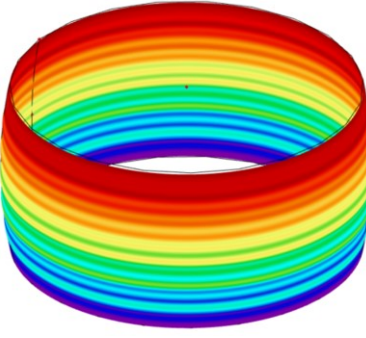
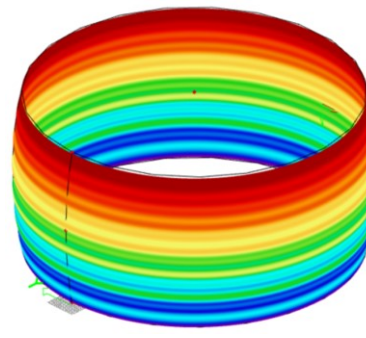
	$p_z < 0$	$p_z = 0$	$p_z > 0$
$k_G < 0$			
	Model 3-2 $n_{xx} = -7844$ $n_{yy} = -8547$ Buckling load factor: 4.06	Model 3-1 $n_{xx} = -5196$ $n_{yy} = -13811$ Buckling load factor: 6.56	Model 3-3 $n_{xx} = 23666$ $n_{yy} = -21705$ Buckling load factor: 10.31
$k_G = 0$			
	Model 1-2 $n_{xx} = -5620$ $n_{yy} = -5620$ Buckling load factor: 2.81	Model 1-1 $n_{xx} = 0$ $n_{yy} = -21880$ Buckling load factor: 10.94	Model 1-3 $n_{xx} = 23120$ $n_{yy} = -23120$ Buckling load factor: 11.56
$k_G > 0$			
	Model 2-2 $n_{xx} = -9581$ $n_{yy} = -8933$ Buckling load factor: 4.69	Model 2-1 $n_{xx} = 7675$ $n_{yy} = -18457$ Buckling load factor: 9.69	Model 2-3 $n_{xx} = 22455$ $n_{yy} = -23219$ Buckling load factor: 12.19

Figure 7.1.1.1 The buckling patterns of the 9 shell structures (NC1), membrane forces and nonlinear buckling load factors included

7.1.2 Imperfection amplitude: 400mm (2t)

In this subsection, the first buckling modes obtained from the linear stability analyses are still chosen as the initial geometrical imperfections with the imperfection

amplitudes of ± 400 mm (twice shell thickness). These amplitudes correspond to two separate nonlinear analyses, identified as NC1 (with +400 mm) and NC2 (with -400 mm). The element size remains at 0.895m ($0.2\sqrt{at}$). The Newton-Raphson method is used. The nonlinear buckling patterns of the 9 models obtained from geometrical nonlinear analyses with imperfection amplitudes of 400 mm (NC1) are as follows and the buckling patterns of NC2 can be referred to in Appendix 3. In Figure 7.1.2.1, the membrane forces labeled under the buckling patterns are calculated using the Sanders-Koiter equations[4], and the calculation details are shown in Appendix 2.

	$p_z < 0$	$p_z = 0$	$p_z > 0$
$k_G < 0$			
	Model 3-2 $n_{xx} = -7844$ $n_{yy} = -8547$ Buckling load factor: 4.06	Model 3-1 $n_{xx} = -5196$ $n_{yy} = -13811$ Buckling load factor: 6.56	Model 3-3 $n_{xx} = 10766$ $n_{yy} = -9874$ Buckling load factor: 4.69
$k_G = 0$			
	Model 1-2 $n_{xx} = -5620$ $n_{yy} = -5620$ Buckling load factor: 2.81	Model 1-1 $n_{xx} = 0$ $n_{yy} = -23120$ Buckling load factor: 11.56	Model 1-3 $n_{xx} = 9380$ $n_{yy} = -9380$ Buckling load factor: 4.69
$k_G > 0$			
	Model 2-2	Model 2-1	Model 2-3

	$n_{xx}=-4473$ $n_{yy}=-4171$ Buckling load factor: 2.19	$n_{xx}=3216$ $n_{yy}=-7733$ Buckling load factor: 4.06	$n_{xx}=8639$ $n_{yy}=-8933$ Buckling load factor: 4.69
--	---	--	--

Figure 7.1.2.1 The buckling patterns of the 9 shell structures (NC1), membrane forces and nonlinear buckling load factors included

7.1.3 Imperfection amplitude: 800mm (4t)

In this subsection, the first buckling modes obtained from the linear stability analyses are still chosen as the initial geometrical imperfections with the imperfection amplitudes of ± 800 mm (four times shell thickness). These amplitudes correspond to two separate nonlinear analyses, identified as NC1 (with +800 mm) and NC2 (with -800 mm). The element size remains at 0.895m ($0.2\sqrt{(a t)}$). The Newton-Raphson method is used. The nonlinear buckling patterns of the 9 models obtained from geometrical nonlinear analyses with imperfection amplitudes of 800 mm (NC1) are as follows and the buckling patterns of NC2 can be referred to in Appendix 3.

In Figure 7.1.3.1, the membrane forces labeled under the buckling patterns are calculated using the Sanders-Koiter equations[4], and the calculation details are shown in Appendix 2.

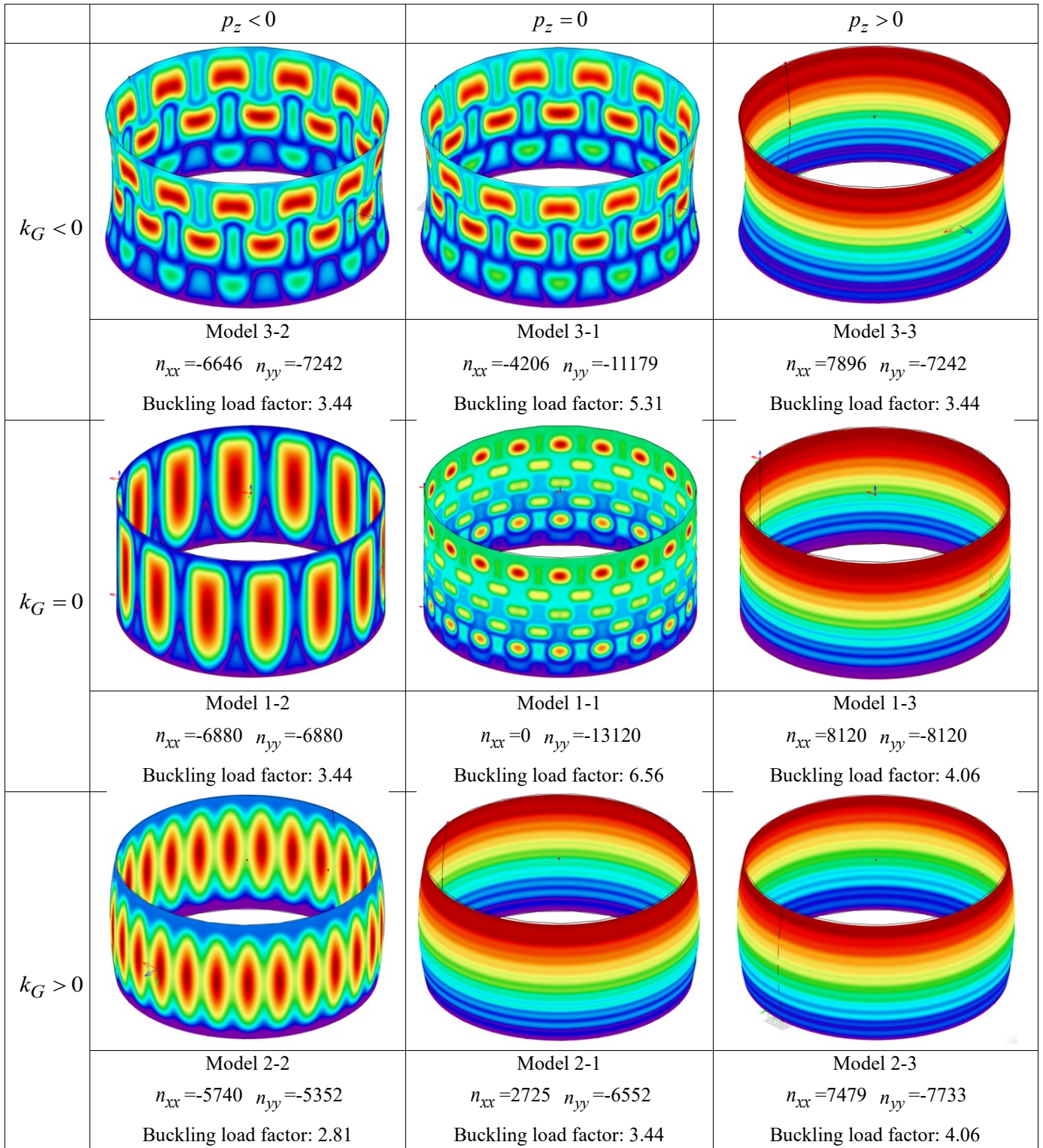


Figure 7.1.3.1 The buckling patterns of the 9 shell structures (NC1), membrane forces and nonlinear

7.1.4 Conclusion

In the parameter analysis of the nonlinear study, it is observed that the amplitude of imperfections significantly influences the buckling behavior of the structure.

Regarding the buckling pattern, a notable shift is identified when compared to the results from the geometric nonlinear analysis presented in Section 6.2. As the imperfection amplitude intensifies, the buckling pattern undergoes substantial changes in certain models. For instance, in some models, as the imperfection amplitude increases from $0.5t$ to $4t$, there is a distinct alteration in the location and severity of local buckling. Take model 1-2 for example, at higher imperfection amplitudes, certain areas of the structure, particularly near the boundaries, experience more pronounced buckling. This may be attributed to the sensitivity of the boundary conditions to imperfections and the localized stress concentrations within the structure. In other models, such as model 2-2, while the overall buckling pattern varies with different imperfection amplitudes, the degree of buckling in some key regions (e.g., the central area of the structure) changes relatively little. This may be because the middle of the structure is relatively uniform and the response to imperfections is relatively stable.

As for the buckling load factor, it is evident that the buckling load factor diminishes with the increase in imperfection amplitude. This trend was suggested in the geometric nonlinear analysis in Section 6.2, but it is more pronounced in the parameter analysis. As the imperfection amplitude increases, the structural capacity to bear loads is reduced, leading to a lower buckling load factor. This is because a larger imperfection amplitude makes the structure more prone to buckling and reaches the critical buckling state at a lower load.

Overall, the imperfection amplitude has a significant impact on the bearing capacity and buckling behavior of the shell. As the imperfection amplitude increases, the bearing capacity of the shell decreases, as indicated by the decrease of the buckling load factor. At the same time, the buckling pattern also changes, and the buckling degree of local areas may change to different extents due to factors such as structural characteristics and boundary conditions.

8 Knockdown factor calculation

Using formula (1.1), we can calculate the knockdown factor values in axial and circumferential directions for the nine shell models by Maple. The calculation details are attached in the Appendix 4. In Section 5.1, it is proved that the element size $0.2\sqrt{(at)}$ is accurate for our analyses, so the membrane forces we use are from Table 5.1.1.1 and Table 5.1.1.2.

8.1 Imperfection amplitude: 200mm (t)

When the amplitude of imperfection is equal to the shell thickness, the knockdown factor calculated by Maple using equation (1.1) yields two or three values, among which only one falls within the range of 0 to 1, and this is the only reasonable value, as follows

Table 8.1.1 The knockdown factor values in circumferential and axial direction and the knockdown factors (imperfection amplitude: t)

	C_x (Circumferential)	C_y (Axial)	C	Buckling Pattern
Model 1-1	0.00	0.25	0.25	ring and column
Model 1-2	0.00	0.22		in-extensional
Model 1-3	0.00	0.29	0.29	ring
Model 2-1	0.39	0.27	0.27	ring
Model 2-2	0.22	0.22	0.22	column
Model 2-3	0.32	0.29	0.29	ring
Model 3-1	0.19	0.24		in-extensional
Model 3-2	0.23	0.22		in-extensional
Model 3-3	0.28	0.28	0.28	ring

8.2 Imperfection amplitude: 100mm (0.5t)

When all other conditions are kept constant, and the imperfection amplitude is set to half the shell thickness, the knockdown factor computed by Maple using equation (1.1) yields two or three values, some of which are too close to zero, some are negative, and some are excessively large. We select only the most reasonable value among them, as follows

Table 8.2.1 The knockdown factor values in circumferential and axial direction and the knockdown factors (imperfection amplitude: 0.5t)

	C_x (Circumferential)	C_y (Axial)	C	Buckling Pattern
Model 1-1	0.00	0.33	0.33	ring and column
Model 1-2	0.00	0.27		in-extensional
Model 1-3	0.00	0.41	0.41	ring
Model 2-1	0.62	0.38	0.38	ring
Model 2-2	0.43	0.28	0.43	column
Model 2-3	0.54	0.43	0.43	ring
Model 3-1	0.21	0.30		in-extensional
Model 3-2	0.25	0.26		in-extensional
Model 3-3	0.34	0.39	0.39	ring

8.3 Imperfection amplitude: 400mm (2t)

Increasing the imperfection amplitude to double the shell thickness, the calculation of the knockdown factor again produces several potential values. We identify and use the single value that lies between 0 and 1, ensuring the validity and practicality of the knockdown factor. The detailed outcomes for this scenario can be found in Table 8.3.1.

Table 8.3.1 The knockdown factor values in circumferential and axial direction and the knockdown factors (imperfection amplitude: 2t)

	C_x (Circumferential)	C_y (Axial)	C	Buckling Pattern
Model 1-1	0.00	0.21	0.21	ring and column
Model 1-2	0.00	0.19		in-extensional
Model 1-3	0.00	0.23	0.23	ring
Model 2-1	0.25	0.22	0.22	ring
Model 2-2	0.18	0.19	0.18	column
Model 2-3	0.22	0.23	0.23	ring
Model 3-1	0.18	0.20		in-extensional
Model 3-2	0.20	0.20		in-extensional
Model 3-3	0.23	0.23	0.23	ring

8.4 Imperfection amplitude: 800mm (4t)

Further increasing the imperfection amplitude to four times the shell thickness, the computation of the knockdown factor using equation (1.1) in Maple once more provides

a set of values. From this set, we choose the only value that is within the acceptable range of 0 to 1, which is the most physically meaningful. The results for this condition are summarized in Table 8.4.1.

Table 8.4.1 The knockdown factor values in circumferential and axial direction and the knockdown factors (imperfection amplitude: 4t)

	C_x (Circumferential)	C_y (Axial)	C	Buckling Pattern
Model 1-1	0.00	0.19	0.19	ring and column
Model 1-2	0.00	0.18		in-extensional
Model 1-3	0.00	0.20	0.20	ring
Model 2-1	0.20	0.19	0.19	ring
Model 2-2	0.17	0.18	0.17	column
Model 2-3	0.19	0.19	0.19	ring
Model 3-1	0.18	0.19		in-extensional
Model 3-2	0.19	0.18		in-extensional
Model 3-3	0.20	0.20	0.20	ring

It can be noticed that in the above 4 tables of chapter 8, the knockdown factor values in the circumferential direction (C_x) for models 1-1, 1-2 and 1-3 are 0. In fact, these three models are perfect cylinders, which means their curvatures in the circumferential direction (k_{yy}) are 0. However, the term k_{yy} should be in the denominator in the knockdown factor formula (1.1) when calculating C_x . This makes the knockdown factor formula invalid for these three models when calculating C_x . The value 0 here describes an infinitely large flat plate which will buckle at any compressive load.

Considering the knockdown factor values in the circumferential (C_x) and axial (C_y) directions obtained from formula (1.1), we can determine the knockdown factor (C) for each model as shown in the last column of Table 8.4.1. For model 1-1, the ring and column buckling pattern occurs. It can be consider as an infinitely large flat plate in the circumferential direction and the knockdown factor (C) is determined by its knockdown factor value in the axial direction (C_y). For models 1-3, 2-1, 2-3 and 3-3, the ring buckling pattern occurs, so their knockdown factors (C) can be determined by their knockdown factor values in the axial direction (C_y). For model 2-2, the column buckling pattern occurs, and the knockdown factor (C) is determined by its knockdown factor value in the circumferential direction (C_x). For other models (models 1-2, 3-1 and 3-2), in-extensional deformation occurs and equation (1.1) is not applicable to in-extensional buckling.

9 Comparison and discussion

The 4 tables below show load factors obtained from linear stability analyses (LBA) and geometrical nonlinear analyses including initial geometrical imperfections (GNIA) for 4 different imperfection amplitudes. The load factor (formula) is determined by the ratio of the critical membrane forces derived from the shell buckling formula (4.1) to the membrane forces obtained through linear elastic analysis, with the value being selected based on the dominant direction according to the buckling mode. And the knockdown factor C based on finite element analyses should be equal to the ratio of the load factors obtained from geometrical nonlinear analysis (GNIA) and linear stability analysis (LBA). The knockdown factors calculated using this method are compared with those obtained from the knockdown factor formula in the tables below

Table 9.1 Load Factors (LBA and GNIA) and Knockdown Factor C (FEM and knockdown factor formula) – Imperfection Amplitude: t

	Load factor (formula)	Load factor (LBA)	Load factor (GNIA)	C (FEM)	C (formula)	Buckling Pattern
model 1-1	25.20	26.07	10.94	0.42	0.25	ring and column
model 1-2	0.00	2.14	2.81	1.31		in-extensional
model 1-3	25.20	26.82	7.19	0.27	0.29	ring
model 2-1	25.20	26.54	6.56	0.25	0.27	ring
model 2-2	9.93	10.58	2.81	0.27	0.22	column
model 2-3	25.86	27.19	7.19	0.26	0.29	ring
model 3-1	25.20	5.68	6.56	1.16		in-extensional
model 3-2	9.70	3.39	4.06	1.20		in-extensional
model 3-3	23.35	24.93	6.56	0.26	0.28	ring

Table 9.2 Load Factors (LBA and GNIA) and Knockdown Factor C (FEM and knockdown factor formula) – Imperfection Amplitude: 0.5t

	Load factor (formula)	Load factor (LBA)	Load factor (GNIA)	C (FEM)	C (formula)	Buckling Pattern
model 1-1	25.20	26.07	10.94	0.42	0.33	ring and column
model 1-2	0.00	2.14	2.81	1.31		in-extensional
model 1-3	25.20	26.82	11.56	0.43	0.41	ring
model 2-1	25.20	26.54	9.69	0.37	0.38	ring
model 2-2	9.93	10.58	4.69	0.44	0.43	column
model 2-3	25.86	27.19	12.19	0.45	0.43	ring

model 3-1	25.20	5.68	6.56	1.16		in-extensional
model 3-2	9.70	3.39	4.06	1.20		in-extensional
model 3-3	23.35	24.93	10.31	0.41	0.39	ring

Table 9.3 Load Factors (LBA and GNIA) and Knockdown Factor C (FEM and knockdown factor formula) – Imperfection Amplitude: 2t

	Load factor (formula)	Load factor (LBA)	Load factor (GNIA)	C (FEM)	C (formula)	Buckling Pattern
model 1-1	25.20	26.07	11.56	0.44	0.21	ring and column
model 1-2	0.00	2.14	2.81	1.31		in-extensional
model 1-3	25.20	26.82	4.69	0.17	0.23	ring
model 2-1	25.20	26.54	4.06	0.15	0.22	ring
model 2-2	9.93	10.58	2.19	0.21	0.18	column
model 2-3	25.86	27.19	4.69	0.17	0.23	ring
model 3-1	25.20	5.68	6.56	1.16		in-extensional
model 3-2	9.70	3.39	4.06	1.20		in-extensional
model 3-3	23.35	24.93	4.69	0.19	0.23	ring

Table 9.4 Load Factors (LBA and GNIA) and Knockdown Factor C (FEM and knockdown factor formula) – Imperfection Amplitude: 4t

	Load factor (formula)	Load factor (LBA)	Load factor (GNIA)	C (FEM)	C (formula)	Buckling Pattern
model 1-1	25.20	26.07	6.56	0.25	0.19	ring and column
model 1-2	0.00	2.14	3.44	1.61		in-extensional
model 1-3	25.20	26.82	4.06	0.15	0.20	ring
model 2-1	25.20	26.54	3.44	0.13	0.19	ring
model 2-2	9.93	10.58	2.81	0.27	0.17	column
model 2-3	25.86	27.19	4.06	0.15	0.19	ring
model 3-1	25.20	5.68	5.31	0.94		in-extensional
model 3-2	9.70	3.39	3.44	1.01		in-extensional
model 3-3	23.35	24.93	3.44	0.14	0.20	ring

By observing the data in the first and second columns of these tables, it can be seen that for most models, the load factor (formula) and the load factor (LBA) are relatively close. This indicates that the shell buckling formula used to calculate the load factor (formula) is generally consistent with the results of the linear stability analysis (LBA) in predicting the buckling behavior of the models. However, for models 1-2, 3 - 1 and 3 -

2, there are significant differences between the two. In these models, the in-extensional buckling pattern occurs, which may lead to a different buckling mechanism compared to other models. This difference in buckling behavior may cause the load factor (formula) calculated based on the shell buckling formula to deviate from the load factor (LBA) obtained from the linear stability analysis.

It can be noticed that models 1-2, 3-1 and 3-2 have knockdown factors C (FEM) larger than 1. This is due to in-extensional deformation. The buckling shapes are constrained by the edges. The critical loads are small, much smaller than the values predicted by the critical load formula. After buckling, the shell can still carry more load, as shown by the non-linear analyses. Shape imperfections give small reductions in the ultimate loads. These shells buckle like flat plates.

The overall error of the knockdown factors derived from the knockdown factor formula, relative to the knockdown factors obtained from finite element analyses (FEM), is assessed using the mean square error metric. The detailed code is provided in the Appendix 5, where it can be observed that the mean square error is 0.0056.

Overall, for most models, the knockdown factor formula gives a reasonable prediction of the buckling load. Under different imperfection amplitudes, there is a certain degree of agreement between the knockdown factor calculated by the formula and the ratio of the load factors obtained by finite element analysis (FEM) (i.e., the comparison between theory and practice), but there are also some differences. For some special models (such as models 1 - 2, 3 - 1 and 3 - 2), due to their special buckling modes (in-extensional deformation), there are challenges to the predictive precision of the knockdown factor formula.

When the knockdown factor is greater than 1 (such as models 1-2, 3-1 and 3-2), from the traditional perspective of judging structural safety based on the knockdown factor, the structure seems to be "safe", but this is because these models have a buckling behavior similar to that of a plate under certain conditions, and the actual load-carrying mechanism and safety need more in-depth analysis.

For most models with knockdown factors within a reasonable range, the safety of the structure is related to the predicted buckling load. If the actual load is less than the critical buckling load considering the knockdown factor, the structure is safe in terms of buckling, but it is also necessary to consider other failure modes (such as yielding, fatigue, etc.) to comprehensively evaluate the safety of the structure.

10 Curve fitted knockdown factor formula

In Chapter 9, it was found that although the knockdown factor formula gives a reasonable prediction of the buckling load for most models, there are still some differences and challenges. Therefore, it is necessary to further improve the accuracy of the knockdown factor formula.

In this chapter, we use the data of model 1-1, 1-3, 2-1, 2-2, 2-3 and 3-3 for fitting (24 data points). The independent variables are k_{yy}/k_{xx} (the ratio of curvatures in different directions), n_{xx}/n_{yy} (the ratio of membrane forces in different directions), and d/t (the ratio of imperfection amplitude to the thickness of the shell structure). However, model 2-2 is an exception. Since it exhibits a column buckling pattern with buckling in the circumferential direction, the fitting is performed using the independent variables k_{xx}/k_{yy} , n_{yy}/n_{xx} , and d/t . The dependent variable is the knockdown factor C based on finite element analyses. Maple is used for nonlinear fitting, and the specific code is shown in Appendix 6. The obtained knockdown factor Formula (10.1) is as follows

$$C = -0.14 \times e^{0.32 \cdot \frac{k_{yy}}{k_{xx}}} + 1.13 \times e^{9.63 \times 10^{-2} \cdot \frac{n_{xx}}{n_{yy}}} - 0.54 \times e^{8.29 \times 10^{-2} \cdot \frac{d}{t}} \quad (10.1)$$

The comparison of the knockdown factor obtained by the finite element analyses C (FEM) and the knockdown factor C (formula) obtained by formula (10.1) is shown in the table below.

Table 10.1 Knockdown Factor C (FEM and fitted knockdown factor formula)

		Model 1-1	Model 1-3	Model 2-1	Model 2-2	Model 2-3	Model 3-3
Imperfection amplitude: 0.5t	C (FEM)	0.42	0.43	0.37	0.44	0.45	0.41
	C (fitted)	0.43	0.32	0.36	0.37	0.30	0.34
Imperfection amplitude: t	C (FEM)	0.42	0.27	0.25	0.27	0.26	0.26
	C (fitted)	0.40	0.29	0.34	0.35	0.28	0.32
Imperfection amplitude: 2t	C (FEM)	0.44	0.17	0.15	0.21	0.17	0.19
	C (fitted)	0.35	0.24	0.28	0.29	0.23	0.27
Imperfection amplitude: 4t	C (FEM)	0.25	0.15	0.13	0.27	0.15	0.14
	C (fitted)	0.24	0.13	0.17	0.18	0.11	0.15

By observing the data in the table, it can be seen that the values of the knockdown factor calculated by the new formula are relatively close to the values obtained from the finite element analysis (FEM). For most models and imperfection amplitudes, the differences between the two are within a certain range. The overall error of the knockdown factors derived from the curve fitted formula, relative to the knockdown factors obtained from finite element analyses (FEM), is assessed using the mean square error metric. The

detailed code is provided in the Appendix 5, where it can be observed that the mean square error is 0.0051, smaller than that of the original knockdown factor formula. This indicates that the new formula has a certain degree of accuracy in predicting the knockdown factor. The residual errors that exist might be attributed to the current limitation in data quantity. As such, it would be beneficial to collect and analyze a more extensive dataset in future studies to refine the fitting process.

It is worth noting that the current formula is used to calculate the knockdown factor for buckling in the axial (y) direction. When the structure has a column buckling mode, which buckles in the circumferential (x) direction, it is necessary to swap the positions of x and y in the formula. In cases similar to model 1-1, where the ring and column buckling mode occurs, meaning that buckling happens in both the circumferential and axial directions, it is essential to verify the formulas for both directions.

11 Conclusions and recommendations

11.1 Linear Analysis Conclusions

Linear Buckling analysis: The buckling modes of the 9 shell models were observed. Ring buckling patterns, which are characterized by the buckling in the axial direction, occurred in:

Model 1-3 (a perfect cylinder under axial compression and radial tension).

Model 2-1 (a nearly cylinder with positive Gaussian curvature under axial compression).

Model 2-3 (a nearly cylinder with positive Gaussian curvature under axial compression and radial tension).

Model 3-3 (a nearly cylinder with negative Gaussian curvature under axial compression and radial tension).

Column buckling pattern, which involves buckling in the circumferential direction, was observed in:

Model 2-2 (a nearly cylinder with positive Gaussian curvature under axial compression and radial compression).

A combination of ring and column buckling, indicating both circumferential and axial deformation, was noted in:

Model 1-1 (a perfect cylinder under axial compression).

And in-extensional buckling patterns, where the load is carried primarily by bending rather than membrane forces, occurred in:

Model 1-2 (a perfect cylinder under axial compression and radial compression).

Model 3-1 (a nearly cylinder with negative Gaussian curvature under axial compression).

Model 3-2 (a nearly cylinder with negative Gaussian curvature under axial compression and radial compression).

For models with ring buckling patterns (1-3, 2-1, 2-3, 3-3), the critical membrane forces in the axial direction obtained from linear buckling and elastic analyses were similar to those from the buckling formula. For the model with a column buckling pattern (2-2), the critical membrane forces in the circumferential direction had a similar relationship. In the model with a ring and column pattern (1-1), the critical membrane forces in both directions were similar to the formula. In the models with in-extensional buckling (1-2, 3-1, 3-2), the buckling load factors were small.

Element Size Study: The influence length formula for choosing a finite element mesh is useful in most cases. It is essential to ensure there are at least 6 elements in an influence length. However, sometimes a smaller element size is required. For example, in some models like 1-3, 2-1, 2-3, 3-3, a smaller element size improved the accuracy as seen when comparing different element sizes such as 1.79m and 0.895m.

Model Scale Study: Changing the model scale while keeping the radius-to-thickness ratio constant generally doesn't affect the buckling patterns and critical membrane forces significantly. For example, when analyzing half-scale models with the same load, the buckling patterns changed as the scaling affected the similarity of membrane forces in the axial and circumferential directions. However, when the radial load was doubled and the Young's modulus was also doubled in the half-scale models to maintain the ratio of axial and circumferential membrane forces, the buckling patterns remained almost unchanged, and the critical membrane forces were very close to those of the original models. This further demonstrated that the scale of the model doesn't have a major impact on the critical membrane forces when the relevant factors are properly adjusted.

Buckling Modes Development: The buckling pattern of a cylinder under axial compression and different radial loads evolves from a ring and column pattern (under pure compression with no radial load) to a column buckling pattern (with increasing radial compression) and finally to a ring buckling pattern (with increasing radial tension). The buckling load factor increases with the increase in radial tension and decreases with the increase in radial compression. The buckling load factor is highly sensitive to the change of radial load, especially in the compression range where the negative impact is substantial, and in the tension range, it shows a trend of first increasing rapidly and then approaching a stable value.

Buckling Behavior Analysis of Model 2-1 when $n_{xx} = 0$: For Model 2-1, when the radial load is set to make the circumferential membrane force (n_{xx}) in the middle of the positively curved shell to be zero, the buckling mode was observed to be a ring buckling pattern and the buckling load factor doesn't change much. This indicates that up to $n_{xx} = 0$, the curvature in the axial direction has little influence. The hoop force n_{xx} does not change the buckling mode or buckling load factor, which confirms the shell buckling formula (4.1).

Boundary Conditions Study: The support conditions (hinged vs. fixed) have a limited impact on the shell's buckling patterns and buckling load factors. Shells with hinged supports are more likely to buckle near the support areas and tend to have slightly lower buckling load factors compared to those with fixed supports.

Model Height Study: For the ring and column buckling pattern (e.g., model 1-1), as the height increases, the buckling load factor shows a slight decrease, and the buckling mode remains relatively consistent with the characteristic ring and column pattern, although the number of "rows" may increase. For the column buckling pattern (e.g., model 1-2), the buckling load factor decreases significantly with the increase in height. For the ring buckling pattern (e.g., model 1-3), the buckling load factor also decreases gradually with height, and the number of ring buckles appears to increase. Overall, when designing shell structures, the height factor needs to be considered

comprehensively according to the specific buckling characteristics to ensure the structural safety and stability.

11.2 Nonlinear Analysis Conclusions

Imperfection Amplitude Study: The amplitude of imperfections significantly influences the buckling behavior of the structure. As the imperfection amplitude increases, the buckling pattern undergoes substantial changes in certain models, and the buckling load factor diminishes. Larger imperfection amplitudes make the structure more prone to buckling and reduce its load - bearing capacity.

Knockdown Factor Calculation: The knockdown factors depend on the curvatures, the imperfection amplitude and membrane forces. For some models, the knockdown factor formula may not be applicable in calculating the circumferential direction when the model has a perfect cylinder geometry (e.g., models 1-1, 1-2, 1-3). The knockdown factor for each model is determined based on the values in the circumferential and axial directions, considering the buckling pattern.

11.3 Overall Conclusions and Recommendations

Formula Verification: The knockdown factor formula gives a reasonable prediction of the buckling load for most models. There is a certain degree of agreement between the knockdown factor calculated by the formula and the ratio of the load factors obtained by finite element analysis. However, the dependence on a/t is substantial and does not occur in the formula. Clearly, the formula does not apply to in-extensional buckling.

Curve Fitted Knockdown Factor Formula: The fitted knockdown factor formula shows relatively close values for most models and imperfection amplitudes, indicating a certain degree of accuracy. The current formula still exhibits some degree of error, which may be due to insufficient data quantity. And the dependence on a/t is substantial and does not occur in the formula.

Future Research: For subsequent research, it will be imperative to enhance the fitting process by incorporating data from a more extensive array of models. Furthermore, the impact of the a/t ratio must be taken into account in future investigations. Future studies could focus on further improving the accuracy of the knockdown factor formula for special models and exploring more complex shell geometries and loading conditions. Moreover, investigating the interaction between different types of imperfections and their combined effect on the buckling behavior could provide more comprehensive understanding of thin - shell structures' behavior.

Literature

- [1] David Bushnell. Buckling of Shells-Pitfall for Designers. *AIAA Journal*, 19(9):1183-1226, September 1981.
- [2] J. Arbocz. Past, present and future of shell stability analysis. Technical report, Department of Aerospace Engineering, Delft University of Technology, Delft, 1981.
- [3] V.I. Weingarten, E.J. Morgan, P. Seide, “Elastic Stability of Thin-Walled Cylindrical and Conical Shells under combined Internal Pressure and Axial Compression”, *AIAA Journal*, Vol. 3, 1965, pp. 500-505.
- [4] P.C.J. Hoogenboom, Notes on shells, reader Delft University of Technology, online (Sept 2020) https://phoogenboom.nl/b17_schedule.html.
- [5] E.J. Giesen Loo, Quantifying the influence of membrane forces, curvature, and imperfections on the nonlinear buckling load of thin-shells, Additional Graduation Work Delft University of Technology, 2017, online (retrieved September 2020) https://phoogenboom.nl/b17_schedule.html.
- [6] J. Blaauwendraad and J.H. Hoefakker. *Structural Shell Analysis: Understanding and Application (Solid Mechanics and Its Application, v.200)*. Dordrecht, the Netherlands: Springer, 2013.
- [7] R.D. Ziemian. *Guide to Stability Design Criteria for Metal Structures*. Structural Research Council, Hoboken, N.J., U.S.: John Wiley and Sons, 2010.
- [8] Fan Ye, Local buckling analysis of thin-wall shell structures, Master’s report Delft University of Technology, 2015, online (retrieved September 2020) https://phoogenboom.nl/MSc_projects/reportFanYe.pdf
- [9] Hutchinson & Koiter W.T.J.W.,. “ Postbuckling Theory.” *Applied Mechanics Reviews*, 23(12), 1970: 1353-1363.
- [10] Koiter, Warner Tjardus. *Stability of Elastic Equilibrium*. Air Force Flight Dynamics Laboratory, 1970.
- [11] G. Cederbaum and J. Arbocz. Reliability of shells via Koiter formulas. *Thin-Walled Structures*, 24(2):173–187, January 1996.
- [12] Tian Chen, On introducing imperfection in the non-linear analysis of buckling of thin shell structures, Master’s report Delft University of Technology, 2014, online (retrieved September 2020) https://phoogenboom.nl/MSc_projects/reportTimChen.pdf
- [13] Xu Jie, Verification and optimisation of nonlinear shell buckling formula of thin-shell structures, Additional Graduation Work Delft University of Technology, 2018, online (retrieved September 2020) http://homepage.tudelft.nl/p3r3s/MSc_projects/reportJieXu.pdf
- [14] L.A. Samuelson, S. Eggwertz, “Shell Stability Handbook”, Elsevier Science Publishers LTD, Essex, 1992.
- [15] J. Arbocz, “Shell Buckling Research at Delft 1976-1996”, Report TU Delft,

1996.

Appendix 1

```

> #1-2-cylinder axial stress-fixed bottom support-double mesh size-radial compression load
> restart;
> a_x := 100-m: kxx := 1/a_x: kyy := 0: kxy := 0:
> nyy := -2000 * (kN/m): nxx := nyy: nxy := 0: eq := kxx-nxx + 2*kxy-nxy + kyy-nyy + pz = 0: pz := solve(eq, pz): evalf((pz-m^2)/kN):
      pz := 20 kN / m^2
      20.
(1)
> #1-3-cylinder axial stress-fixed bottom support-double mesh size-radial tensile load
> restart;
> a_x := 100-m: kxx := 1/a_x: kyy := 0: kxy := 0:
> nyy := -2000 * (kN/m): nxx := -nyy: nxy := 0: eq := kxx-nxx + 2*kxy-nxy + kyy-nyy + pz = 0: pz := solve(eq, pz): evalf((pz-m^2)/kN):
      pz := -20 kN / m^2
      -20.
(2)
> #2-2-Nearly cylinder with positive Gaussian Curvature under axial compression and radial compression
> restart;
> a_x := 100-m: kxx := -1/a_x: s := 5-m: l := 100-m: a_y := 0.5-s + 1/8 * (l^2/s): kyy := -1/a_y: kxy := 0:
> nyy := -2210.83 * (kN/m): nxx := nyy: nxy := 0: eq := kxx-nxx + 2*kxy-nxy + kyy-nyy + pz = 0: pz := solve(eq, pz): evalf((pz-m^2)/kN):
      pz := -30.86406238 kN / m^2
      -30.86406238
(3)
> #2-3-Nearly cylinder with positive Gaussian Curvature under axial compression and radial tension
> restart;
> a_x := 100-m: kxx := -1/a_x: s := 5-m: l := 100-m: a_y := 0.5-s + 1/8 * (l^2/s): kyy := 1/a_y: kxy := 0:
> nyy := -1856 * (kN/m): nxx := -nyy: nxy := 0: eq := kxx-nxx + 2*kxy-nxy + kyy-nyy + pz = 0: pz := solve(eq, pz): evalf((pz-m^2)/kN):
      pz := 11.20950495 kN / m^2
      11.20950495
(4)
> #3-2-Nearly cylinder with negative Gaussian Curvature under axial compression and radial compression
> restart;
> a_x := 100-m: kxx := -1/a_x: s := 5-m: l := 100-m: a_y := 0.5-s + 1/8 * (l^2/s): kyy := 1/a_y: kxy := 0:
> nyy := -2000 * (kN/m): nxx := nyy: nxy := 0: eq := kxx-nxx + 2*kxy-nxy + kyy-nyy + pz = 0: pz := solve(eq, pz): evalf((pz-m^2)/kN):
      pz := -12.07920792 kN / m^2
      -12.07920792
(5)
> #3-3-Nearly cylinder with negative Gaussian Curvature under axial compression and radial tension
> restart;
> a_x := 100-m: kxx := -1/a_x: s := 5-m: l := 100-m: a_y := 0.5-s + 1/8 * (l^2/s): kyy := 1/a_y: kxy := 0:
> nyy := -2096 * (kN/m): nxx := -nyy: nxy := 0: eq := kxx-nxx + 2*kxy-nxy + kyy-nyy + pz = 0: pz := solve(eq, pz): evalf((pz-m^2)/kN):
      pz := 29.26099010 kN / m^2
      29.26099010
(6)

```

Appendix 2

Imperfection amplitude: t

$\beta_1=1$			
\triangleright restart;			
\triangleright loadfactor = 10.94; P = -2000 $\frac{HN}{m}$; a_x_top = 100 m; a_x_middle = 100 m; a_y = m; pz = 0 $\frac{HN}{m^2}$; k_xx_middle = - $\frac{1}{a_x_middle}$; k_yy = $\frac{1}{a_y}$; k_xy = 0; r_xxy = 0;	$k_{xx_middle} = -\frac{1}{100\text{ m}}$	$k_{yy} = 0$	(1)
\triangleright r_yy = loadfactor P $\frac{a_x_top}{a_x_middle}$; evalf($\frac{r_{yy} m}{HN}$);	$r_{yy} = -\frac{21880.00000\text{ HN}}{m}$	-21880.00000	(2)
\triangleright eq = k_xx_middle r_xx + 2 k_xy r_xy + k_yy r_yy + loadfactor pz = 0; r_xx = solve(eq, r_xx); evalf($\frac{r_{xx} m}{HN}$);	$r_{xx} = 0$	0.	(3)
$\beta_1=2$			
\triangleright restart;			
\triangleright loadfactor = 2.81; P = -2000 $\frac{HN}{m}$; a_x_top = 100 m; a_x_middle = 100 m; a_y = m; pz = -20 $\frac{HN}{m^2}$; k_xx_middle = - $\frac{1}{a_x_middle}$; k_yy = $\frac{1}{a_y}$; k_xy = 0; r_xxy = 0;	$k_{xx_middle} = -\frac{1}{100\text{ m}}$	$k_{yy} = 0$	(4)
\triangleright r_yy = loadfactor P $\frac{a_x_top}{a_x_middle}$; evalf($\frac{r_{yy} m}{HN}$);	$r_{yy} = -\frac{5620.000000\text{ HN}}{m}$	-5620.000000	(5)
\triangleright eq = k_xx_middle r_xx + 2 k_xy r_xy + k_yy r_yy + loadfactor pz = 0; r_xx = solve(eq, r_xx); evalf($\frac{r_{xx} m}{HN}$);	$r_{xx} = \frac{5620.0\text{ HN}}{m}$	$-5620.$	(6)
$\beta_1=3$			
\triangleright restart;			
\triangleright loadfactor = 7.19; P = -2000 $\frac{HN}{m}$; a_x_top = 100 m; a_x_middle = 100 m; a_y = m; pz = 20 $\frac{HN}{m^2}$; k_xx_middle = - $\frac{1}{a_x_middle}$; k_yy = $\frac{1}{a_y}$; k_xy = 0; r_xxy = 0;	$k_{xx_middle} = -\frac{1}{100\text{ m}}$	$k_{yy} = 0$	(7)
\triangleright r_yy = loadfactor P $\frac{a_x_top}{a_x_middle}$; evalf($\frac{r_{yy} m}{HN}$);	$r_{yy} = -\frac{14380.00000\text{ HN}}{m}$	-14380.00000	(8)
\triangleright eq = k_xx_middle r_xx + 2 k_xy r_xy + k_yy r_yy + loadfactor pz = 0; r_xx = solve(eq, r_xx); evalf($\frac{r_{xx} m}{HN}$);	$r_{xx} = \frac{14380.0\text{ HN}}{m}$	14380.	(9)
$\beta_2=1$			
\triangleright restart;			
\triangleright loadfactor = 6.56; P = -2000 $\frac{HN}{m}$; a_x_top = 100 m; a_x_middle = 105 m; a_y = 252.5 m; pz = 0 $\frac{HN}{m^2}$; k_xx_middle = - $\frac{1}{a_x_middle}$; k_yy = $\frac{1}{a_y}$; k_xy = 0; r_xxy = 0;	$k_{xx_middle} = -\frac{1}{105\text{ m}}$	$k_{yy} = \frac{1}{252.5\text{ m}}$	(10)
\triangleright r_yy = loadfactor P $\frac{a_x_top}{a_x_middle}$; evalf($\frac{r_{yy} m}{HN}$);	$r_{yy} = -\frac{12495.23810\text{ HN}}{m}$	-12495.23810	(11)
\triangleright eq = k_xx_middle r_xx + 2 k_xy r_xy + k_yy r_yy + loadfactor pz = 0; r_xx = solve(eq, r_xx); evalf($\frac{r_{xx} m}{HN}$);	$r_{xx} = \frac{5196.039606\text{ HN}}{m}$	5196.039606	(12)
$\beta_2=2$			
\triangleright restart;			
\triangleright loadfactor = 2.81; P = -2000 $\frac{HN}{m}$; a_x_top = 100 m; a_x_middle = 105 m; a_y = 252.5 m; pz = -20 $\frac{HN}{m^2}$; k_xx_middle = - $\frac{1}{a_x_middle}$; k_yy = $\frac{1}{a_y}$; k_xy = 0; r_xxy = 0;	$k_{xx_middle} = -\frac{1}{105\text{ m}}$	$k_{yy} = \frac{1}{252.5\text{ m}}$	(13)
\triangleright r_yy = loadfactor P $\frac{a_x_top}{a_x_middle}$; evalf($\frac{r_{yy} m}{HN}$);	$r_{yy} = -\frac{5352.380952\text{ HN}}{m}$	-5352.380952	(14)
\triangleright eq = k_xx_middle r_xx + 2 k_xy r_xy + k_yy r_yy + loadfactor pz = 0; r_xx = solve(eq, r_xx); evalf($\frac{r_{xx} m}{HN}$);	$r_{xx} = \frac{5740.607425\text{ HN}}{m}$	-5740.607425	(15)
$\beta_2=3$			
\triangleright restart;			
\triangleright loadfactor = 7.19; P = -2000 $\frac{HN}{m}$; a_x_top = 100 m; a_x_middle = 105 m; a_y = 252.5 m; pz = 10 $\frac{HN}{m^2}$; k_xx_middle = - $\frac{1}{a_x_middle}$; k_yy = $\frac{1}{a_y}$; k_xy = 0; r_xxy = 0;	$k_{xx_middle} = -\frac{1}{105\text{ m}}$	$k_{yy} = \frac{1}{252.5\text{ m}}$	(16)
\triangleright r_yy = loadfactor P $\frac{a_x_top}{a_x_middle}$; evalf($\frac{r_{yy} m}{HN}$);	$r_{yy} = -\frac{13895.23810\text{ HN}}{m}$	-13895.23810	(17)
\triangleright eq = k_xx_middle r_xx + 2 k_xy r_xy + k_yy r_yy + loadfactor pz = 0; r_xx = solve(eq, r_xx); evalf($\frac{r_{xx} m}{HN}$);	$r_{xx} = \frac{13244.54950\text{ HN}}{m}$	13244.54950	(18)

```

> s3-1
> restart;
> loadfactor = 6.56 : P = -2000  $\frac{kN}{m}$  ; a_x_top = 100 m ; a_x_middle = 95 m ; a_y = 252.5 m ; p2 = 0  $\frac{kN}{m^2}$  ; k_xx_middle = - $\frac{1}{a_x\_middle}$  ; k_yy =  $\frac{1}{a_y}$  ; k_xy = 0 ; n_x = 0 ;
      k_xx_middle = - $\frac{1}{95 \text{ m}}$ 
      k_yy =  $\frac{0.003960396040}{\text{m}}$ 
(19)
> n_yy = loadfactor P  $\frac{a_x\_top}{a_x\_middle}$  ; evalf( $\frac{n_yy \text{ m}}{kN}$ );
      n_yy = - $\frac{13810.52832 \text{ kN}}{\text{m}}$ 
      -13810.52832
(20)
> eq = k_xx_middle n_xx + 2 k_xy n_xy + k_yy n_yy + loadfactor p2 = 0 ; n_xx = solve(eq, n_xx); evalf( $\frac{n_xx \text{ m}}{kN}$ );
      n_xx = - $\frac{5196.039606 \text{ kN}}{\text{m}}$ 
      -5196.039606
(21)
> s3-2
> restart;
> loadfactor = 4.00 : P = -2000  $\frac{kN}{m}$  ; a_x_top = 100 m ; a_x_middle = 95 m ; a_y = 252.5 m ; p2 = -12  $\frac{kN}{m^2}$  ; k_xx_middle = - $\frac{1}{a_x\_middle}$  ; k_yy =  $\frac{1}{a_y}$  ; k_xy = 0 ; n_x = 0 ;
      k_xx_middle = - $\frac{1}{95 \text{ m}}$ 
      k_yy =  $\frac{0.003960396040}{\text{m}}$ 
(22)
> n_yy = loadfactor P  $\frac{a_x\_top}{a_x\_middle}$  ; evalf( $\frac{n_yy \text{ m}}{kN}$ );
      n_yy = - $\frac{8547.368421 \text{ kN}}{\text{m}}$ 
      -8547.368421
(23)
> eq = k_xx_middle n_xx + 2 k_xy n_xy + k_yy n_yy + loadfactor p2 = 0 ; n_xx = solve(eq, n_xx); evalf( $\frac{n_xx \text{ m}}{kN}$ );
      n_xx = - $\frac{7844.241585 \text{ kN}}{\text{m}}$ 
      -7844.241585
(24)
> s3-3
> restart;
> loadfactor = 6.56 : P = -2000  $\frac{kN}{m}$  ; a_x_top = 100 m ; a_x_middle = 95 m ; a_y = 252.5 m ; p2 = 32.5  $\frac{kN}{m^2}$  ; k_xx_middle = - $\frac{1}{a_x\_middle}$  ; k_yy =  $\frac{1}{a_y}$  ; k_xy = 0 ; n_x = 0 ;
      k_xx_middle = - $\frac{1}{95 \text{ m}}$ 
      k_yy =  $\frac{0.003960396040}{\text{m}}$ 
(25)
> n_yy = loadfactor P  $\frac{a_x\_top}{a_x\_middle}$  ; evalf( $\frac{n_yy \text{ m}}{kN}$ );
      n_yy = - $\frac{13810.52832 \text{ kN}}{\text{m}}$ 
      -13810.52832
(26)
> eq = k_xx_middle n_xx + 2 k_xy n_xy + k_yy n_yy + loadfactor p2 = 0 ; n_xx = solve(eq, n_xx); evalf( $\frac{n_xx \text{ m}}{kN}$ );
      n_xx =  $\frac{15057.96039 \text{ kN}}{\text{m}}$ 
      15057.96039
(27)

```

Imperfection amplitude: 0.5t

```

> s1-1
> restart;
> loadfactor = 10.94 : P = -2000  $\frac{kN}{m}$  ; a_x_top = 100 m ; a_x_middle = 100 m ; a_y = 0 ; p2 = 0  $\frac{kN}{m^2}$  ; k_xx_middle = - $\frac{1}{a_x\_middle}$  ; k_yy =  $\frac{1}{a_y}$  ; k_xy = 0 ; n_x = 0 ;
      k_xx_middle = - $\frac{1}{100 \text{ m}}$ 
      k_yy = 0
(1)
> n_yy = loadfactor P  $\frac{a_x\_top}{a_x\_middle}$  ; evalf( $\frac{n_yy \text{ m}}{kN}$ );
      n_yy = - $\frac{21880.00000 \text{ kN}}{\text{m}}$ 
      -21880.00000
(2)
> eq = k_xx_middle n_xx + 2 k_xy n_xy + k_yy n_yy + loadfactor p2 = 0 ; n_xx = solve(eq, n_xx); evalf( $\frac{n_xx \text{ m}}{kN}$ );
      n_xx = 0
      0.
(3)
> s1-2
> restart;
> loadfactor = 2.81 : P = -2000  $\frac{kN}{m}$  ; a_x_top = 100 m ; a_x_middle = 100 m ; a_y = 0 ; p2 = -20  $\frac{kN}{m^2}$  ; k_xx_middle = - $\frac{1}{a_x\_middle}$  ; k_yy =  $\frac{1}{a_y}$  ; k_xy = 0 ; n_x = 0 ;
      k_xx_middle = - $\frac{1}{100 \text{ m}}$ 
      k_yy = 0
(4)
> n_yy = loadfactor P  $\frac{a_x\_top}{a_x\_middle}$  ; evalf( $\frac{n_yy \text{ m}}{kN}$ );
      n_yy = - $\frac{5620.00000 \text{ kN}}{\text{m}}$ 
      -5620.00000
(5)
> eq = k_xx_middle n_xx + 2 k_xy n_xy + k_yy n_yy + loadfactor p2 = 0 ; n_xx = solve(eq, n_xx); evalf( $\frac{n_xx \text{ m}}{kN}$ );
      n_xx = - $\frac{5620. \text{ kN}}{\text{m}}$ 
      -5620.
(6)
> s1-3
> restart;
> loadfactor = 11.56 : P = -2000  $\frac{kN}{m}$  ; a_x_top = 100 m ; a_x_middle = 100 m ; a_y = 0 ; p2 = 20  $\frac{kN}{m^2}$  ; k_xx_middle = - $\frac{1}{a_x\_middle}$  ; k_yy =  $\frac{1}{a_y}$  ; k_xy = 0 ; n_x = 0 ;
      k_xx_middle = - $\frac{1}{100 \text{ m}}$ 
      k_yy = 0
(7)
> n_yy = loadfactor P  $\frac{a_x\_top}{a_x\_middle}$  ; evalf( $\frac{n_yy \text{ m}}{kN}$ );
      n_yy = - $\frac{23120.00000 \text{ kN}}{\text{m}}$ 
      -23120.00000
(8)
> eq = k_xx_middle n_xx + 2 k_xy n_xy + k_yy n_yy + loadfactor p2 = 0 ; n_xx = solve(eq, n_xx); evalf( $\frac{n_xx \text{ m}}{kN}$ );
      n_xx =  $\frac{23120. \text{ kN}}{\text{m}}$ 
      23120.
(9)
> s2-1
> restart;
> loadfactor = 8.69 : P = -2000  $\frac{kN}{m}$  ; a_x_top = 100 m ; a_x_middle = 105 m ; a_y = 252.5 m ; p2 = 0  $\frac{kN}{m^2}$  ; k_xx_middle = - $\frac{1}{a_x\_middle}$  ; k_yy =  $\frac{1}{a_y}$  ; k_xy = 0 ; n_x = 0 ;
      k_xx_middle = - $\frac{1}{105 \text{ m}}$ 
      k_yy =  $\frac{0.003960396040}{\text{m}}$ 
(10)
> n_yy = loadfactor P  $\frac{a_x\_top}{a_x\_middle}$  ; evalf( $\frac{n_yy \text{ m}}{kN}$ );
      n_yy = - $\frac{18457.14296 \text{ kN}}{\text{m}}$ 
      -18457.14296
(11)
> eq = k_xx_middle n_xx + 2 k_xy n_xy + k_yy n_yy + loadfactor p2 = 0 ; n_xx = solve(eq, n_xx); evalf( $\frac{n_xx \text{ m}}{kN}$ );
      n_xx =  $\frac{7675.247526 \text{ kN}}{\text{m}}$ 
      7675.247526
(12)

```

```

s2-2
> restart;
> loadfactor = 4.69 : P = -2000  $\frac{kN}{m}$  : a_x_top = 100 m : a_x_middle = 105 m : a_y = 252.5 m : pz = -27  $\frac{kN}{m^2}$  : k_xx_middle = - $\frac{1}{a_x\_middle}$  : k_yy = - $\frac{1}{a_y}$  : k_xy = 0 : n_xy = 0 :
k_xx_middle = - $\frac{1}{105}$ 
k_yy =  $\frac{0.003960396040}{m}$ 
(13)
> n_yy = loadfactor P  $\frac{a_x\_top}{a_x\_middle}$  : evalf( $\frac{n_yy}{kN}$ ):
n_yy =  $\frac{-8933.333333}{m}$ 
-8933.333333
(14)
> eq = k_xx_middle n_xx + 2 k_xy n_xy + k_yy n_yy + loadfactor pz = 0 : n_xx = solve(eq, n_xx); evalf( $\frac{n_xx}{kN}$ ):
n_xx =  $\frac{-9581.298514}{m}$ 
-9581.298514
(15)

s2-3
> restart;
> loadfactor = 12.19 : P = -2000  $\frac{kN}{m}$  : a_x_top = 100 m : a_x_middle = 105 m : a_y = 252.5 m : pz = 10  $\frac{kN}{m^2}$  : k_xx_middle = - $\frac{1}{a_x\_middle}$  : k_yy = - $\frac{1}{a_y}$  : k_xy = 0 : n_xy = 0 :
k_xx_middle = - $\frac{1}{105}$ 
k_yy =  $\frac{0.003960396040}{m}$ 
(16)
> n_yy = loadfactor P  $\frac{a_x\_top}{a_x\_middle}$  : evalf( $\frac{n_yy}{kN}$ ):
n_yy =  $\frac{-23219.04762}{m}$ 
-23219.04762
(17)
> eq = k_xx_middle n_xx + 2 k_xy n_xy + k_yy n_yy + loadfactor pz = 0 : n_xx = solve(eq, n_xx); evalf( $\frac{n_xx}{kN}$ ):
n_xx =  $\frac{22454.94554}{m}$ 
22454.94554
(18)

s3-1
> restart;
> loadfactor = 6.56 : P = -2000  $\frac{kN}{m}$  : a_x_top = 100 m : a_x_middle = 95 m : a_y = 252.5 m : pz = 0  $\frac{kN}{m^2}$  : k_xx_middle = - $\frac{1}{a_x\_middle}$  : k_yy =  $\frac{1}{a_y}$  : k_xy = 0 : n_xy = 0 :
k_xx_middle = - $\frac{1}{95}$ 
k_yy =  $\frac{0.003960396040}{m}$ 
(19)
> n_yy = loadfactor P  $\frac{a_x\_top}{a_x\_middle}$  : evalf( $\frac{n_yy}{kN}$ ):
n_yy =  $\frac{-13810.52832}{m}$ 
-13810.52832
(20)
> eq = k_xx_middle n_xx + 2 k_xy n_xy + k_yy n_yy + loadfactor pz = 0 : n_xx = solve(eq, n_xx); evalf( $\frac{n_xx}{kN}$ ):
n_xx =  $\frac{-5196.039606}{m}$ 
-5196.039606
(21)

s3-2
> restart;
> loadfactor = 4.06 : P = -2000  $\frac{kN}{m}$  : a_x_top = 100 m : a_x_middle = 95 m : a_y = 252.5 m : pz = -12  $\frac{kN}{m^2}$  : k_xx_middle = - $\frac{1}{a_x\_middle}$  : k_yy =  $\frac{1}{a_y}$  : k_xy = 0 : n_xy = 0 :
k_xx_middle = - $\frac{1}{95}$ 
k_yy =  $\frac{0.003960396040}{m}$ 
(22)
> n_yy = loadfactor P  $\frac{a_x\_top}{a_x\_middle}$  : evalf( $\frac{n_yy}{kN}$ ):
n_yy =  $\frac{-8547.368421}{m}$ 
-8547.368421
(23)
> eq = k_xx_middle n_xx + 2 k_xy n_xy + k_yy n_yy + loadfactor pz = 0 : n_xx = solve(eq, n_xx); evalf( $\frac{n_xx}{kN}$ ):
n_xx =  $\frac{-7844.241585}{m}$ 
-7844.241585
(24)

s3-3
> restart;
> loadfactor = 10.31 : P = -2000  $\frac{kN}{m}$  : a_x_top = 100 m : a_x_middle = 95 m : a_y = 252.5 m : pz = 32.5  $\frac{kN}{m^2}$  : k_xx_middle = - $\frac{1}{a_x\_middle}$  : k_yy =  $\frac{1}{a_y}$  : k_xy = 0 : n_xy = 0 :
k_xx_middle = - $\frac{1}{95}$ 
k_yy =  $\frac{0.003960396040}{m}$ 
(25)
> n_yy = loadfactor P  $\frac{a_x\_top}{a_x\_middle}$  : evalf( $\frac{n_yy}{kN}$ ):
n_yy =  $\frac{-21705.28316}{m}$ 
-21705.28316
(26)
> eq = k_xx_middle n_xx + 2 k_xy n_xy + k_yy n_yy + loadfactor pz = 0 : n_xx = solve(eq, n_xx); evalf( $\frac{n_xx}{kN}$ ):
n_xx =  $\frac{23665.78836}{m}$ 
23665.78836
(27)

```

Imperfection amplitude: 2t

```

s1-1
> restart;
> loadfactor = 11.56 : P = -2000  $\frac{kN}{m}$  : a_x_top = 100 m : a_x_middle = 100 m : a_y = : pz = 0  $\frac{kN}{m^2}$  : k_xx_middle = - $\frac{1}{a_x\_middle}$  : k_yy =  $\frac{1}{a_y}$  : k_xy = 0 : n_xy = 0 :
k_xx_middle = - $\frac{1}{100}$ 
k_yy = 0
(1)
> n_yy = loadfactor P  $\frac{a_x\_top}{a_x\_middle}$  : evalf( $\frac{n_yy}{kN}$ ):
n_yy =  $\frac{-23120.00000}{m}$ 
-23120.00000
(2)
> eq = k_xx_middle n_xx + 2 k_xy n_xy + k_yy n_yy + loadfactor pz = 0 : n_xx = solve(eq, n_xx); evalf( $\frac{n_xx}{kN}$ ):
n_xx = 0
0
(3)

s1-2
> restart;
> loadfactor = 2.81 : P = -2000  $\frac{kN}{m}$  : a_x_top = 100 m : a_x_middle = 100 m : a_y = : pz = -20  $\frac{kN}{m^2}$  : k_xx_middle = - $\frac{1}{a_x\_middle}$  : k_yy =  $\frac{1}{a_y}$  : k_xy = 0 : n_xy = 0 :
k_xx_middle = - $\frac{1}{100}$ 
k_yy = 0
(4)
> n_yy = loadfactor P  $\frac{a_x\_top}{a_x\_middle}$  : evalf( $\frac{n_yy}{kN}$ ):
n_yy =  $\frac{-5620.000000}{m}$ 
-5620.000000
(5)
> eq = k_xx_middle n_xx + 2 k_xy n_xy + k_yy n_yy + loadfactor pz = 0 : n_xx = solve(eq, n_xx); evalf( $\frac{n_xx}{kN}$ ):
n_xx =  $\frac{-5620.}{m}$ 
-5620.
(6)

```

```

k1-3
restart;
> loadfactor = 4.69; P = -2000  $\frac{kN}{m}$ ; a_x_top = 100 m; a_x_middle = 100 m; a_y = 0; ps = 20  $\frac{kN}{m^2}$ ; k_xx_middle = - $\frac{1}{a_x\_middle}$ ; k_yy =  $\frac{1}{a_y}$ ; k_xy = 0; n_xy = 0;
k_xx_middle = - $\frac{1}{100 m}$ 
k_yy = 0
(7)
> n_yy = loadfactor P  $\frac{a_x\_top}{a_x\_middle}$  evalf( $\frac{n_yy m}{kN}$ );
n_yy = - $\frac{9380.000000 kN}{m}$ 
-9380.000000
(8)
> eq = k_xx_middle n_xx + 2 k_xy n_xy + k_yy n_yy + loadfactor ps = 0; n_xx = solve(eq, n_xx); evalf( $\frac{n_xx m}{kN}$ );
n_xx =  $\frac{9380. kN}{m}$ 
9380.
(9)

k2-1
restart;
> loadfactor = 4.06; P = -2000  $\frac{kN}{m}$ ; a_x_top = 100 m; a_x_middle = 105 m; a_y = 252.5 m; ps = 0  $\frac{kN}{m^2}$ ; k_xx_middle = - $\frac{1}{a_x\_middle}$ ; k_yy = - $\frac{1}{a_y}$ ; k_xy = 0; n_xy = 0;
k_xx_middle = - $\frac{1}{105 m}$ 
k_yy = - $\frac{0.003960396040}{m}$ 
(10)
> n_yy = loadfactor P  $\frac{a_x\_top}{a_x\_middle}$  evalf( $\frac{n_yy m}{kN}$ );
n_yy = - $\frac{7733.333333 kN}{m}$ 
-7733.333333
(11)
> eq = k_xx_middle n_xx + 2 k_xy n_xy + k_yy n_yy + loadfactor ps = 0; n_xx = solve(eq, n_xx); evalf( $\frac{n_xx m}{kN}$ );
n_xx =  $\frac{3215.841585 kN}{m}$ 
3215.841585
(12)

k2-2
restart;
> loadfactor = 2.19; P = -2000  $\frac{kN}{m}$ ; a_x_top = 100 m; a_x_middle = 105 m; a_y = 252.5 m; ps = -27  $\frac{kN}{m^2}$ ; k_xx_middle = - $\frac{1}{a_x\_middle}$ ; k_yy = - $\frac{1}{a_y}$ ; k_xy = 0; n_xy = 0;
k_xx_middle = - $\frac{1}{105 m}$ 
k_yy = - $\frac{0.003960396040}{m}$ 
(13)
> n_yy = loadfactor P  $\frac{a_x\_top}{a_x\_middle}$  evalf( $\frac{n_yy m}{kN}$ );
n_yy = - $\frac{4171.428571 kN}{m}$ 
-4171.428571
(14)
> eq = k_xx_middle n_xx + 2 k_xy n_xy + k_yy n_yy + loadfactor ps = 0; n_xx = solve(eq, n_xx); evalf( $\frac{n_xx m}{kN}$ );
n_xx = - $\frac{4473.996535 kN}{m}$ 
-4473.996535
(15)

k2-3
restart;
> loadfactor = 4.69; P = -2000  $\frac{kN}{m}$ ; a_x_top = 100 m; a_x_middle = 105 m; a_y = 252.5 m; ps = 10  $\frac{kN}{m^2}$ ; k_xx_middle = - $\frac{1}{a_x\_middle}$ ; k_yy = - $\frac{1}{a_y}$ ; k_xy = 0; n_xy = 0;
k_xx_middle = - $\frac{1}{105 m}$ 
k_yy = - $\frac{0.003960396040}{m}$ 
(16)
> n_yy = loadfactor P  $\frac{a_x\_top}{a_x\_middle}$  evalf( $\frac{n_yy m}{kN}$ );
n_yy =  $\frac{8933.333333 kN}{m}$ 
-8933.333333
(17)
> eq = k_xx_middle n_xx + 2 k_xy n_xy + k_yy n_yy + loadfactor ps = 0; n_xx = solve(eq, n_xx); evalf( $\frac{n_xx m}{kN}$ );
n_xx =  $\frac{8639.351486 kN}{m}$ 
8639.351486
(18)

k3-1
restart;
> loadfactor = 6.56; P = -2000  $\frac{kN}{m}$ ; a_x_top = 100 m; a_x_middle = 95 m; a_y = 252.5 m; ps = 0  $\frac{kN}{m^2}$ ; k_xx_middle = - $\frac{1}{a_x\_middle}$ ; k_yy =  $\frac{1}{a_y}$ ; k_xy = 0; n_xy = 0;
k_xx_middle = - $\frac{1}{95 m}$ 
k_yy =  $\frac{0.003960396040}{m}$ 
(19)
> n_yy = loadfactor P  $\frac{a_x\_top}{a_x\_middle}$  evalf( $\frac{n_yy m}{kN}$ );
n_yy = - $\frac{13810.52832 kN}{m}$ 
-13810.52832
(20)
> eq = k_xx_middle n_xx + 2 k_xy n_xy + k_yy n_yy + loadfactor ps = 0; n_xx = solve(eq, n_xx); evalf( $\frac{n_xx m}{kN}$ );
n_xx = - $\frac{5196.039606 kN}{m}$ 
-5196.039606
(21)

k3-2
restart;
> loadfactor = 4.06; P = -2000  $\frac{kN}{m}$ ; a_x_top = 100 m; a_x_middle = 95 m; a_y = 252.5 m; ps = -12  $\frac{kN}{m^2}$ ; k_xx_middle = - $\frac{1}{a_x\_middle}$ ; k_yy =  $\frac{1}{a_y}$ ; k_xy = 0; n_xy = 0;
k_xx_middle = - $\frac{1}{95 m}$ 
k_yy =  $\frac{0.003960396040}{m}$ 
(22)
> n_yy = loadfactor P  $\frac{a_x\_top}{a_x\_middle}$  evalf( $\frac{n_yy m}{kN}$ );
n_yy = - $\frac{8547.368421 kN}{m}$ 
-8547.368421
(23)
> eq = k_xx_middle n_xx + 2 k_xy n_xy + k_yy n_yy + loadfactor ps = 0; n_xx = solve(eq, n_xx); evalf( $\frac{n_xx m}{kN}$ );
n_xx = - $\frac{7844.241585 kN}{m}$ 
-7844.241585
(24)

k3-3
restart;
> loadfactor = 4.69; P = -2000  $\frac{kN}{m}$ ; a_x_top = 100 m; a_x_middle = 95 m; a_y = 252.5 m; ps = 32.5  $\frac{kN}{m^2}$ ; k_xx_middle = - $\frac{1}{a_x\_middle}$ ; k_yy =  $\frac{1}{a_y}$ ; k_xy = 0; n_xy = 0;
k_xx_middle = - $\frac{1}{95 m}$ 
k_yy =  $\frac{0.003960396040}{m}$ 
(25)
> n_yy = loadfactor P  $\frac{a_x\_top}{a_x\_middle}$  evalf( $\frac{n_yy m}{kN}$ );
n_yy = - $\frac{9873.684211 kN}{m}$ 
-9873.684211
(26)
> eq = k_xx_middle n_xx + 2 k_xy n_xy + k_yy n_yy + loadfactor ps = 0; n_xx = solve(eq, n_xx); evalf( $\frac{n_xx m}{kN}$ );
n_xx =  $\frac{10765.52352 kN}{m}$ 
10765.52352
(27)

```

Imperfection amplitude: 4t

```

s1-1
restart;
> loadfactor = 0.56; P = -2000  $\frac{HN}{m}$ ; a_x_top = 100 m; a_x_middle = 100 m; a_y = m; pz = 0  $\frac{HN}{m^2}$ ; k_xx_middle = - $\frac{1}{a_x\_middle}$ ; k_yy =  $\frac{1}{a_y}$ ; k_xy = 0; n_xy = 0;

$$k\_xx\_middle = -\frac{1}{100 m}$$


$$k\_yy = 0$$

(1)
> n_yy = loadfactor P  $\frac{a_x\_top}{a_x\_middle}$ ; evalf( $\frac{n\_yy m}{HN}$ );

$$n\_yy = -\frac{13120.00000 HN}{m}$$

(2)
> eq = k_xx\_middle n_xx + 2 k_xy n_xy + k_yy n_yy + loadfactor pz = 0; n_xx = solve(eq, n_xx); evalf( $\frac{n\_xx m}{HN}$ );

$$n\_xx = 0$$

(3)

s1-2
restart;
> loadfactor = 3.44; P = -2000  $\frac{HN}{m}$ ; a_x_top = 100 m; a_x_middle = 100 m; a_y = m; pz = -20  $\frac{HN}{m^2}$ ; k_xx_middle = - $\frac{1}{a_x\_middle}$ ; k_yy =  $\frac{1}{a_y}$ ; k_xy = 0; n_xy = 0;

$$k\_xx\_middle = -\frac{1}{100 m}$$


$$k\_yy = 0$$

(4)
> n_yy = loadfactor P  $\frac{a_x\_top}{a_x\_middle}$ ; evalf( $\frac{n\_yy m}{HN}$ );

$$n\_yy = -\frac{6880.00000 HN}{m}$$

(5)
> eq = k_xx\_middle n_xx + 2 k_xy n_xy + k_yy n_yy + loadfactor pz = 0; n_xx = solve(eq, n_xx); evalf( $\frac{n\_xx m}{HN}$ );

$$n\_xx = -\frac{6880. HN}{m}$$

(6)

s1-3
restart;
> loadfactor = 4.06; P = -2000  $\frac{HN}{m}$ ; a_x_top = 100 m; a_x_middle = 100 m; a_y = m; pz = 20  $\frac{HN}{m^2}$ ; k_xx_middle = - $\frac{1}{a_x\_middle}$ ; k_yy =  $\frac{1}{a_y}$ ; k_xy = 0; n_xy = 0;

$$k\_xx\_middle = -\frac{1}{100 m}$$


$$k\_yy = 0$$

(7)
> n_yy = loadfactor P  $\frac{a_x\_top}{a_x\_middle}$ ; evalf( $\frac{n\_yy m}{HN}$ );

$$n\_yy = -\frac{8120.00000 HN}{m}$$

(8)
> eq = k_xx\_middle n_xx + 2 k_xy n_xy + k_yy n_yy + loadfactor pz = 0; n_xx = solve(eq, n_xx); evalf( $\frac{n\_xx m}{HN}$ );

$$n\_xx = \frac{8120. HN}{m}$$

(9)

s2-1
restart;
> loadfactor = 3.44; P = -2000  $\frac{HN}{m}$ ; a_x_top = 100 m; a_x_middle = 105 m; a_y = 252.5 m; pz = 0  $\frac{HN}{m^2}$ ; k_xx_middle = - $\frac{1}{a_x\_middle}$ ; k_yy =  $\frac{1}{a_y}$ ; k_xy = 0; n_xy = 0;

$$k\_xx\_middle = -\frac{1}{105 m}$$


$$k\_yy = \frac{0.003960396040}{m}$$

(10)
> n_yy = loadfactor P  $\frac{a_x\_top}{a_x\_middle}$ ; evalf( $\frac{n\_yy m}{HN}$ );

$$n\_yy = -\frac{5932.380992 HN}{m}$$

(11)
> eq = k_xx\_middle n_xx + 2 k_xy n_xy + k_yy n_yy + loadfactor pz = 0; n_xx = solve(eq, n_xx); evalf( $\frac{n\_xx m}{HN}$ );

$$n\_xx = \frac{2724.732475 HN}{m}$$

(12)

s2-2
restart;
> loadfactor = 2.81; P = -2000  $\frac{HN}{m}$ ; a_x_top = 100 m; a_x_middle = 105 m; a_y = 252.5 m; pz = -27  $\frac{HN}{m^2}$ ; k_xx_middle = - $\frac{1}{a_x\_middle}$ ; k_yy =  $\frac{1}{a_y}$ ; k_xy = 0; n_xy = 0;

$$k\_xx\_middle = -\frac{1}{105 m}$$


$$k\_yy = \frac{0.003960396040}{m}$$

(13)
> n_yy = loadfactor P  $\frac{a_x\_top}{a_x\_middle}$ ; evalf( $\frac{n\_yy m}{HN}$ );

$$n\_yy = -\frac{5932.380992 HN}{m}$$

(14)
> eq = k_xx\_middle n_xx + 2 k_xy n_xy + k_yy n_yy + loadfactor pz = 0; n_xx = solve(eq, n_xx); evalf( $\frac{n\_xx m}{HN}$ );

$$n\_xx = -\frac{5740.607425 HN}{m}$$

(15)

s2-3
restart;
> loadfactor = 4.06; P = -2000  $\frac{HN}{m}$ ; a_x_top = 100 m; a_x_middle = 105 m; a_y = 252.5 m; pz = 10  $\frac{HN}{m^2}$ ; k_xx_middle = - $\frac{1}{a_x\_middle}$ ; k_yy =  $\frac{1}{a_y}$ ; k_xy = 0; n_xy = 0;

$$k\_xx\_middle = -\frac{1}{105 m}$$


$$k\_yy = \frac{0.003960396040}{m}$$

(16)
> n_yy = loadfactor P  $\frac{a_x\_top}{a_x\_middle}$ ; evalf( $\frac{n\_yy m}{HN}$ );

$$n\_yy = -\frac{7733.333333 HN}{m}$$

(17)
> eq = k_xx\_middle n_xx + 2 k_xy n_xy + k_yy n_yy + loadfactor pz = 0; n_xx = solve(eq, n_xx); evalf( $\frac{n\_xx m}{HN}$ );

$$n\_xx = \frac{7478.841385 HN}{m}$$

(18)

s3-1
restart;
> loadfactor = 5.31; P = -2000  $\frac{HN}{m}$ ; a_x_top = 100 m; a_x_middle = 95 m; a_y = 252.5 m; pz = 0  $\frac{HN}{m^2}$ ; k_xx_middle = - $\frac{1}{a_x\_middle}$ ; k_yy =  $\frac{1}{a_y}$ ; k_xy = 0; n_xy = 0;

$$k\_xx\_middle = -\frac{1}{95 m}$$


$$k\_yy = \frac{0.003960396040}{m}$$

(19)
> n_yy = loadfactor P  $\frac{a_x\_top}{a_x\_middle}$ ; evalf( $\frac{n\_yy m}{HN}$ );

$$n\_yy = -\frac{11178.94737 HN}{m}$$

(20)
> eq = k_xx\_middle n_xx + 2 k_xy n_xy + k_yy n_yy + loadfactor pz = 0; n_xx = solve(eq, n_xx); evalf( $\frac{n\_xx m}{HN}$ );

$$n\_xx = -\frac{4205.940596 HN}{m}$$

(21)

s3-2
restart;
> loadfactor = 3.44; P = -2000  $\frac{HN}{m}$ ; a_x_top = 100 m; a_x_middle = 95 m; a_y = 252.5 m; pz = -12  $\frac{HN}{m^2}$ ; k_xx_middle = - $\frac{1}{a_x\_middle}$ ; k_yy =  $\frac{1}{a_y}$ ; k_xy = 0; n_xy = 0;

$$k\_xx\_middle = -\frac{1}{95 m}$$


$$k\_yy = \frac{0.003960396040}{m}$$

(22)
> n_yy = loadfactor P  $\frac{a_x\_top}{a_x\_middle}$ ; evalf( $\frac{n\_yy m}{HN}$ );

$$n\_yy = -\frac{7242.103263 HN}{m}$$

(23)
> eq = k_xx\_middle n_xx + 2 k_xy n_xy + k_yy n_yy + loadfactor pz = 0; n_xx = solve(eq, n_xx); evalf( $\frac{n\_xx m}{HN}$ );

$$n\_xx = -\frac{6646.352475 HN}{m}$$

(24)

```

```

> a3-3
> restart;
> loadfactor := 3.44; P := -2000  $\frac{\text{kN}}{\text{m}}$ ; a_x_top := 100 \text{ m}; a_x_middle := 95 \text{ m}; a_y := 252.5 \text{ m}; ps := 32.5  $\frac{\text{kN}}{\text{m}^2}$ ; k_xx_middle := - $\frac{1}{a_x\_middle}$ ; k_yy :=  $\frac{1}{a_y}$ ; k_xy := 0; n_xy := 0;
k_xx_middle := - $\frac{1}{95 \text{ m}}$ 
k_yy :=  $\frac{0.003960396040}{\text{m}}$ 
(25)
> n_yy := loadfactor P  $\frac{a_x\_top}{a_x\_middle}$ ; evalf( $\frac{n_yy \text{ m}}{\text{kN}}$ );
n_yy := - $\frac{7242.105283 \text{ kN}}{\text{m}}$ 
-7242.105283
(26)
> eq := k_xx_middle n_xx + 2 k_xy n_xy + k_yy n_yy + loadfactor ps = 0; n_xx := solve(eq, n_xx); evalf( $\frac{n_xx \text{ m}}{\text{kN}}$ );
n_xx :=  $\frac{7896.247325 \text{ kN}}{7896.247325}$ 
(27)

```

Appendix 3

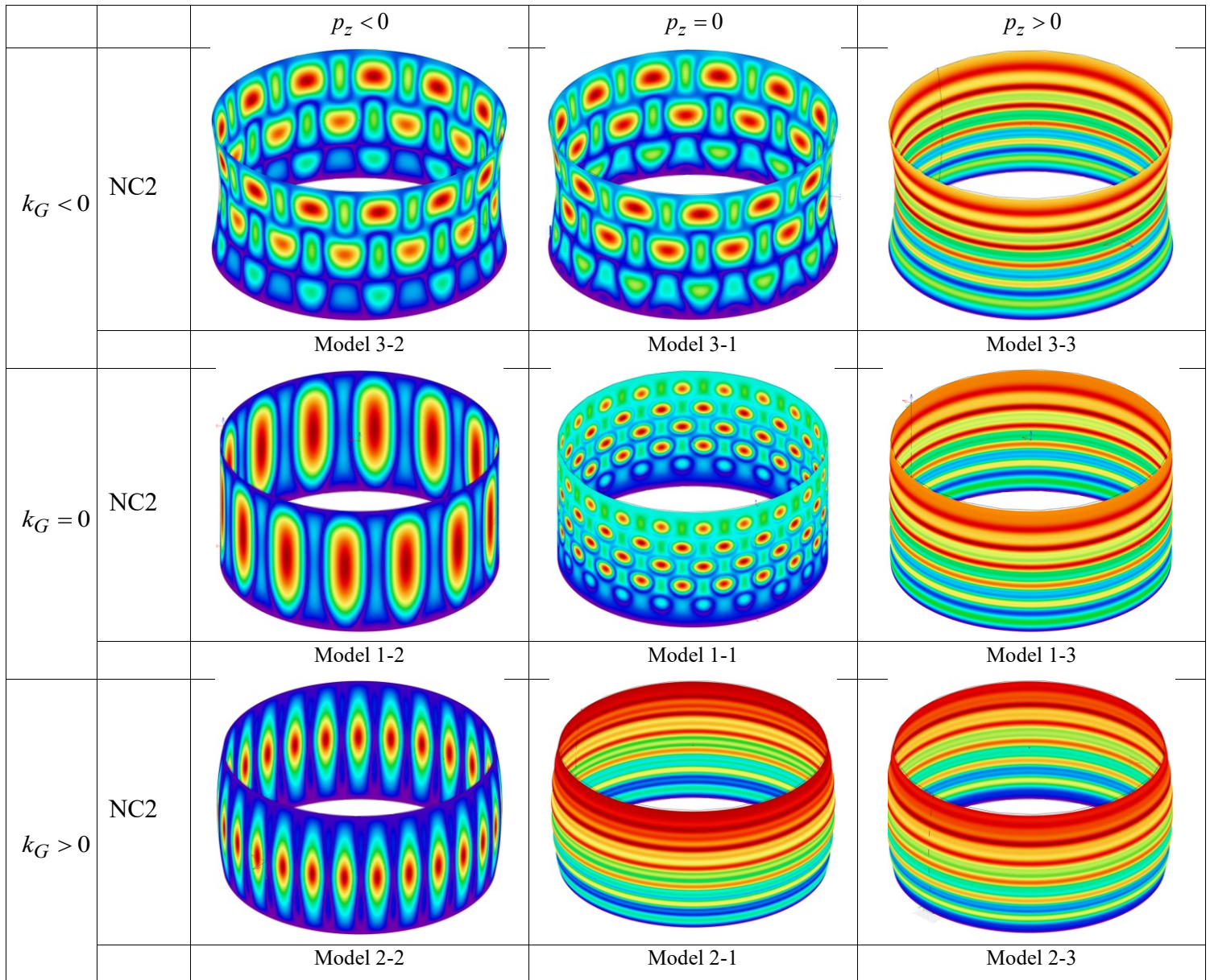


Figure 2.1 The nonlinear buckling patterns of the 9 shell structures (NC2), imperfection amplitude: t

		$p_z < 0$	$p_z = 0$	$p_z > 0$
--	--	-----------	-----------	-----------

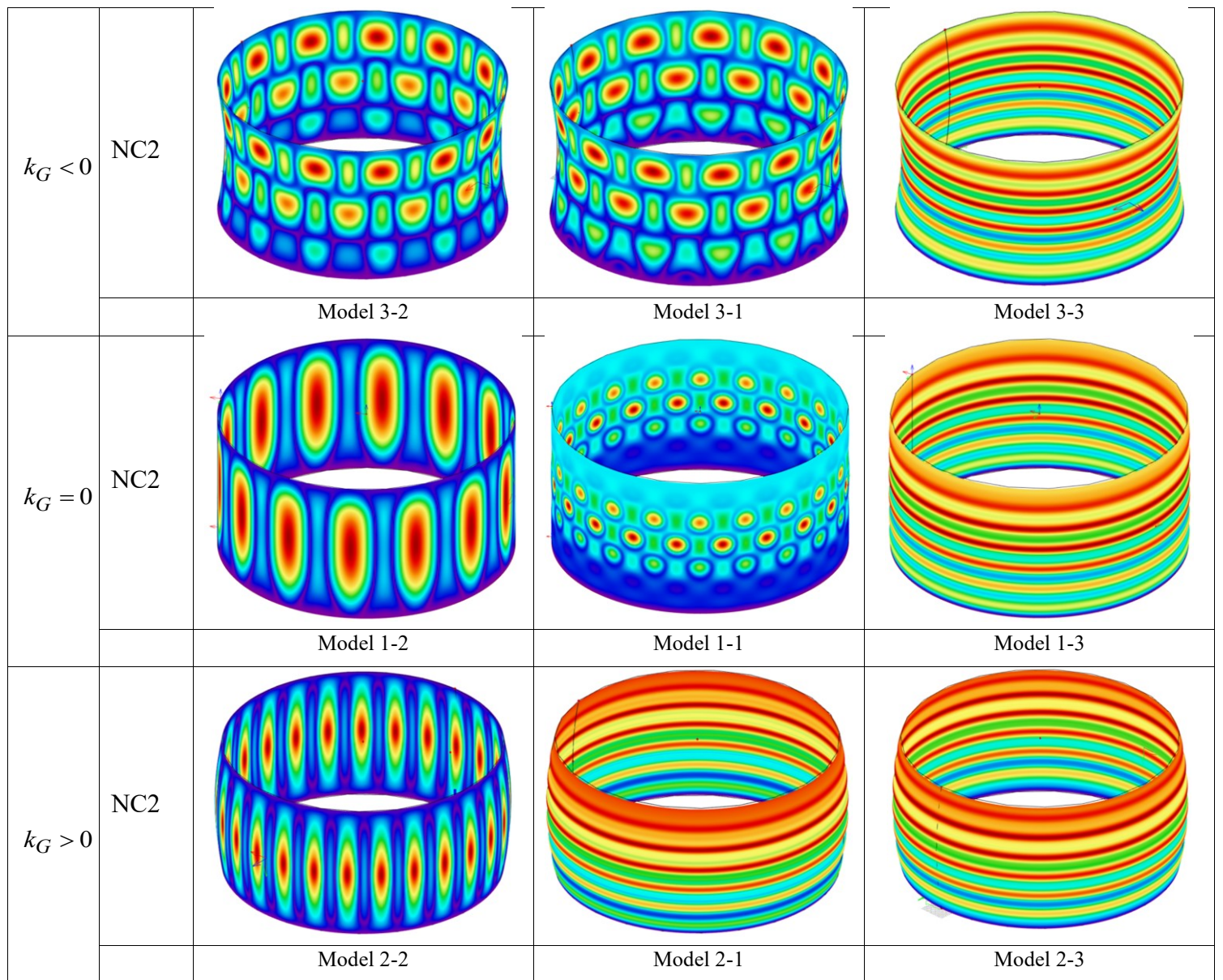
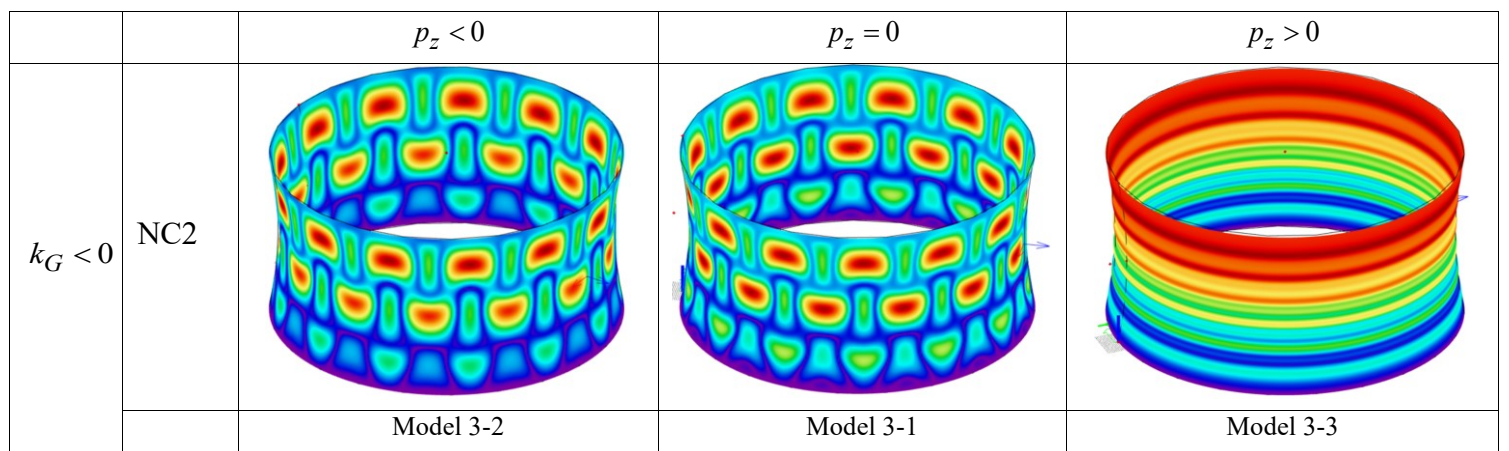


Figure 2.2 The nonlinear buckling patterns of the 9 shell structures (NC2), imperfection amplitude: $0.5t$



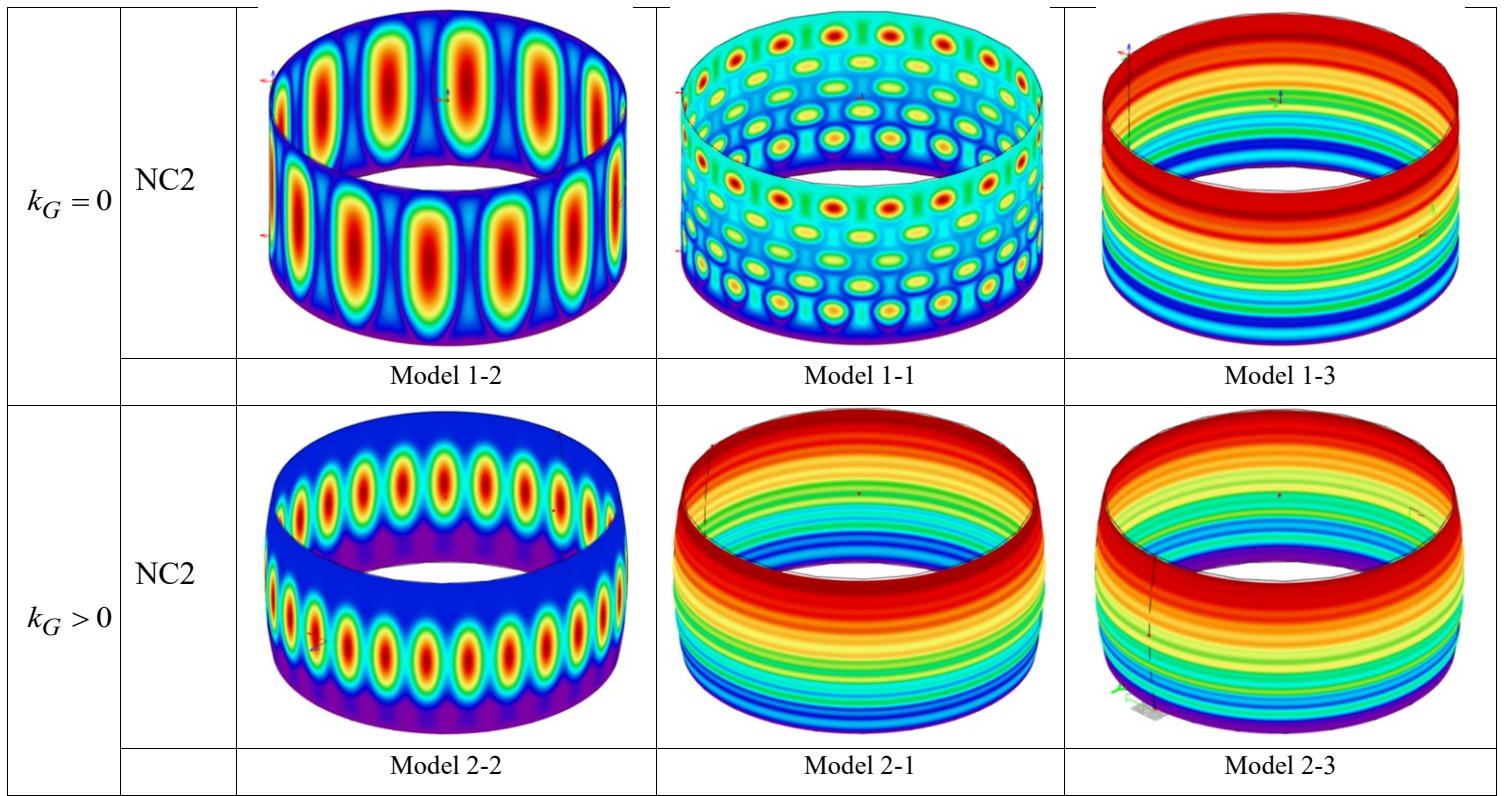
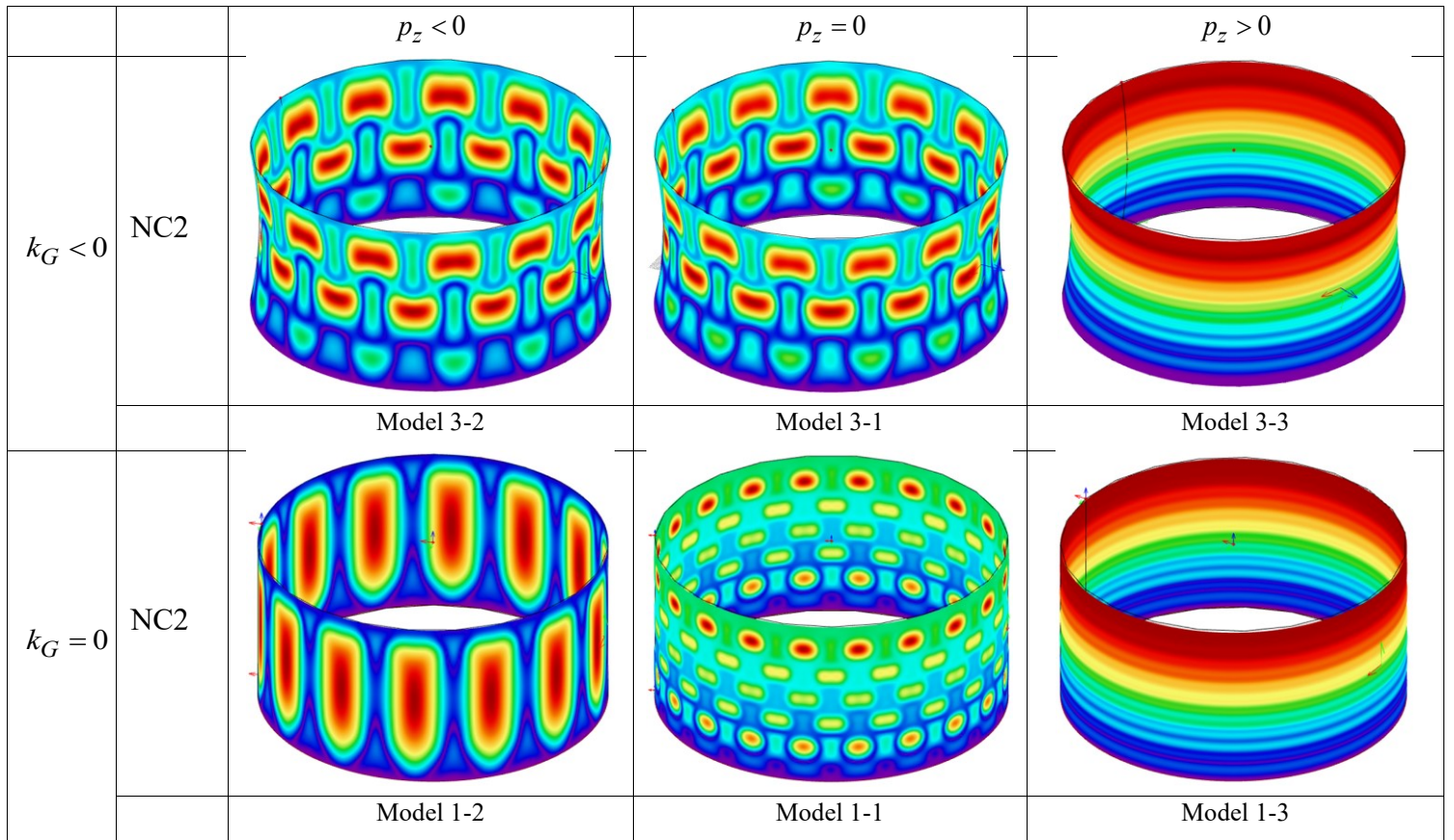


Figure 2.3 The nonlinear buckling patterns of the 9 shell structures (NC2), imperfection amplitude: $2t$



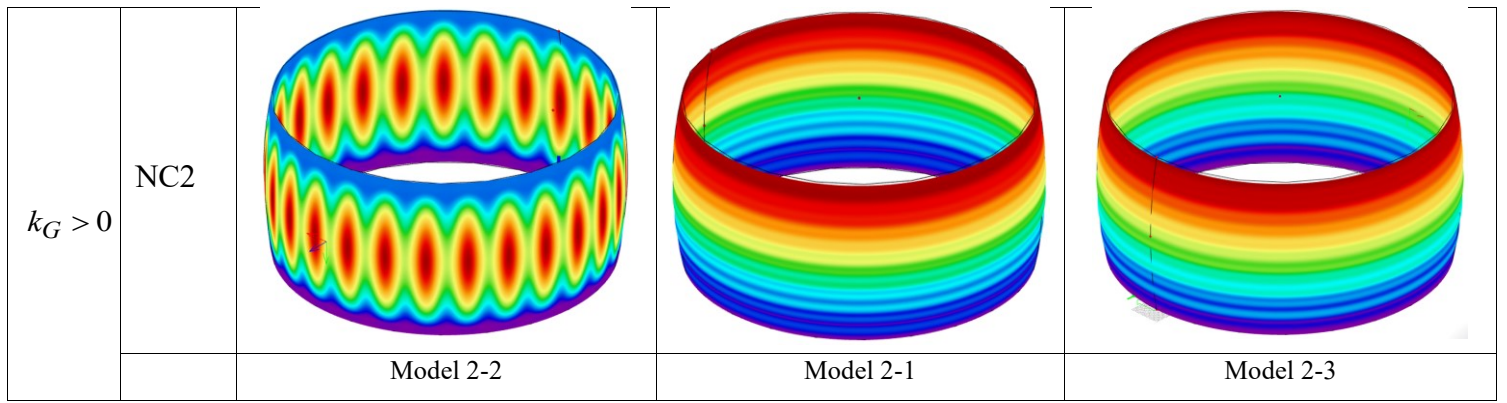


Figure 2.4 The nonlinear buckling patterns of the 9 shell structures (NC2), imperfection amplitude: $4t$

Appendix 4

Knockdown factor calculation by Maple when the imperfection amplitude equals to the shell thickness t :

```
> restart;
> #1-1
> a_x := 100 : kxx :=  $\frac{1}{a_x}$  : kyy := 0 : kxy := 0 : t := 0.2 : d := 0.2 : v := 0.3 : nxx := -657.5 : nyy := -2000 : eta :=
 $\frac{\sqrt{3 \cdot (1 - v^2)}}{1 - C}$ ;
> # eq1 :=  $C - \frac{\left(\frac{kxx}{kyy} - 1 - \frac{2 \cdot \eta \cdot d}{t}\right)^2}{4 \cdot \left(\frac{kxx}{kyy} - \frac{nyy}{nxx} - \frac{3 \cdot \eta \cdot d}{t}\right) \cdot \left(\frac{kxx}{kyy} - \frac{2 \cdot \eta \cdot d}{t}\right)} = 0$  : C := solve(eq1, C);
> eq2 :=  $C - \frac{\left(\frac{kyy}{kxx} - 1 - \frac{2 \cdot \eta \cdot d}{t}\right)^2}{4 \cdot \left(\frac{kyy}{kxx} - \frac{nxx}{nyy} - \frac{3 \cdot \eta \cdot d}{t}\right) \cdot \left(\frac{kyy}{kxx} - \frac{2 \cdot \eta \cdot d}{t}\right)} = 0$  : C := solve(eq2, C);
C := 14.44052272, 0.2400407074 (1)
```

```
> #1-2
> restart;
> a_x := 100 : kxx :=  $\frac{1}{a_x}$  : kyy := 0 : kxy := 0 : t := 0.2 : d := 0.2 : v := 0.3 : nxx := -2012 : nyy := -2000 : eta :=
 $\frac{\sqrt{3 \cdot (1 - v^2)}}{1 - C}$ ;
> eq2 :=  $C - \frac{\left(\frac{kyy}{kxx} - 1 - \frac{2 \cdot \eta \cdot d}{t}\right)^2}{4 \cdot \left(\frac{kyy}{kxx} - \frac{nxx}{nyy} - \frac{3 \cdot \eta \cdot d}{t}\right) \cdot \left(\frac{kyy}{kxx} - \frac{2 \cdot \eta \cdot d}{t}\right)} = 0$  : C := solve(eq2, C);
C := 5.894981233, 0.2198427215 (2)
```

```
> #1-3
> restart;
> a_x := 100 : kxx :=  $\frac{1}{a_x}$  : kyy := 0 : kxy := 0 : t := 0.2 : d := 0.2 : v := 0.3 : nxx := 2000 : nyy := -2000 : eta :=
 $\frac{\sqrt{3 \cdot (1 - v^2)}}{1 - C}$ ;
> eq2 :=  $C - \frac{\left(\frac{kyy}{kxx} - 1 - \frac{2 \cdot \eta \cdot d}{t}\right)^2}{4 \cdot \left(\frac{kyy}{kxx} - \frac{nxx}{nyy} - \frac{3 \cdot \eta \cdot d}{t}\right) \cdot \left(\frac{kyy}{kxx} - \frac{2 \cdot \eta \cdot d}{t}\right)} = 0$  : C := solve(eq2, C);
C := 0.2876072813, -5.272880752 (3)
```

```
> #2-1
> restart;
> a_x := 100 * m : kxx :=  $-\frac{1}{a_x}$  : s := 5 * m : l := 100 * m : a_y := 0.5 * s +  $\frac{1}{8} \cdot \frac{l^2}{s}$  : kyy :=  $-\frac{1}{a_y}$  : kxy := 0 : t := 0.2 : d := 0.2 :
v := 0.3 : nxx := 791.81 : nyy := -1905 : eta :=  $\frac{\sqrt{3 \cdot (1 - v^2)}}{1 - C}$ ;
> eq1 :=  $C - \frac{\left(\frac{kxx}{kyy} - 1 - \frac{2 \cdot \eta \cdot d}{t}\right)^2}{4 \cdot \left(\frac{kxx}{kyy} - \frac{nyy}{nxx} - \frac{3 \cdot \eta \cdot d}{t}\right) \cdot \left(\frac{kxx}{kyy} - \frac{2 \cdot \eta \cdot d}{t}\right)} = 0$  : C := solve(eq1, C);
C := 0.3995985530, -0.3334450134 + 0.2189578413 I, -0.3334450134 - 0.2189578413 I (4)
```

```
> restart;
> a_x := 100 * m : kxx :=  $-\frac{1}{a_x}$  : s := 5 * m : l := 100 * m : a_y := 0.5 * s +  $\frac{1}{8} \cdot \frac{l^2}{s}$  : kyy :=  $-\frac{1}{a_y}$  : kxy := 0 : t := 0.2 : d := 0.2 :
v := 0.3 : nxx := 791.81 : nyy := -1905 : eta :=  $\frac{\sqrt{3 \cdot (1 - v^2)}}{1 - C}$ ;
> eq2 :=  $C - \frac{\left(\frac{kyy}{kxx} - 1 - \frac{2 \cdot \eta \cdot d}{t}\right)^2}{4 \cdot \left(\frac{kyy}{kxx} - \frac{nxx}{nyy} - \frac{3 \cdot \eta \cdot d}{t}\right) \cdot \left(\frac{kyy}{kxx} - \frac{2 \cdot \eta \cdot d}{t}\right)} = 0$  : C := solve(eq2, C);
C := 0.2670021253, -6.217044247 + 2.417457642 I, -6.217044247 - 2.417457642 I (5)
```

```

> #2-2
> restart;
> a_x := 100 * m : kxx := -1/a_x : s := 5 * m : l := 100 * m : a_y := 0.5 * s + 1/8 * l^2 / s : kyy := -1/a_y : kxy := 0 : t := 0.2 : d := 0.2 :
v := 0.3 : eta := sqrt(3 * (1 - v^2)) / (1 - C) : nxx := -1966 : nyy := -2036 :
eq1 := C - ( (kxx - 1 - 2 * eta * d / t)^2 / (4 * (kyy - nxx - 3 * eta * d / t) * (kyy - 2 * eta * d / t)) ) = 0 : C := solve(eq1, C);
C := 0.2206158087, -0.4175537214, -2.285264516
(6)

```

```

> restart;
> a_x := 100 * m : kxx := -1/a_x : s := 5 * m : l := 100 * m : a_y := 0.5 * s + 1/8 * l^2 / s : kyy := -1/a_y : kxy := 0 : t := 0.2 : d := 0.2 :
v := 0.3 : eta := sqrt(3 * (1 - v^2)) / (1 - C) : nxx := -1966 : nyy := -2036 :
eq2 := C - ( (kyy - 1 - 2 * eta * d / t)^2 / (4 * (kxx - nyy - 3 * eta * d / t) * (kxx - 2 * eta * d / t)) ) = 0 : C := solve(eq2, C);
C := 0.2202482198, 9.677363703, -7.943256638
(7)

```

```

> #2-3
> restart;
> a_x := 100 : kxx := -1/a_x : s := 5 : l := 100 : a_y := 0.5 * s + 1/8 * l^2 / s : kyy := -1/a_y : kxy := 0 : t := 0.2 : d := 0.2 : v := 0.3 :
eta := sqrt(3 * (1 - v^2)) / (1 - C) : nxx := 1821.3 : nyy := -1856.42 :
eq1 := C - ( (kxx - 1 - 2 * eta * d / t)^2 / (4 * (kyy - nxx - 3 * eta * d / t) * (kyy - 2 * eta * d / t)) ) = 0 : C := solve(eq1, C);
C := 0.3186475309, -0.4804741759 + 0.2162594130 I, -0.4804741759 - 0.2162594130 I
(8)

```

```

> restart;
> a_x := 100 : kxx := -1/a_x : s := 5 : l := 100 : a_y := 0.5 * s + 1/8 * l^2 / s : kyy := -1/a_y : kxy := 0 : t := 0.2 : d := 0.2 : v := 0.3 :
eta := sqrt(3 * (1 - v^2)) / (1 - C) : nxx := 1821.3 : nyy := -1856.42 :
eq2 := C - ( (kyy - 1 - 2 * eta * d / t)^2 / (4 * (kxx - nyy - 3 * eta * d / t) * (kxx - 2 * eta * d / t)) ) = 0 : C := solve(eq2, C);
C := 0.2897135383, -3.955797411, -6.110083529
(9)

```

```

> #3-1
> restart;
> a_x := 100 : kxx := -1/a_x : s := 5 : l := 100 : a_y := 0.5 * s + 1/8 * l^2 / s : kyy := 1/a_y : kxy := 0 : t := 0.2 : d := 0.2 : v := 0.3 :
eta := sqrt(3 * (1 - v^2)) / (1 - C) : nxx := -791.85 : nyy := -2104 :
eq1 := C - ( (kxx - 1 - 2 * eta * d / t)^2 / (4 * (kyy - nxx - 3 * eta * d / t) * (kxx - 2 * eta * d / t)) ) = 0 : C := solve(eq1, C);
C := 0.1936168083, 1.956408089, 2.352643592
(10)

```

```

> restart;
> a_x := 100 : kxx := -1/a_x : s := 5 : l := 100 : a_y := 0.5 * s + 1/8 * l^2 / s : kyy := 1/a_y : kxy := 0 : t := 0.2 : d := 0.2 : v := 0.3 :
eta := sqrt(3 * (1 - v^2)) / (1 - C) : nxx := -791.85 : nyy := -2104 :
eq2 := C - ( (kyy - 1 - 2 * eta * d / t)^2 / (4 * (kxx - nyy - 3 * eta * d / t) * (kxx - 2 * eta * d / t)) ) = 0 : C := solve(eq2, C);
C := 0.2385003794, 6.541756272, 11.57396664
(11)

```

```

> #3-2
> restart;
> a_x := 100 : kxx := -1/a_x : s := 5 : l := 100 : a_y := 0.5*s + 1/8 * l^2/s : kyy := 1/a_y : kxy := 0 : t := 0.2 : d := 0.2 : v := 0.3 :
eta := sqrt(3*(1-v^2))/(1-C) : nxx := -2072.61 : nyy := -2072 :
|
|
|
> eq1 := C - ( (kxx/kyy - 1 - 2*eta*d/t)^2 ) / ( 4 * ( (kxx/nxx - nyy/nxx - 3*eta*d/t) * (kxx/kyy - 2*eta*d/t) ) ) = 0 : C := solve(eq1, C);
|
|
|
C := 0.2251842539, 2.231430598, 2.607459468 (12)
|
|
|
> restart;
> a_x := 100 : kxx := -1/a_x : s := 5 : l := 100 : a_y := 0.5*s + 1/8 * l^2/s : kyy := 1/a_y : kxy := 0 : t := 0.2 : d := 0.2 : v := 0.3 :
eta := sqrt(3*(1-v^2))/(1-C) : nxx := -2072.61 : nyy := -2072 :
|
|
|
> eq2 := C - ( (kyy/kxx - 1 - 2*eta*d/t)^2 ) / ( 4 * ( (kyy/nxx - nyy/nxx - 3*eta*d/t) * (kyy/kxx - 2*eta*d/t) ) ) = 0 : C := solve(eq2, C);
|
|
|
C := 0.2208301584, 4.498164385, 10.05591569 (13)
|
|
|
> #3-3
> restart;
> a_x := 100 : kxx := -1/a_x : s := 5 : l := 100 : a_y := 0.5*s + 1/8 * l^2/s : kyy := 1/a_y : kxy := 0 : t := 0.2 : d := 0.2 : v := 0.3 :
eta := sqrt(3*(1-v^2))/(1-C) : nxx := 2232.40 : nyy := -2271.5 :
|
|
|
> eq1 := C - ( (kxx/kyy - 1 - 2*eta*d/t)^2 ) / ( 4 * ( (kxx/nxx - nyy/nxx - 3*eta*d/t) * (kxx/kyy - 2*eta*d/t) ) ) = 0 : C := solve(eq1, C);
|
|
|
C := 0.2762022878, 2.286949022, 4.849813192 (14)
|
|
|
> restart;
> a_x := 100 : kxx := -1/a_x : s := 5 : l := 100 : a_y := 0.5*s + 1/8 * l^2/s : kyy := 1/a_y : kxy := 0 : t := 0.2 : d := 0.2 : v := 0.3 :
eta := sqrt(3*(1-v^2))/(1-C) : nxx := 2232.40 : nyy := -2271.5 :
|
|
|
> eq2 := C - ( (kyy/kxx - 1 - 2*eta*d/t)^2 ) / ( 4 * ( (kyy/nxx - nyy/nxx - 3*eta*d/t) * (kyy/kxx - 2*eta*d/t) ) ) = 0 : C := solve(eq2, C);
|
|
|
C := 0.2844301747, 8.902590015, -9.387752925 (15)

```

Knockdown factor calculation by Maple when the imperfection amplitude equals to half the shell thickness 0.5t:

```

> restart;
> #1-1
> a_x := 100 : kxx := 1/a_x : kyy := 0 : kxy := 0 : t := 0.2 : d := 0.1 : v := 0.3 : nxx := 0 : nyy := -2000 : eta := sqrt(3*(1-v^2))/(1-C) :
|
|
|
> #eq1 := C - ( (kxx/kyy - 1 - 2*eta*d/t)^2 ) / ( 4 * ( (kxx/nxx - nyy/nxx - 3*eta*d/t) * (kxx/kyy - 2*eta*d/t) ) ) = 0 : C := solve(eq1, C);
|
|
|
> eq2 := C - ( (kyy/kxx - 1 - 2*eta*d/t)^2 ) / ( 4 * ( (kyy/nxx - nyy/nxx - 3*eta*d/t) * (kyy/kxx - 2*eta*d/t) ) ) = 0 : C := solve(eq2, C);
|
|
|
C := 21.35513479, 0.3294075357

```

```

> #1-2
> restart;
> a_x := 100 : kxx :=  $\frac{1}{a_x}$  : kyy := 0 : kxy := 0 : t := 0.2 : d := 0.1 : v := 0.3 : nxx := -2060.97 : nyy := -2000 : eta :=  $\frac{\text{sqrt}(3 \cdot (1 - v^2))}{1 - C}$  :
> eq2 :=  $C - \frac{\left(\frac{kyy}{kxx} - 1 - \frac{2 \cdot \text{eta} \cdot d}{t}\right)^2}{4 \cdot \left(\frac{kyy}{kxx} - \frac{nxx}{nyy} - \frac{3 \cdot \text{eta} \cdot d}{t}\right) \cdot \left(\frac{kyy}{kxx} - \frac{2 \cdot \text{eta} \cdot d}{t}\right)} = 0$  : C := solve(eq2, C);
C := 3.381970458, 0.2663076976

> #1-3
> restart;
> a_x := 100 : kxx :=  $\frac{1}{a_x}$  : kyy := 0 : kxy := 0 : t := 0.2 : d := 0.1 : v := 0.3 : nxx := 2113.25 : nyy := -2000 : eta :=  $\frac{\text{sqrt}(3 \cdot (1 - v^2))}{1 - C}$  :
> eq2 :=  $C - \frac{\left(\frac{kyy}{kxx} - 1 - \frac{2 \cdot \text{eta} \cdot d}{t}\right)^2}{4 \cdot \left(\frac{kyy}{kxx} - \frac{nxx}{nyy} - \frac{3 \cdot \text{eta} \cdot d}{t}\right) \cdot \left(\frac{kyy}{kxx} - \frac{2 \cdot \text{eta} \cdot d}{t}\right)} = 0$  : C := solve(eq2, C);
C := 0.4100635492, -2.867095471

> #2-1
> restart;
> a_x := 100·m : kxx :=  $-\frac{1}{a_x}$  : s := 5·m : l := 100·m : a_y := 0.5·s +  $\frac{1}{8} \cdot \frac{f^2}{s}$  : kyy :=  $-\frac{1}{a_y}$  : kxy := 0 : t := 0.2 : d := 0.1 : v := 0.3 : nxx := 873.28 : nyy := -1904.78 : eta :=  $\frac{\text{sqrt}(3 \cdot (1 - v^2))}{1 - C}$  :
circumferential direction:
> eq1 :=  $C - \frac{\left(\frac{kxx}{kyy} - 1 - \frac{2 \cdot \eta \cdot d}{t}\right)^2}{4 \cdot \left(\frac{kxx}{kyy} - \frac{nyy}{nxx} - \frac{3 \cdot \eta \cdot d}{t}\right) \cdot \left(\frac{kxx}{kyy} - \frac{2 \cdot \eta \cdot d}{t}\right)} = 0$  : C := solve(eq1, C);
C := 0.002219672849, 0.2489017612, 0.6168126574

> restart;
axial direction
> a_x := 100·m : kxx :=  $-\frac{1}{a_x}$  : s := 5·m : l := 100·m : a_y := 0.5·s +  $\frac{1}{8} \cdot \frac{f^2}{s}$  : kyy :=  $-\frac{1}{a_y}$  : kxy := 0 : t := 0.2 : d := 0.1 : v := 0.3 : nxx := 873.28 : nyy := -1904.78 : eta :=  $\frac{\text{sqrt}(3 \cdot (1 - v^2))}{1 - C}$  :
> eq2 :=  $C - \frac{\left(\frac{kyy}{kxx} - 1 - \frac{2 \cdot \text{eta} \cdot d}{t}\right)^2}{4 \cdot \left(\frac{kyy}{kxx} - \frac{nxx}{nyy} - \frac{3 \cdot \text{eta} \cdot d}{t}\right) \cdot \left(\frac{kyy}{kxx} - \frac{2 \cdot \text{eta} \cdot d}{t}\right)} = 0$  : C := solve(eq2, C);
C := 0.3764020041, -2.589657228 + 1.812317177 I, -2.589657228 - 1.812317177 I

> #2-2
> restart;
> a_x := 100·m : kxx :=  $-\frac{1}{a_x}$  : s := 5·m : l := 100·m : a_y := 0.5·s +  $\frac{1}{8} \cdot \frac{f^2}{s}$  : kyy :=  $-\frac{1}{a_y}$  : kxy := 0 : t := 0.2 : d := 0.1 : v := 0.3 : eta :=  $\frac{\text{sqrt}(3 \cdot (1 - v^2))}{1 - C}$  : nxx := -2009.24 : nyy := -2036.55 :
> eq1 :=  $C - \frac{\left(\frac{kxx}{kyy} - 1 - \frac{2 \cdot \eta \cdot d}{t}\right)^2}{4 \cdot \left(\frac{kxx}{kyy} - \frac{nyy}{nxx} - \frac{3 \cdot \eta \cdot d}{t}\right) \cdot \left(\frac{kxx}{kyy} - \frac{2 \cdot \eta \cdot d}{t}\right)} = 0$  : C := solve(eq1, C);
C := 0.4331194913, -0.004293234118, -0.5706432705

> restart;
> a_x := 100·m : kxx :=  $-\frac{1}{a_x}$  : s := 5·m : l := 100·m : a_y := 0.5·s +  $\frac{1}{8} \cdot \frac{f^2}{s}$  : kyy :=  $-\frac{1}{a_y}$  : kxy := 0 : t := 0.2 : d := 0.1 : v := 0.3 : eta :=  $\frac{\text{sqrt}(3 \cdot (1 - v^2))}{1 - C}$  : nxx := -2009.24 : nyy := -2036.55 :
> eq2 :=  $C - \frac{\left(\frac{kyy}{kxx} - 1 - \frac{2 \cdot \text{eta} \cdot d}{t}\right)^2}{4 \cdot \left(\frac{kyy}{kxx} - \frac{nxx}{nyy} - \frac{3 \cdot \text{eta} \cdot d}{t}\right) \cdot \left(\frac{kyy}{kxx} - \frac{2 \cdot \text{eta} \cdot d}{t}\right)} = 0$  : C := solve(eq2, C);
C := 0.2752155140, 5.178014636, -3.818348215

> #2-3
> restart;
> a_x := 100 : kxx :=  $-\frac{1}{a_x}$  : s := 5 : l := 100 : a_y := 0.5·s +  $\frac{1}{8} \cdot \frac{f^2}{s}$  : kyy :=  $-\frac{1}{a_y}$  : kxy := 0 : t := 0.2 : d := 0.1 : v := 0.3 : eta :=  $\frac{\text{sqrt}(3 \cdot (1 - v^2))}{1 - C}$  : nxx := 1940.83 : nyy := -1855.98 :
> eq1 :=  $C - \frac{\left(\frac{kxx}{kyy} - 1 - \frac{2 \cdot \eta \cdot d}{t}\right)^2}{4 \cdot \left(\frac{kxx}{kyy} - \frac{nyy}{nxx} - \frac{3 \cdot \eta \cdot d}{t}\right) \cdot \left(\frac{kxx}{kyy} - \frac{2 \cdot \eta \cdot d}{t}\right)} = 0$  : C := solve(eq1, C);
C := 0.005435443725, 0.1580019518, 0.5364164028

> restart;
> a_x := 100 : kxx :=  $-\frac{1}{a_x}$  : s := 5 : l := 100 : a_y := 0.5·s +  $\frac{1}{8} \cdot \frac{f^2}{s}$  : kyy :=  $-\frac{1}{a_y}$  : kxy := 0 : t := 0.2 : d := 0.1 : v := 0.3 : eta :=  $\frac{\text{sqrt}(3 \cdot (1 - v^2))}{1 - C}$  : nxx := 1940.83 : nyy := -1855.98 :
> eq2 :=  $C - \frac{\left(\frac{kyy}{kxx} - 1 - \frac{2 \cdot \text{eta} \cdot d}{t}\right)^2}{4 \cdot \left(\frac{kyy}{kxx} - \frac{nxx}{nyy} - \frac{3 \cdot \text{eta} \cdot d}{t}\right) \cdot \left(\frac{kyy}{kxx} - \frac{2 \cdot \text{eta} \cdot d}{t}\right)} = 0$  : C := solve(eq2, C);
C := 0.4252312437, -2.078263389 + 0.9603504517 I, -2.078263389 - 0.9603504517 I

```

```

> #3-1
> restart;
> a_x := 100 : kxx := -1/a_x : s := 5 : l := 100 : a_y := 0.5*s + 1/8 * F^2/s : kyy := 1/a_y : kxy := 0 : t := 0.2 : d := 0.1 : v := 0.3 : eta := sqrt(3*(1-v^2))/(1-C) : nxx := -790 : nyy := -2105.25 :
> eq1 := C - (kxx/kyy - 1 - 2*eta*d/t)^2 / (4 * (kxx/nxx - nyy/t - 3*eta*d/t) * (kxx/t - 2*eta*d/t)) = 0 : C := solve(eq1, C);
C := 0.2052509656, 1.477477255, 1.686233341
> restart;
> a_x := 100 : kxx := -1/a_x : s := 5 : l := 100 : a_y := 0.5*s + 1/8 * F^2/s : kyy := 1/a_y : kxy := 0 : t := 0.2 : d := 0.1 : v := 0.3 : eta := sqrt(3*(1-v^2))/(1-C) : nxx := -790 : nyy := -2105.25 :
> eq2 := C - (kyy/kxx - 1 - 2*eta*d/t)^2 / (4 * (kyy/nxx - nyy/t - 3*eta*d/t) * (kyy/t - 2*eta*d/t)) = 0 : C := solve(eq2, C);
C := 0.297292143, 3.623683810, 7.059391081
> #3-2
> restart;
> a_x := 100 : kxx := -1/a_x : s := 5 : l := 100 : a_y := 0.5*s + 1/8 * F^2/s : kyy := 1/a_y : kxy := 0 : t := 0.2 : d := 0.1 : v := 0.3 : eta := sqrt(3*(1-v^2))/(1-C) : nxx := -2058.13 : nyy := -2043.9 :
> eq1 := C - (kxx/kyy - 1 - 2*eta*d/t)^2 / (4 * (kxx/nxx - nyy/t - 3*eta*d/t) * (kxx/t - 2*eta*d/t)) = 0 : C := solve(eq1, C);
C := 0.2540353079, 1.609276238, 1.845224970
> restart;
> a_x := 100 : kxx := -1/a_x : s := 5 : l := 100 : a_y := 0.5*s + 1/8 * F^2/s : kyy := 1/a_y : kxy := 0 : t := 0.2 : d := 0.1 : v := 0.3 : eta := sqrt(3*(1-v^2))/(1-C) : nxx := -2058.13 : nyy := -2043.9 :
> eq2 := C - (kyy/kxx - 1 - 2*eta*d/t)^2 / (4 * (kyy/nxx - nyy/t - 3*eta*d/t) * (kyy/t - 2*eta*d/t)) = 0 : C := solve(eq2, C);
C := 0.2631578504, 2.727576750, 5.824629939
> #3-3
> restart;
> a_x := 100 : kxx := -1/a_x : s := 5 : l := 100 : a_y := 0.5*s + 1/8 * F^2/s : kyy := 1/a_y : kxy := 0 : t := 0.2 : d := 0.1 : v := 0.3 : eta := sqrt(3*(1-v^2))/(1-C) : nxx := 2232.65 : nyy := -2272.01 :
> eq1 := C - (kxx/kyy - 1 - 2*eta*d/t)^2 / (4 * (kxx/nxx - nyy/t - 3*eta*d/t) * (kxx/t - 2*eta*d/t)) = 0 : C := solve(eq1, C);
C := 0.3427854891, 1.639853297, 3.132080731
> restart;
> a_x := 100 : kxx := -1/a_x : s := 5 : l := 100 : a_y := 0.5*s + 1/8 * F^2/s : kyy := 1/a_y : kxy := 0 : t := 0.2 : d := 0.1 : v := 0.3 : eta := sqrt(3*(1-v^2))/(1-C) : nxx := 2232.65 : nyy := -2272.01 :
> eq2 := C - (kyy/kxx - 1 - 2*eta*d/t)^2 / (4 * (kyy/nxx - nyy/t - 3*eta*d/t) * (kyy/t - 2*eta*d/t)) = 0 : C := solve(eq2, C);
C := 0.3901824363, 4.799367561, -5.339480952

```

Knockdown factor calculation by Maple when the imperfection amplitude equals to twice the shell thickness 2t:

```

> restart;
> #1-1
> a_x := 100 : kxx := 1/a_x : kyy := 0 : kxy := 0 : t := 0.2 : d := 0.4 : v := 0.3 : nxx := 0 : nyy := -2000 : eta := sqrt(3*(1-v^2))/(1-C) :
> # eq1 := C - (kxx/kyy - 1 - 2*eta*d/t)^2 / (4 * (kxx/nxx - nyy/t - 3*eta*d/t) * (kxx/t - 2*eta*d/t)) = 0 : C := solve(eq1, C);
> eq2 := C - (kyy/kxx - 1 - 2*eta*d/t)^2 / (4 * (kyy/nxx - nyy/t - 3*eta*d/t) * (kyy/t - 2*eta*d/t)) = 0 : C := solve(eq2, C);
C := 277.0892178, 0.2089513615

```

```

> #1-2
> restart;
> a_x := 100 : kxx :=  $\frac{1}{a_x}$  : kyy := 0 : kxy := 0 : t := 0.2 : d := 0.4 : v := 0.3 : nxx := -2060.97 : nyy := -2000 : eta :=  $\frac{\text{sqrt}(3 \cdot (1 - v^2))}{1 - C}$  :
> eq2 :=  $C - \frac{\left(\frac{kyy}{kxx} - 1 - \frac{2 \cdot \text{eta} \cdot d}{t}\right)^2}{4 \cdot \left(\frac{kyy}{kxx} - \frac{nxx}{nyy} - \frac{3 \cdot \text{eta} \cdot d}{t}\right) \cdot \left(\frac{kyy}{kxx} - \frac{2 \cdot \text{eta} \cdot d}{t}\right)} = 0$  : C := solve(eq2, C)
C := 10.58955777, 0.1935921347

> #1-3
> restart;
> a_x := 100 : kxx :=  $\frac{1}{a_x}$  : kyy := 0 : kxy := 0 : t := 0.2 : d := 0.4 : v := 0.3 : nxx := 2113.25 : nyy := -2000 : eta :=  $\frac{\text{sqrt}(3 \cdot (1 - v^2))}{1 - C}$  :
> eq2 :=  $C - \frac{\left(\frac{kyy}{kxx} - 1 - \frac{2 \cdot \text{eta} \cdot d}{t}\right)^2}{4 \cdot \left(\frac{kyy}{kxx} - \frac{nxx}{nyy} - \frac{3 \cdot \text{eta} \cdot d}{t}\right) \cdot \left(\frac{kyy}{kxx} - \frac{2 \cdot \text{eta} \cdot d}{t}\right)} = 0$  : C := solve(eq2, C)
C := 0.2266349045, -9.485244404

> #2-1
> restart;
> a_x := 100 : m : kxx :=  $-\frac{1}{a_x}$  : s := 5 : m : I := 100 : m : a_y := 0.5 : s +  $\frac{1}{8} \cdot \frac{f^2}{s}$  : kyy :=  $-\frac{1}{a_y}$  : kxy := 0 : t := 0.2 : d := 0.4 : v := 0.3 : nxx := 873.28 : nyy := -1904.78 : eta :=  $\frac{\text{sqrt}(3 \cdot (1 - v^2))}{1 - C}$  :
circumferential direction:
> eq1 :=  $C - \frac{\left(\frac{kxx}{kyy} - 1 - \frac{2 \cdot \eta \cdot d}{t}\right)^2}{4 \cdot \left(\frac{kxx}{kyy} - \frac{nyy}{nxx} - \frac{3 \cdot \eta \cdot d}{t}\right) \cdot \left(\frac{kxx}{kyy} - \frac{2 \cdot \eta \cdot d}{t}\right)} = 0$  : C := solve(eq1, C)
C := 0.2483582237, -1.461701646 + 0.2301955466 I, -1.461701646 - 0.2301955466 I

axial direction
> a_x := 100 : m : kxx :=  $-\frac{1}{a_x}$  : s := 5 : m : I := 100 : m : a_y := 0.5 : s +  $\frac{1}{8} \cdot \frac{f^2}{s}$  : kyy :=  $-\frac{1}{a_y}$  : kxy := 0 : t := 0.2 : d := 0.4 : v := 0.3 : nxx := 873.28 : nyy := -1904.78 : eta :=  $\frac{\text{sqrt}(3 \cdot (1 - v^2))}{1 - C}$  :
> eq2 :=  $C - \frac{\left(\frac{kyy}{kxx} - 1 - \frac{2 \cdot \text{eta} \cdot d}{t}\right)^2}{4 \cdot \left(\frac{kyy}{kxx} - \frac{nxx}{nyy} - \frac{3 \cdot \text{eta} \cdot d}{t}\right) \cdot \left(\frac{kyy}{kxx} - \frac{2 \cdot \text{eta} \cdot d}{t}\right)} = 0$  : C := solve(eq2, C)
C := 0.2154345474, -13.11773986 + 2.515975061 I, -13.11773986 - 2.515975061 I

> #2-2
> restart;
> a_x := 100 : m : kxx :=  $-\frac{1}{a_x}$  : s := 5 : m : I := 100 : m : a_y := 0.5 : s +  $\frac{1}{8} \cdot \frac{f^2}{s}$  : kyy :=  $-\frac{1}{a_y}$  : kxy := 0 : t := 0.2 : d := 0.4 : v := 0.3 : eta :=  $\frac{\text{sqrt}(3 \cdot (1 - v^2))}{1 - C}$  : nxx := -2009.24 : nyy := -2036.55 :
> eq1 :=  $C - \frac{\left(\frac{kxx}{kyy} - 1 - \frac{2 \cdot \eta \cdot d}{t}\right)^2}{4 \cdot \left(\frac{kxx}{kyy} - \frac{nyy}{nxx} - \frac{3 \cdot \eta \cdot d}{t}\right) \cdot \left(\frac{kxx}{kyy} - \frac{2 \cdot \eta \cdot d}{t}\right)} = 0$  : C := solve(eq1, C)
C := 0.1822751305, -1.681272382, -5.525314695

> restart;
> a_x := 100 : m : kxx :=  $-\frac{1}{a_x}$  : s := 5 : m : I := 100 : m : a_y := 0.5 : s +  $\frac{1}{8} \cdot \frac{f^2}{s}$  : kyy :=  $-\frac{1}{a_y}$  : kxy := 0 : t := 0.2 : d := 0.4 : v := 0.3 : eta :=  $\frac{\text{sqrt}(3 \cdot (1 - v^2))}{1 - C}$  : nxx := -2009.24 : nyy := -2036.55 :
> eq2 :=  $C - \frac{\left(\frac{kyy}{kxx} - 1 - \frac{2 \cdot \text{eta} \cdot d}{t}\right)^2}{4 \cdot \left(\frac{kyy}{kxx} - \frac{nxx}{nyy} - \frac{3 \cdot \text{eta} \cdot d}{t}\right) \cdot \left(\frac{kyy}{kxx} - \frac{2 \cdot \text{eta} \cdot d}{t}\right)} = 0$  : C := solve(eq2, C)
C := 0.1926693519, 17.76485705, -16.24827695

> #2-3
> restart;
> a_x := 100 : kxx :=  $-\frac{1}{a_x}$  : s := 5 : I := 100 : a_y := 0.5 : s +  $\frac{1}{8} \cdot \frac{f^2}{s}$  : kyy :=  $-\frac{1}{a_y}$  : kxy := 0 : t := 0.2 : d := 0.4 : v := 0.3 : eta :=  $\frac{\text{sqrt}(3 \cdot (1 - v^2))}{1 - C}$  : nxx := 1940.83 : nyy := -1855.98 :
> eq1 :=  $C - \frac{\left(\frac{kxx}{kyy} - 1 - \frac{2 \cdot \eta \cdot d}{t}\right)^2}{4 \cdot \left(\frac{kxx}{kyy} - \frac{nyy}{nxx} - \frac{3 \cdot \eta \cdot d}{t}\right) \cdot \left(\frac{kxx}{kyy} - \frac{2 \cdot \eta \cdot d}{t}\right)} = 0$  : C := solve(eq1, C)
C := 0.2198826945, -1.809447170 + 0.2630405316 I, -1.809447170 - 0.2630405316 I

> restart;
> a_x := 100 : kxx :=  $-\frac{1}{a_x}$  : s := 5 : I := 100 : a_y := 0.5 : s +  $\frac{1}{8} \cdot \frac{f^2}{s}$  : kyy :=  $-\frac{1}{a_y}$  : kxy := 0 : t := 0.2 : d := 0.4 : v := 0.3 : eta :=  $\frac{\text{sqrt}(3 \cdot (1 - v^2))}{1 - C}$  : nxx := 1940.83 : nyy := -1855.98 :
> eq2 :=  $C - \frac{\left(\frac{kyy}{kxx} - 1 - \frac{2 \cdot \text{eta} \cdot d}{t}\right)^2}{4 \cdot \left(\frac{kyy}{kxx} - \frac{nxx}{nyy} - \frac{3 \cdot \text{eta} \cdot d}{t}\right) \cdot \left(\frac{kyy}{kxx} - \frac{2 \cdot \text{eta} \cdot d}{t}\right)} = 0$  : C := solve(eq2, C)
C := 0.2258037884, -6.804694155, -14.82541540

```

```

> #3-1
> restart;
> a_x := 100 : kxx := -1/a_x : s := 5 : I := 100 : a_y := 0.5*s + 1/8 * f^2/s : kyy := 1/a_y : kxy := 0 : t := 0.2 : d := 0.4 : v := 0.3 : eta := sqrt(3*(1-v^2))/(1-C) : nxx := -790 : nyy := -2105.25 :
> eq1 := C - (kxx/kyy - 1 - 2*eta*d^2/t) = 0 : C := solve(eq1, C);
C := 0.1833901388, 2.910044578, 3.671261294
> restart;
> a_x := 100 : kxx := -1/a_x : s := 5 : I := 100 : a_y := 0.5*s + 1/8 * f^2/s : kyy := 1/a_y : kxy := 0 : t := 0.2 : d := 0.4 : v := 0.3 : eta := sqrt(3*(1-v^2))/(1-C) : nxx := -790 : nyy := -2105.25 :
> eq2 := C - (kyy/kxx - 1 - 2*eta*d^2/t) = 0 : C := solve(eq2, C);
C := 0.2043931121, 12.65415749, 20.27772629
> #3-2
> restart;
> a_x := 100 : kxx := -1/a_x : s := 5 : I := 100 : a_y := 0.5*s + 1/8 * f^2/s : kyy := 1/a_y : kxy := 0 : t := 0.2 : d := 0.4 : v := 0.3 : eta := sqrt(3*(1-v^2))/(1-C) : nxx := -2058.13 : nyy := -2043.9 :
> eq1 := C - (kxx/kyy - 1 - 2*eta*d^2/t) = 0 : C := solve(eq1, C);
C := 0.2022894044, 3.496923622, 4.085845620
> restart;
> a_x := 100 : kxx := -1/a_x : s := 5 : I := 100 : a_y := 0.5*s + 1/8 * f^2/s : kyy := 1/a_y : kxy := 0 : t := 0.2 : d := 0.4 : v := 0.3 : eta := sqrt(3*(1-v^2))/(1-C) : nxx := -2058.13 : nyy := -2043.9 :
> eq2 := C - (kyy/kxx - 1 - 2*eta*d^2/t) = 0 : C := solve(eq2, C);
C := 0.1953908464, 8.007547417, 18.42788910
> #3-3
> restart;
> a_x := 100 : kxx := -1/a_x : s := 5 : I := 100 : a_y := 0.5*s + 1/8 * f^2/s : kyy := 1/a_y : kxy := 0 : t := 0.2 : d := 0.4 : v := 0.3 : eta := sqrt(3*(1-v^2))/(1-C) : nxx := 2232.65 : nyy := -2272.01 :
> eq1 := C - (kxx/kyy - 1 - 2*eta*d^2/t) = 0 : C := solve(eq1, C);
C := 0.2294599472, 3.588427074, 8.192502667
> restart;
> a_x := 100 : kxx := -1/a_x : s := 5 : I := 100 : a_y := 0.5*s + 1/8 * f^2/s : kyy := 1/a_y : kxy := 0 : t := 0.2 : d := 0.4 : v := 0.3 : eta := sqrt(3*(1-v^2))/(1-C) : nxx := 2232.65 : nyy := -2272.01 :
> eq2 := C - (kyy/kxx - 1 - 2*eta*d^2/t) = 0 : C := solve(eq2, C);
C := 0.2259705799, 17.20351462, -17.73778405

```

Knockdown factor calculation by Maple when the imperfection amplitude equals to four times the shell thickness $4t$:

```

> restart;
> #1-1
> a_x := 100 : kxx := 1/a_x : kyy := 0 : kxy := 0 : t := 0.2 : d := 0.8 : v := 0.3 : nxx := 0 : nyy := -2000 : eta := sqrt(3*(1-v^2))/(1-C) :
> # eq1 := C - (kxx/kyy - 1 - 2*eta*d^2/t) = 0 : C := solve(eq1, C);
> eq2 := C - (kyy/kxx - 1 - 2*eta*d^2/t) = 0 : C := solve(eq2, C);
C := 1076.568559, 0.1877784158

```

```

> #I-2
> restart:
> a_x := 100 : kxx :=  $\frac{1}{a_x}$  : kyy := 0 : kxy := 0 : t := 0.2 : d := 0.8 : v := 0.3 : nxx := -2060.97 : nyy := -2000 : eta :=  $\frac{\sqrt{3 \cdot (1 - v^2)}}{1 - C}$  :
> eq2 :=  $C - \frac{\left(\frac{kyy}{kxx} - 1 - \frac{2 \cdot \text{eta} \cdot d}{t}\right)^2}{4 \cdot \left(\frac{kyy}{kxx} - \frac{nxx}{nyy} - \frac{3 \cdot \text{eta} \cdot d}{t}\right) \cdot \left(\frac{kyy}{kxx} - \frac{2 \cdot \text{eta} \cdot d}{t}\right)} = 0$  : C := solve(eq2, C);
C := 20.20811400, 0.1802975797

> #I-3
> restart:
> a_x := 100 : kxx :=  $\frac{1}{a_x}$  : kyy := 0 : kxy := 0 : t := 0.2 : d := 0.8 : v := 0.3 : nxx := 2113.25 : nyy := -2000 : eta :=  $\frac{\sqrt{3 \cdot (1 - v^2)}}{1 - C}$  :
> eq2 :=  $C - \frac{\left(\frac{kyy}{kxx} - 1 - \frac{2 \cdot \text{eta} \cdot d}{t}\right)^2}{4 \cdot \left(\frac{kyy}{kxx} - \frac{nxx}{nyy} - \frac{3 \cdot \text{eta} \cdot d}{t}\right) \cdot \left(\frac{kyy}{kxx} - \frac{2 \cdot \text{eta} \cdot d}{t}\right)} = 0$  : C := solve(eq2, C);
C := 0.1959560564, -18.80272016

> #2-1
> restart:
> a_x := 100·m : kxx :=  $-\frac{1}{a_x}$  : s := 5·m : l := 100·m : a_y := 0.5·s +  $\frac{1}{8} \cdot \frac{l^2}{s}$  : kyy :=  $-\frac{1}{a_y}$  : kxy := 0 : t := 0.2 : d := 0.8 : v := 0.3 : nxx := 873.28 : nyy := -1904.78 : eta :=  $\frac{\sqrt{3 \cdot (1 - v^2)}}{1 - C}$  :
circumferectial direction:
> eq1 :=  $C - \frac{\left(\frac{kxx}{kyy} - 1 - \frac{2 \cdot \eta \cdot d}{t}\right)^2}{4 \cdot \left(\frac{kxx}{kyy} - \frac{nyy}{nxx} - \frac{3 \cdot \eta \cdot d}{t}\right) \cdot \left(\frac{kxx}{kyy} - \frac{2 \cdot \eta \cdot d}{t}\right)} = 0$  : C := solve(eq1, C);
C := 0.2000809045, -3.555523242, -4.043574941

axial direction
> a_x := 100·m : kxx :=  $-\frac{1}{a_x}$  : s := 5·m : l := 100·m : a_y := 0.5·s +  $\frac{1}{8} \cdot \frac{l^2}{s}$  : kyy :=  $-\frac{1}{a_y}$  : kxy := 0 : t := 0.2 : d := 0.8 : v := 0.3 : nxx := 873.28 : nyy := -1904.78 : eta :=  $\frac{\sqrt{3 \cdot (1 - v^2)}}{1 - C}$  :
> eq2 :=  $C - \frac{\left(\frac{kyy}{kxx} - 1 - \frac{2 \cdot \text{eta} \cdot d}{t}\right)^2}{4 \cdot \left(\frac{kyy}{kxx} - \frac{nxx}{nyy} - \frac{3 \cdot \text{eta} \cdot d}{t}\right) \cdot \left(\frac{kyy}{kxx} - \frac{2 \cdot \text{eta} \cdot d}{t}\right)} = 0$  : C := solve(eq2, C);
C := 0.1903239867, -26.24670561, -28.25317385

> #2-2
> restart:
> a_x := 100·m : kxx :=  $-\frac{1}{a_x}$  : s := 5·m : l := 100·m : a_y := 0.5·s +  $\frac{1}{8} \cdot \frac{l^2}{s}$  : kyy :=  $-\frac{1}{a_y}$  : kxy := 0 : t := 0.2 : d := 0.8 : v := 0.3 : eta :=  $\frac{\sqrt{3 \cdot (1 - v^2)}}{1 - C}$  : nxx := -2009.24 : nyy := -2036.55 :
> eq1 :=  $C - \frac{\left(\frac{kxx}{kyy} - 1 - \frac{2 \cdot \eta \cdot d}{t}\right)^2}{4 \cdot \left(\frac{kxx}{kyy} - \frac{nyy}{nxx} - \frac{3 \cdot \eta \cdot d}{t}\right) \cdot \left(\frac{kxx}{kyy} - \frac{2 \cdot \eta \cdot d}{t}\right)} = 0$  : C := solve(eq1, C);
C := 0.1728658288, -4.286787664, -12.08705002

> restart:
> a_x := 100·m : kxx :=  $-\frac{1}{a_x}$  : s := 5·m : l := 100·m : a_y := 0.5·s +  $\frac{1}{8} \cdot \frac{l^2}{s}$  : kyy :=  $-\frac{1}{a_y}$  : kxy := 0 : t := 0.2 : d := 0.8 : v := 0.3 : eta :=  $\frac{\sqrt{3 \cdot (1 - v^2)}}{1 - C}$  : nxx := -2009.24 : nyy := -2036.55 :
> eq2 :=  $C - \frac{\left(\frac{kyy}{kxx} - 1 - \frac{2 \cdot \text{eta} \cdot d}{t}\right)^2}{4 \cdot \left(\frac{kyy}{kxx} - \frac{nxx}{nyy} - \frac{3 \cdot \text{eta} \cdot d}{t}\right) \cdot \left(\frac{kyy}{kxx} - \frac{2 \cdot \text{eta} \cdot d}{t}\right)} = 0$  : C := solve(eq2, C);
C := 0.1795310218, 34.55124545, -32.92237032

> #2-3
> restart:]
> a_x := 100 : kxx :=  $-\frac{1}{a_x}$  : s := 5 : l := 100 : a_y := 0.5·s +  $\frac{1}{8} \cdot \frac{l^2}{s}$  : kyy :=  $-\frac{1}{a_y}$  : kxy := 0 : t := 0.2 : d := 0.8 : v := 0.3 : eta :=  $\frac{\sqrt{3 \cdot (1 - v^2)}}{1 - C}$  : nxx := 1940.83 : nyy := -1855.98 :
> eq1 :=  $C - \frac{\left(\frac{kxx}{kyy} - 1 - \frac{2 \cdot \eta \cdot d}{t}\right)^2}{4 \cdot \left(\frac{kxx}{kyy} - \frac{nyy}{nxx} - \frac{3 \cdot \eta \cdot d}{t}\right) \cdot \left(\frac{kxx}{kyy} - \frac{2 \cdot \eta \cdot d}{t}\right)} = 0$  : C := solve(eq1, C);
C := 0.1889473607, -4.526556465 + 0.3018735363 I, -4.526556465 - 0.3018735363 I

> restart:
> a_x := 100 : kxx :=  $-\frac{1}{a_x}$  : s := 5 : l := 100 : a_y := 0.5·s +  $\frac{1}{8} \cdot \frac{l^2}{s}$  : kyy :=  $-\frac{1}{a_y}$  : kxy := 0 : t := 0.2 : d := 0.8 : v := 0.3 : eta :=  $\frac{\sqrt{3 \cdot (1 - v^2)}}{1 - C}$  : nxx := 1940.83 : nyy := -1855.98 :
> eq2 :=  $C - \frac{\left(\frac{kyy}{kxx} - 1 - \frac{2 \cdot \text{eta} \cdot d}{t}\right)^2}{4 \cdot \left(\frac{kyy}{kxx} - \frac{nxx}{nyy} - \frac{3 \cdot \text{eta} \cdot d}{t}\right) \cdot \left(\frac{kyy}{kxx} - \frac{2 \cdot \text{eta} \cdot d}{t}\right)} = 0$  : C := solve(eq2, C);
C := 0.1949950383, -13.58429708, -31.57901737

```

```

> #3-1
> restart;
> a_x := 100 : kxx := -1/a_x : s := 5 : l := 100 : a_y := 0.5*s + 1/8 * F^2/s : kyy := 1/a_y : kxy := 0 : t := 0.2 : d := 0.8 : v := 0.3 : eta := sqrt(3*(1-v^2))/(1-C) : nxx := -790 : nyy :=
-2105.25 :
> eq1 := C - (kxx/kyy - 1 - 2*eta*d/t)^2 / (4 * (kxx/nxx - nyy/nxx - 3*eta*d/t) * (kxx/kyy - 2*eta*d/t)) = 0 : C := solve(eq1, C);
C := 0.1762273401, 4.820201204, 6.295913397
> restart;
> a_x := 100 : kxx := -1/a_x : s := 5 : l := 100 : a_y := 0.5*s + 1/8 * F^2/s : kyy := 1/a_y : kxy := 0 : t := 0.2 : d := 0.8 : v := 0.3 : eta := sqrt(3*(1-v^2))/(1-C) : nxx := -790 : nyy :=
-2105.25 :
> eq2 := C - (kyy/kxx - 1 - 2*eta*d/t)^2 / (4 * (kyy/nxx - nyy/nxx - 3*eta*d/t) * (kyy/kxx - 2*eta*d/t)) = 0 : C := solve(eq2, C);
C := 0.1859868206, 25.20727316, 37.28422995
> #3-2
> restart;
> a_x := 100 : kxx := -1/a_x : s := 5 : l := 100 : a_y := 0.5*s + 1/8 * F^2/s : kyy := 1/a_y : kxy := 0 : t := 0.2 : d := 0.8 : v := 0.3 : eta := sqrt(3*(1-v^2))/(1-C) : nxx := -2058.13 : nyy :=
-2043.9 :
> eq1 := C - (kxx/kyy - 1 - 2*eta*d/t)^2 / (4 * (kxx/nxx - nyy/nxx - 3*eta*d/t) * (kxx/kyy - 2*eta*d/t)) = 0 : C := solve(eq1, C);
C := 0.1866771706, 6.061884985, 6.971859329
> restart;
> a_x := 100 : kxx := -1/a_x : s := 5 : l := 100 : a_y := 0.5*s + 1/8 * F^2/s : kyy := 1/a_y : kxy := 0 : t := 0.2 : d := 0.8 : v := 0.3 : eta := sqrt(3*(1-v^2))/(1-C) : nxx := -2058.13 : nyy :=
-2043.9 :
> eq2 := C - (kyy/kxx - 1 - 2*eta*d/t)^2 / (4 * (kyy/nxx - nyy/nxx - 3*eta*d/t) * (kyy/kxx - 2*eta*d/t)) = 0 : C := solve(eq2, C);
C := 0.1815059069, 15.06824892, 35.13502295
> #3-3
> restart;
> a_x := 100 : kxx := -1/a_x : s := 5 : l := 100 : a_y := 0.5*s + 1/8 * F^2/s : kyy := 1/a_y : kxy := 0 : t := 0.2 : d := 0.8 : v := 0.3 : eta := sqrt(3*(1-v^2))/(1-C) : nxx := 2232.65 : nyy :=
-2272.01 :
> eq1 := C - (kxx/kyy - 1 - 2*eta*d/t)^2 / (4 * (kxx/nxx - nyy/nxx - 3*eta*d/t) * (kxx/kyy - 2*eta*d/t)) = 0 : C := solve(eq1, C);
C := 0.2006128054, 6.200107093, 14.80389668
> restart;
> a_x := 100 : kxx := -1/a_x : s := 5 : l := 100 : a_y := 0.5*s + 1/8 * F^2/s : kyy := 1/a_y : kxy := 0 : t := 0.2 : d := 0.8 : v := 0.3 : eta := sqrt(3*(1-v^2))/(1-C) : nxx := 2232.65 : nyy :=
-2272.01 :
> eq2 := C - (kyy/kxx - 1 - 2*eta*d/t)^2 / (4 * (kyy/nxx - nyy/nxx - 3*eta*d/t) * (kyy/kxx - 2*eta*d/t)) = 0 : C := solve(eq2, C);
C := 0.1962182866, 33.86732032, -34.58299464

```

Appendix 5

```

> restart;
> # Standard values
> C := [0.42, 0.43, 0.37, 0.44, 0.45, 0.41, 0.42, 0.27, 0.25, 0.27, 0.26, 0.26, 0.44, 0.17, 0.15, 0.21, 0.17, 0.19, 0.25, 0.15, 0.13, 0.27, 0.15, 0.14];
C := [0.42, 0.43, 0.37, 0.44, 0.45, 0.41, 0.42, 0.27, 0.25, 0.27, 0.26, 0.26, 0.44, 0.17, 0.15, 0.21, 0.17, 0.19, 0.25, 0.15, 0.13, 0.27, 0.15, 0.14] (1)
> # Fitted values
> C_fitted := [0.427146636, 0.317822118, 0.359426053, 0.368928935, 0.299978937, 0.341780891, 0.403326094, 0.294001576, 0.33560551, 0.345108393, 0.276158395, 0.317960349, 0.352618014,
0.243293496, 0.284897431, 0.294400314, 0.225450315, 0.267252269, 0.237674452, 0.128349934, 0.169953869, 0.179456752, 0.110506753, 0.152308707];
C_fitted := [0.427146636, 0.317822118, 0.359426053, 0.368928935, 0.299978937, 0.341780891, 0.403326094, 0.294001576, 0.33560551, 0.345108393, 0.276158395, 0.317960349, 0.352618014,
0.243293496, 0.284897431, 0.294400314, 0.225450315, 0.267252269, 0.237674452, 0.128349934, 0.169953869, 0.179456752, 0.110506753, 0.152308707] (2)
> # Formula values
> C_formula := [0.33, 0.41, 0.38, 0.43, 0.43, 0.39, 0.25, 0.29, 0.27, 0.22, 0.29, 0.28, 0.21, 0.23, 0.22, 0.18, 0.23, 0.23, 0.19, 0.2, 0.19, 0.17, 0.19, 0.2];
C_formula := [0.33, 0.41, 0.38, 0.43, 0.43, 0.39, 0.25, 0.29, 0.27, 0.22, 0.29, 0.28, 0.21, 0.23, 0.22, 0.18, 0.23, 0.23, 0.19, 0.2, 0.19, 0.17, 0.19, 0.2] (3)
> # Number of data points
> n := nops(C);
n := 24 (4)
> # Mean Squared Error (MSE) for formula values
> MSE_formula := (1/n)*add((C[i]-C_formula[i])^2, i = 1..n);
MSE_formula := 0.005641666667 (5)
> # Mean Squared Error (MSE) for fitted values
> MSE_fitted := (1/n)*add((C[i]-C_fitted[i])^2, i = 1..n);
MSE_fitted := 0.005079140512 (6)
> print(MSE_formula, MSE_fitted);
0.005641666667, 0.005079140512 (7)

```

